PhD degree in Molecular Medicine (curriculum in Molecular Oncology)

European School of Molecular Medicine (SEMM),

University of Milan and University of Naples "Federico II"

Settore disciplinare: BIO/11

Regulatory mechanisms implicated in the control of Numb asymmetric partitioning at mitosis of adult mammary stem cells

UNIVERSITÀ DEGLI STUDI DI MILANO

Restelli Silvia

IFOM, Milan

Matricola n. R10319

Supervisor: Prof. Salvatore Pece

IEO, Milan

Anno accademico 2015-2016

This work was supported by:

Index

Figure and table legend

Abbreviations

ACD	Asymmetric cell division
BM	Basement membrane
CSC	Cancer stem cell
Ctr	Control
CYT	Cytosol
DMEM	Dulbecco's modified Eagle medium
EB	Enteroblast
EC	Enterocyte
EDM	Enzyme digestion medium
EH	Epsin15 homology region
EMT	Epithelial-to-mesenchymal transition
FACS	Fluorescence activated cell sorting
GMC	Ganglion mother cell
Hh	Hedgehog
ICM	Inner cell mass
IF	Immunofluorescence
Insc	Inscuteable
ISC	Intestinal stem cell
K14	Keratine 14
K8	Keratine 8
KD	knockdown
KO1	Numb knockout 1 tumour cell line
MAPK	Mitogen-activated protein kinase
MaSC	Mammary stem cell
MEC	Mammary epithelial cell
MESCM	Mammary epithelial stem cell medium
mPar3	Mammalian Par3
MRU	Mammary repopulating unit
MS	Mammosphere
NICD	Notch intracellular domain
PBS	Phosphate-buffered saline
PCP	Planar cell polarity
PKC	Protein kinase C
PM	Plasma membrane
PRR	Prolin-rich region
pSer-276	Phosphorylated Serine 276
PTB	Phosphotyrosine binding domain
RT	Room temperature
rt-qPCR	Real time quantitative Polymerase Chain Reaction
SC	Stem Cell
SCD	Symmetric cell division
SDS	Sodium dodecyl sulfate
SOP	Sensory organ precursor cell
TAE	Tris-Acetate EDTA

TBS	Tris-buffered saline
TL	Time Lapse
WB	Western blot

Abstract

The role of Numb as a cell fate determinant has been very well described in *Drosophila melanogaster (D. melanogaster)* neuroblasts (Knoblich, 2010; Caussinus and Gonzales, 2005). In this system, the asymmetric partitioning of Numb in one of the two daughter cells is controlled by its phosphorylation status, which determines its subcellular localization. It is well established that the polarized distribution of Numb in dividing *D. melanogaster* neuroblasts relies on the proper functioning of a group of proteins including the Par polarity complex (composed of Par3, Par6 and aPKC) and Aurora A. aPKC phosphorylates Numb, and is essential for specifying neuroblast polarity and for ensuring the asymmetric localization of Numb (Wirtz-Peitz, Nishimura et al., 2008).

In mammals, Numb acts as a cell fate determinant in mammary adult stem cells, in which it segregates into the daughter cell that retains the stem cell fate. In this cell, Numb forms a tri-complex with p53 and the E3-ubiquitin ligase HDM2, thus preventing p53 degradation by HDM2 and contributing to its stabilization (Colaluca, Tosoni et al. 2008). For these reasons, loss of Numb in the mammary stem cell compartment reduces p53 levels, disrupts mammary tissue homeostasis and causes the appearance of breast cancer stem cells (Tosoni, Zecchini et al. 2015).

The data generated in this thesis suggest that the molecular machinery responsible for the phosphorylation of Numb during mitosis is partially conserved from *D. melanogaster* neuroblasts to adult mammary stem cells. In mammary epithelial cells (MECs), treatment with TPA - a potent PKC activator - induces Numb phosphorylation at a conserved serine residue (Ser276) and causes a re-localization of the protein from cellular biomembranes to the cytosol. Moreover, while the overexpression of PKCζ (the mammalian homologue of *D. melanogaster* aPKC) in MECs enhances the phosphorylation of Numb on Ser276 and re-localizes Numb to the cytosol, PKCζ knockdown impairs Numb phosphorylation, resulting in the accumulation of Numb at the plasma membrane (PM). In addition, Par3 knockdown in MECs not only reduces pSer276 levels but also reinforces Numb staining at the PM. All together, these data indicate that PKCζ could promote Numb phosphorylation and that the Par polarity complex could regulate Numb localization in mammary cells. Furthermore, we show that treatment of mammary stem cells with TPA imparts a shift from asymmetric to symmetric distribution of Numb at mitosis, indicating that Numb phosphorylation status might impact on Numb distribution. The same effect is obtained by Par3 knockdown in mammary stem cells, suggesting that Par3 could regulate Numb partitioning during mitosis of mammary stem cells.

To gain more insight into this issue, we generated two different Numb phosphomutants, in which we mutated three serine residues previously characterized as PKCζ phosphorylation targets (Ser7, Ser276 and Ser295) (Smith et al., 2007) (Nishimura and Kaibuchi, 2007) to either alanine (phosphodeficient mutant) or aspartic acid (phosphomimetic mutant). We found that both mutants segregate symmetrically during mitosis of mammary stem cells, suggesting that a proper cycle of Numb phosphorylation and de-phosphorylation is necessary to allow its asymmetric partitioning, thus confirming the role of Numb phosphorylation on its subcellular distribution.

We also found that both the phosphomimetic and the phosphodeficient mutants cannot rescue the low p53 levels displayed by Numb knockout cells. Furthermore, in our experiments the phosphomimetic mutant showed a reduced ability to bind p53. These latter findings argue that Numb phosphorylation could impact on its binding to p53, thus introducing an additional level of regulation in the Numb/p53 circuitry in mammary stem cell homeostasis.

Altogether, our data suggest that a correct cycle of phosphorylation and de-phosphorylation at specific serine residues is essential to ensure the asymmetric segregation of Numb at mitosis of MaSCs. Given the importance of Numb in the maintenance of mammary tissue homeostasis, in the next future it would be interesting to investigate the correlation between the dysfunction of the mechanisms governing Numb phosphorylation in MaSCs and breast tumourigenesis.

Chapter 1

Introduction

1.1 Stem cells and tissue homeostasis: focus on the mammary epithelium

1.1.1 Definition and features of stem cells and adult stem cells

Stem cells are unique cells present in almost all multicellular organisms. The definition of a "stem cell" comprises two general properties: the capacity to self-renew (to produce more stem cells by cell division) and the ability to differentiate into specialized, committed cells.

Stem cells can be classified on the basis of their differentiating potential, or *potency*. **Embryonic stem cells** derive from the inner cell mass (ICM) of the developing blastocyst and are *pluripotent* stem cells, which means that they can differentiate into any cell type of the three embryonic germ layers: endoderm, mesoderm, and ectoderm. During development, pluripotent stem cells generate more differentiated stem cells called *multipotent* stem cells. These cells can give rise to a limited range of cell types within a specific tissue. For example, multipotent blood stem cells can develop into red blood cells, white blood cells or platelets (Chamberlain, Fox et al. 2007).

Stem cells are also present in the adult tissues, where they are referred to as **adult stem cells**. These cells are essential for the maintenance of tissue homeostasis and repair after injury. Adult stem cells can be *multipotent* or *unipotent*, depending on the tissue they belong to (Visvader and Clevers 2016). For example, the epidermis contains unipotent stem cells that can produce only a specific cell type (keratinocytes), while the bone marrow contains several multipotent stem cells that can generate multiple differentiated cell types (red blood cells, white blood cells and platelets, but also bone, cartilage and fat cells) (Chamberlain, Fox et al. 2007; Fuchs 2008; Fuchs and Nowak 2008).

The history of adult stem cells began more than 60 years ago with the discovery of hematopoietic pluripotent stem cells (Becker, Mc et al. 1963). Since then, adult stem cells have been discovered in a variety of organs and tissues, including blood vessels, skeletal muscle, skin, brain, gut, heart, mammary gland and liver. Within their tissue, stem cells

reside in specific microenvironments, called “niches”, that have a fundamental role in controlling the stem cell behavior. Signals from the niche influence their cell cycle and contribute to the maintenance of their undifferentiated state (Hsu and Fuchs 2012).

In most tissues, adult stem cells are quiescent, which means that they rarely divide and spend most of their lives in the G0 phase of the cell cycle. Based on their quiescent behavior, stem cells can be classified into two categories: those with high turnover and those with low turnover. In tissues with high turnover rates, such as the intestine or the epidermis, stem cells divide regularly to maintain the homeostasis of the active tissue. In tissues such as the brain or the skeletal muscle, which display a low turnover, stem cells remain quiescent for extended periods of time and are woken up only in particular conditions, such as during accidental injury (Hsu and Fuchs 2012). It is worth to note that in malignant tissues, cancer cells appear to mimic some of the mechanisms used to regulate normal stem cell functions. Therefore, it is essential to understand the behavior of normal stem cells under physiological conditions in order to study its possible dysfunction in pathological conditions (Hsu and Fuchs 2012).

1.1.2 Mammary adult stem cells

The mammary epithelium is a unique organ that not only distinguishes mammals from all other animals, but it is also the only glandular organ that reaches a complete development after birth. The mammary gland is generally composed of two tissue compartments: the epithelium, which consists of *ducts* and milk-producing alveolar structures (*alveoli*), and the *stroma* or connective tissue, which is also called the mammary fat pad and is composed of fibroblasts, adipocytes, endothelial cells and immune cells (Hennighausen and Robinson 2005).

The mammary epithelium is structurally organized into two layers: an external, luminal layer, containing secretory cells that undergo functional differentiation to produce milk

during pregnancy, and a basal, inner layer, made of myoepithelial cells, which are contractile cells and participates in the delivery of milk towards the nipple. Macroscopically, the epithelium displays a tree-like structure, with branches and lobules (groups of alveoli) that are embedded in the stroma (***Fig. 1***). At different stages of development (pre-pubertal, pubertal and pregnancy), the mammary epithelium undergoes severe structural changes, suggesting the presence of adult stem cells within this tissue (Inman, Robertson et al. 2015).

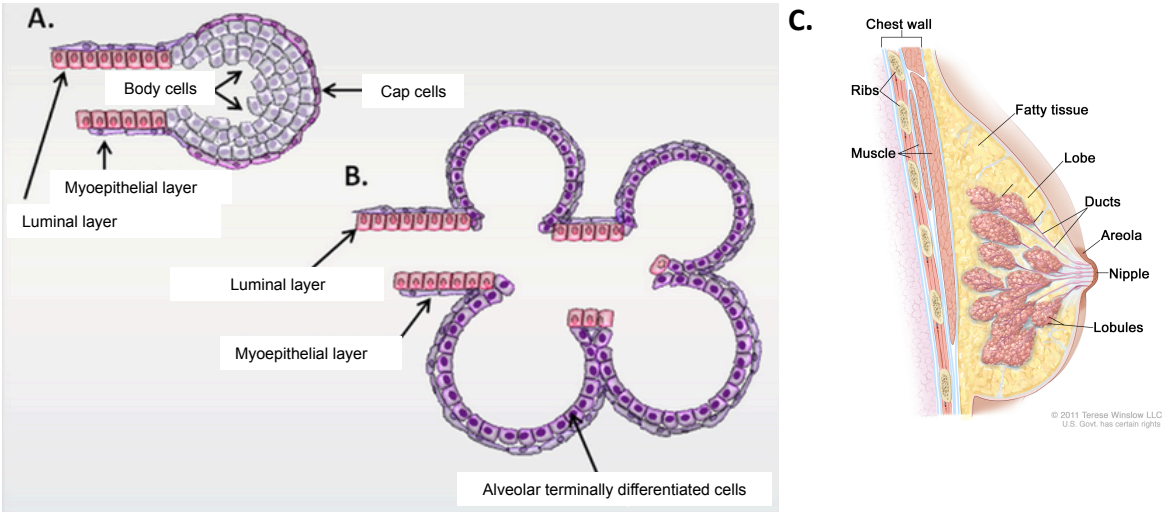

Figure 1. Structure and development of the mammary gland epithelium
a) The prepubertal and pubertal mammary gland is composed of highly proliferative ducts, which end up in terminal end buds (or TEBs). TEBs comprise cap cells (basal), which are in direct contact with the basement membrane, and luminal Body cells, which form the internal cellular bulk of the TEB.
b) Pregnancy induces profound morphological changes in the epithelium, including ductal branching and formation of alveolar structures. Alveoli are composed of a single layer of milk-producing cells that are surrounded by myoepithelial or contractile cells. (A and B are taken form Gajewska et al. 2013)
c) Schematic drawing of the human mammary gland with the epithelial tree (ducts and lobules) embedded in the stroma (fatty tissue). Groups of lobules are organized in lobes, which are responsible for the production of milk during lactation. The milk is transported to the nipple through specialized ducts (adapted from Terese Winslow, National Cancer Institute).

The first evidences of mammary adult stem cells came from studies in the late 1950s, when Deome and colleagues demonstrated that an entire mammary gland could be regenerated by transplantation of a fragment of mammary epithelium into the cleared fat pad of a

recipient mouse (Deome, Faulkin et al. 1959). In the following years, further studies demonstrated that mammary epithelial outgrowths could be obtained in cleared mammary fat pads transplanted with either explants or cell suspensions (Hoshino and Gardner 1967) (Daniel, De Ome et al. 1968) (Smith 1996). Moreover, explants from different regions of the epithelial tree were shown to reconstitute fully functional outgrowths, indicating that the repopulating cells are spread throughout the entire epithelial tree (Hoshino 1962) (Daniel, De Ome et al. 1968) (Smith and Medina 1988) (Visvader 2009). In 2006, Shackleton and colleagues demonstrated that a single cell from the mouse mammary gland could reconstitute an entire gland *in vivo* (Shackleton, Vaillant et al. 2006). The transplanted cell contributed to the development of both the luminal and the myoepiythelial lineages and generated functional lobulo-alveolar structures during pregnancy. This cell displayed also self-renewal capacity and, for all these reasons, it was initially thought to be a multipotent, self-renewing adult stem cell (***Fig. 2***). However, studies from Blanpain's laboratory have questioned the reliability of transplantation assays in extrapolating the differentiation potential of stem cells under physiological conditions. They found that the mammary gland initially develops from Keratin 14-positive (K14+) multipotent embryonic cells that can give rise to both myoepithelial and luminal cells. Strikingly, during puberty and pregnancy, it seems that two different populations of lineage-restricted adult stem cells (Keratin 8+ / luminal and Keratin 14+ / myoepithelial adult stem cells) are responsible for the expansion of the mammary epithelium. According to this study, the two populations of mammary adult stem cells appear to be unipotent rather than multipotent, and their differentiation potential relies on the physiological condition they experience (Van Keymeulen, Rocha et al. 2011).

By contrast, recent studies, based on *in vivo* clonal cell-fate mapping and 3D imaging techniques, showed that the mouse pubertal gland contains different stem and progenitor

cell populations, including also bipotent stem cells that can generate both luminal and myoepithelial cells (Rios, Fu et al. 2014). Thus, the mammary tissue homeostasis appears to rely on a hierarchical population of stem and progenitor cells, which contribute differently to the development of the epithelium (***Fig. 2***).

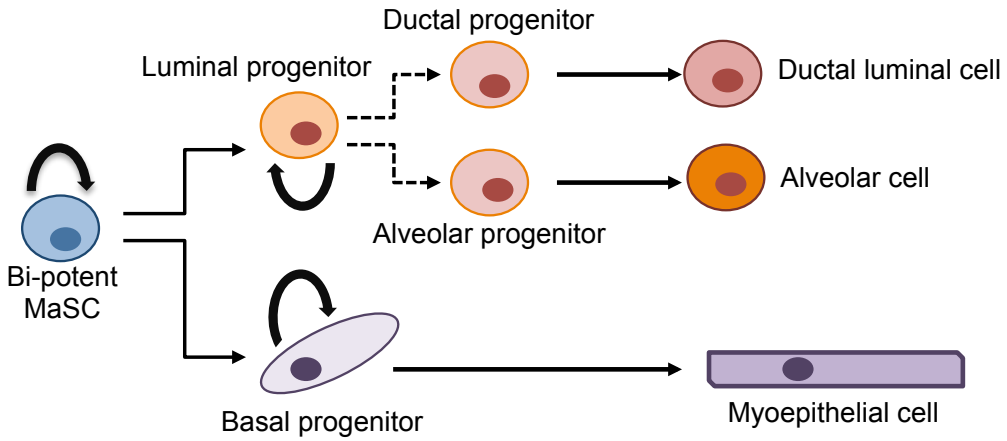

Figure 2. Schematic model of the mammary gland stem cell hierarchy
Bipotent mammary stem cells (MaSCs) give rise to unipotent stem cells or long-lived progenitors, which in turn give rise to basal/myoepithelial and luminal lineages. In addition to these cells, two types of committed progenitors (alveolar and ductal) have been experimentally isolated. Bipotent basal MaSCs have been recently tracked in vivo (Rios et al. 2014) (adapted from Visvader and Clevers, 2016).

Even though the discussion on their multipotency remains open, the existence of mammary stem cells (MaSCs) is widely accepted nowadays. In particular, adult MaSCs are thought to reside within a specialized niche in the basal epithelial compartment that is highly controlled (Stingl, Eirew et al. 2006). As with most adult stem cells, these cells are considered quiescent unless activated at specific events occurring during female development, that is, puberty and pregnancy. During these phases, the activation of stem cells by ovarian hormones (e.g., progesterone and 17β-estradiol) have a profound impact on the homeostasis of the mammary tissue, and results in the morphological changes associated to these stages of the mammary gland development (Joshi, Jackson et al. 2010). Many questions in the field still remain unanswered. For example, which specific signals are required to specify a particular lineage path? Or, what is the essential role of the tissue

microenvironment in the activation and lineage specification of MaSCs? At the moment, we know that a correct tissue architecture, together with the right amount of growth factors, cytokines and proteinases, provided by the stem cell niche, are essential for a proper development and functioning of the mammary gland (Inman, Robertson et al. 2015)

1.1.3 Isolation of adult mammary stem cells

Different approaches have been used to isolate and characterize MaSCs, however, no studies have identified bona fide markers of a pure population of MaSCs. MaSCs-enriched population of cells from mouse mammary glands were identified by coupling the fluorescence activated cell-sorting (FACS), based on cell-surface marker expression, with transplantation assays (Badders, Goel et al. 2009) (dos Santos, Rebbeck et al. 2013) (Plaks, Brenot et al. 2013) (Shackleton, Vaillant et al. 2006) (Stingl, Eirew et al. 2006) (Zeng and Nusse 2010). Mammary epithelial cells can be isolated by selecting the Lin^- cell surface signature, which comprises CD45 (hematopoietic, immune cells), Ter119 (erythrocytes) and CD31 (endothelial cells). These epithelial cells are then sorted for the expression of high levels of CD24 (heat-stable antigen), CD29 (β1 integrin) and CD49f (α6 integrin) (Badders, Goel et al. 2009) (dos Santos, Rebbeck et al. 2013) (Plaks, Brenot et al. 2013) (Shackleton, Vaillant et al. 2006) (Stingl, Eirew et al. 2006) (Zeng and Nusse 2010). Recently, several studies have attempted to identify additional markers in order to isolate pure MaSCs from the Lin^- $CD24^{high}$ $CD29^{high}$ $CD49f^{high}$ population. In 2013, dos Santos and colleagues proposed CD1d (a glycoprotein expressed by antigen-presenting cells) as a marker for MaSCs, as adding this marker to the current sorting technique led to a fivefold increase in the mammary gland reconstituting units (MRUs) found in the Lin^- $CD24^+$ $CD29^{high}$ $CD49f^{high}$ population (dos Santos, Rebbeck et al. 2013). In the same year, Plaks and colleagues showed that the $Lgr5^+$ subset of basal mammary cells display reconstitution capabilities (Plaks, Brenot et al. 2013). However, a recent paper from Wang and

colleagues, showed the opposite: Lgr^- cells that express the protein C receptor (ProcR) showed stronger MRU behaviour than $Lgr5^+$ cells (Wang, Cai et al. 2015). Based on this finding, they proposed ProcR as a new MaSCs marker (Wang, Cai et al. 2015).

Beyond doubts, FACS-based studies have been useful in the identification of new markers for the isolation of MaSCs. However, variations in FACS results and in the frequency of MaSCs detected in different studies exist. This could be explained by differences in the methodologies used, from transplantation conditions to FACS settings, and the age of the mice used (Inman, Robertson et al. 2015).

Most of the studies dedicated to the isolation of MaSCs were carried out in mice. Little is known about human normal MaSCs. As in the case of the mouse, human MaSCs are extremely rare within the mammary gland and several efforts have been made to isolate these cells in order to characterize this small but fundamental population. In our laboratory, the isolation of human MaSCs has been performed by coupling the PKH26 labelling technique with a mammosphere assay (Cicalese, Bonizzi et al. 2009) (Pece, Tosoni et al. 2010). This approach exploits two peculiar characteristics of mammary stem cells: first, their quiescent phenotype, as compared to their progeny; and second, their ability to survive and divide in anchorage-independent conditions (Pece, Tosoni et al. 2010).

Briefly, the critical steps in this procedure involve:

1. The mammosphere culture method, which is the production of clonal three-dimensional spheroids in suspension growth conditions, relies on the specific ability of stem cells to proliferate in suspension by anoikis (Tosoni, Di Fiore et al. 2012) (Dontu, Al-Hajj et al. 2003) (Cicalese, Bonizzi et al. 2009) (Pece, Tosoni et al. 2010).

2. PKH26, which is a lipophilic and fluorescent dye, is used to label the entire dissociated bulk mammary epithelial cell population. As mammospheres grow, PKH26 is selectively retained in the (quiescent) stem cell present in each mammosphere, but not in its

proliferating progeny (that dilutes the dye while dividing);

3. Purification of PKH26-labeled mammary stem cells from the bulk of progenitors by FACS sorting of cells obtained from the dissociation of mammospheres (***Fig. 3***).

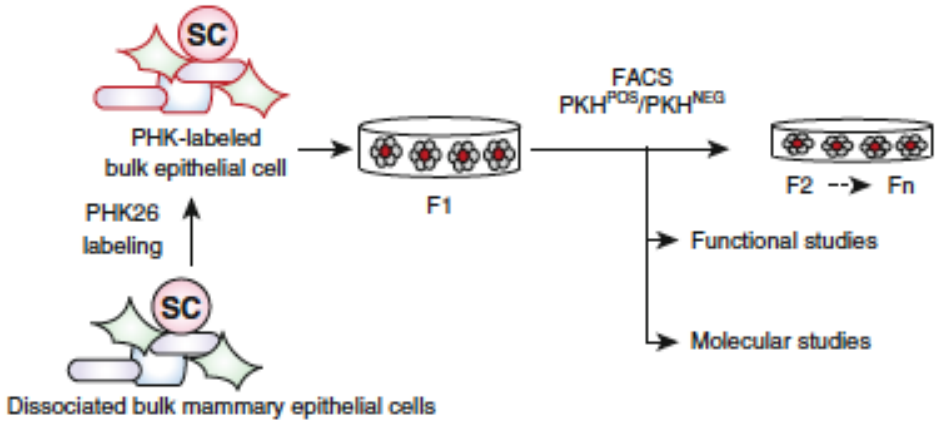

Figure 3. Functional purification of mammary stem cells
Schematic representation of the experimental method used to produce PKH26-labeled mammosphere cultures. Cells from the mammary gland are freshly isolated and called "the dissociated bulk of mammary epithelial cells" (bottom). This entire population is then labeled with the PKH26 dye (top) and plated in suspension culture to allow the formation of primary generation mammospheres (F1). F1 mammospheres can be dissociated and cells can be replated in suspension to yield multiple generations of mammospheres (F1, F2, F3... Fn). Dissociated cells can also be subjected to FACS analysis to isolate PKH26 POS (positive) or PKH26 NEG (negative) cells for further analysis (adapted from Tosoni et al. 2012).

This technique allows to purify pure populations of MaSCs, with mammary initiating capability and stem features (Pece, Tosoni et al., 2010).

In contrast to previous studies, this strategy does not rely on the usage of immunophenotypical markers, going beyond some of the limitations imposed by the use of such markers (Tosoni, Di Fiore et al. 2012).

1.1.4 Mammary stem cells and breast cancer

The interest in MaSCs has grown in the last decade due to their recent implication in breast carcinogenesis (Al-Hajj, Wicha et al. 2003). Nowadays, there is substantial evidence that

only a small subpopulation of cancer cells is able to initiate tumour growth. This small fraction of cancer cells, referred to as Cancer Stem Cells, or CSCs, was initially described in human leukaemia (Bonnet and Dick 1997) and only later in solid tumours, including the breast (Al-Hajj, Wicha et al. 2003). CSCs are generally localized either in interior hypoxic zones of the tumour or at the tumour invasive boundaries, and share some important features of normal adult stem cells, such as self-renewal and differentiation abilities, capacity to migrate and survive in non-adherent conditions, and resistance to apoptosis (Dontu, Al-Hajj et al. 2003). In breast cancer, CSCs can drive the formation of metastasis and cause resistance to therapy (Brooks, Burness et al. 2015). Of note, breast cancers with a high proportion of CSCs correlate with a poor outcome (Pece, Tosoni et al. 2010). Thus, cancer therapy that targets this small subpopulation of cancer cells might be necessary to prevent breast cancer recurrence (Reya, Morrison et al. 2001; Woodward, Chen et al. 2005).

In the next Section, I will describe the process of asymmetric cell division, or ACD, which is considered a unique mechanism employed by stem cells to control tissue homeostasis. Our laboratory recently demonstrated that subversion of this mechanism could cause breast CSCs emergence (Tosoni, Zecchini et al. 2015).

1.2 Asymmetric cell division: a unique "property" of stem cells

1.2.1 Stem cell division

Stem cells can undergo two main types of cell division: symmetric and asymmetric. Symmetric cell division (SCD) produces two identical daughter cells, resulting in an expansion of the stem cell pool. Conversely, asymmetric cell division (ACD) gives rise to two daughter cells with different developmental fates: one daughter cell retains the stem cell identity and the other daughter cell differentiates along a specific lineage. Hence, ACD guarantees both differentiation and stem cell self-renewal, the two hallmarks of stem cells. Different molecular, cellular and environmental cues can influence the choice between symmetric and asymmetric cell division (Berika, Elgayyar et al. 2014). In particular, stem cells divide asymmetrically in response to either intrinsic or extrinsic signals. In the first case, stem cells can set up a polarity axis that is used to localize cell fate determinants asymmetrically at mitosis. The same axis is then used to orient the mitotic spindle and ensure the asymmetric segregation of the determinants in only one daughter cell, which will acquire a different cell fate (Betschinger and Knoblich 2004) (Yu, Kuo et al. 2006). In the latter situation, extrinsic signals from the surrounding environment (e.g., the niche) are essential to maintain the self-renewal abilities of stem cells (Li and Xie 2005). By orienting the mitotic spindle perpendicularly to the niche surface, stem cells can ensure that only one daughter cell loses the contact with the niche and becomes committed to differentiation (***Fig. 4***) (Knoblich 2008). Moreover, while intrinsically determined ACDs usually follow a predefined developmental program, and thus predominate during development, niche-controlled ACDs offer a higher degree of flexibility and, for this reason, are more common in adult stem cells (Knoblich 2008).

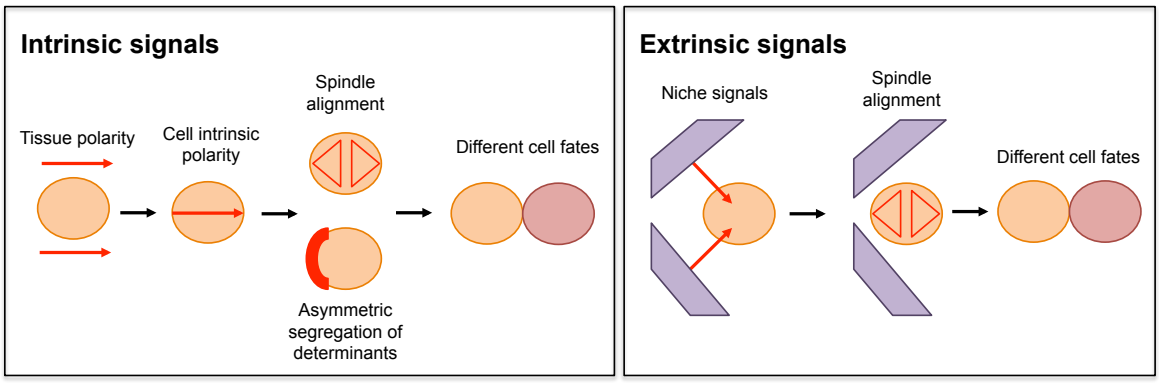

Figure 4. Intrinsic and extrinsic regulation of ACD
In intrinsic regulation of ACD (upper panel), cytoplasmic cell fate determinants are asymmetrically localized and inherited by only one daughter cell. In extrinsic regulation of ACD (bottom panel), instead, daughter cells that loose contacts with the niche are committed to differentiation (adapted from Knoblich, 2008).

I will now focus the attention on intrinsic regulation of ACD and discuss some of the better-described models of this mechanism, from its discovery in the developing nervous system of *Drosophila melanogaster* (*D. melanogaster*) to mammalian adult stem cells.

1.2.2 Asymmetric cell division in invertebrate model systems

Most of the progress in the understanding of ACD has been made in invertebrate systems, such as *D. melanogaster* and *Caenorhabditis elegans* (*C.elegans*). One of the first model systems in which ACD was observed is ***D. melanogaster*** **neuroblasts**, which are embryonic stem cells that delaminate from the ventral neuroectoderm. During embryonic development, neuroblasts divide asymmetrically to generate neurons of the larval nervous system and then become quiescent. During the larval stages, neuroblasts re-enter the cell cycle and divide asymmetrically to generate the neurons of the adult fly brain (Ito and Hotta 1992). Neuroblasts can be divided into two types based on their lineage and localization: type I and type II. Type I neuroblasts divide asymmetrically to produce another neuroblast and a ganglion mother cell (GMC), which divides symmetrically and gives rise to two neurons. Type II neuroblasts generate transit-amplifying populations of self-renewing progenitors, called intermediate neural precursor (INP), which divide

asymmetrically as Type I neuroblasts (Bello, Izergina et al. 2008; Boone and Doe 2008) (Bowman, Rolland et al. 2008). Independently of the type, the mechanisms that regulate ACD are equal in all *D. melanogaster* neuroblasts. In this model, ACD is the result of the unequal distribution and the asymmetric inheritance of cell fate determinants, such as the Numb protein, at mitosis (Buchman and Tsai 2007) (Fuerstenberg, Broadus et al. 1998) (Fishell and Kriegstein 2003) (Knoblich 2008) (Lechler and Fuchs 2005) (Wodarz and Huttner 2003). This mechanism relies on a specific set of proteins that is highly conserved throughout evolution and comprises the Par polarity complex - composed of Par6, Par3 and atypical protein kinase C (aPKC) – the aPKC inhibitor Lgl2 and the mitotic kinase Aurora A (Wirtz-Peitz, Nishimura et al. 2008).

In interphase neuroblasts, aPKC forms an apical complex with Par6 and Lgl2. When mitosis starts, Aurora A phosphorylates Par6, leading to the activation of aPKC and consequent phosphorylation of Lgl2. This phosphorylation reduces the affinity of Lgl2 for Par6 and aPKC, leading to its release from the complex and allowing Par3 to enter it. This subunit exchange initiates the phosphorylation of Numb by aPKC. In particular, Par3, by recruiting the cell fate determinant Numb to the aPKC site, acts as an adaptor between the kinase and its substrate. In this way, phosphorylated Numb is excluded from the apical side of the cell cortex and the unmodified protein is retained in the basal side, resulting in unequal distribution of the protein between the two daughter cells (***Fig. 5***) (Wirtz-Peitz, Nishimura et al. 2008).

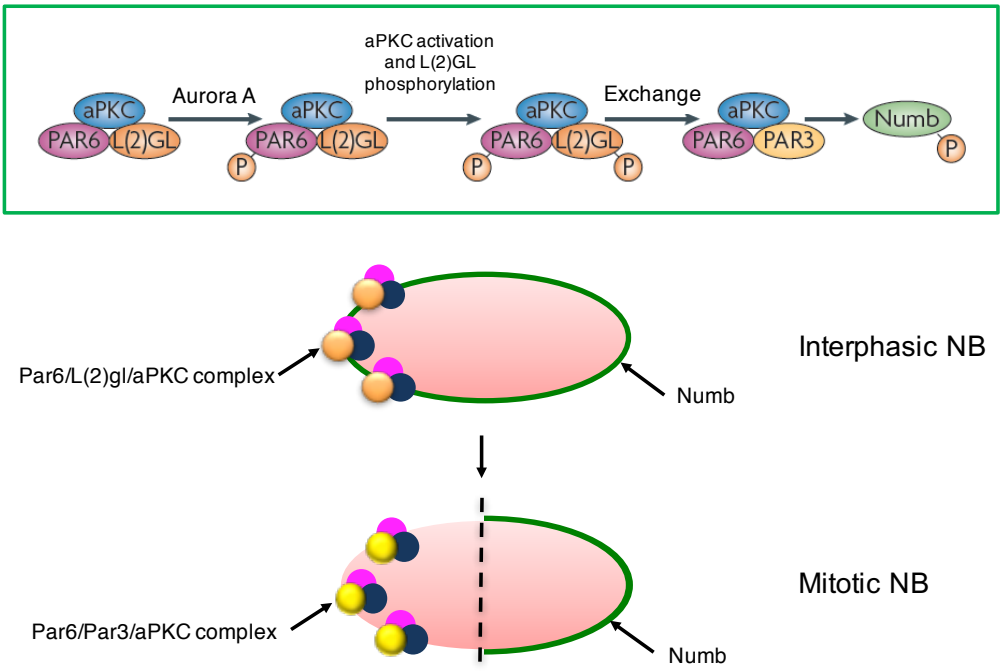

Figure 5. Asymmetric segregation of fate determinants in D. melanogaster neuroblasts
The molecular mechanism of Numb asymmetric segregation has been clearly described in D. melanogaster neuroblasts. At the onset of mitosis, Aurora-mediated phosphorylation of Par6 leads to the activation of aPKC, which in turn phosphorylates Lgl2. This phosphorylation event causes the exclusion of Lgl2 and the recruitment of Par3 in the Par complex. Par3 is responsible for the recruitment of Numb to the same complex so that aPKC can phosphorylate Numb and exclude it from the apical cortex. As a result, Numb accumulates at the basal cortex and it is inherited only by the basal cell (adapted from Knoblich 2010).

During ACD of *D. melanogaster* neuroblasts, the mitotic spindle is aligned with the polarity axis determined by the Par complex and depends on a protein called Inscuteable (Insc) (Kraut and Campos-Ortega 1996). At mitosis, Inscuteable localizes apically by binding to Par3 and recruits two additional proteins called Pins and Gαi into the apical complex. The binding of Pins to Gαi changes the conformation of complex from an inactive to an active state where the N-terminus binds an additional protein called Mud. Mud is a dynein binding protein and provides a docking site for astral microtubules, thus attracting one of the spindle poles to orient the mitotic spindle along the polarity axis (Siller, Cabernard et al. 2006) (Izumi, Ohta et al. 2006) (Bowman, Neumuller et al. 2006).

Additional cell fate determinants have been described in *D. melanogaster* neuroblasts. Prospero, for example, is a homeodomain transcription factor that segregates only in the

GMC and specifies its lineage (Choksi, Southall et al. 2006) (Doe, Chu-LaGraff et al. 1991). Brat is a translational repressor that is required for suppression of neuroblast identity in GMCs, thus promoting differentiation. Staufen is an mRNA binding protein that is responsible for segregating Prospero mRNA in the GMC, boosting the asymmetry between neuroblasts and GMCs (Inaba and Yamashita 2012).

Another important contribution in the field of ACD came from studies in the ***D. melanogaster*** **sensory organ precursor cells**, or SOP cells. These cells generate the four cells that constitute the external sensory organs of the adult fly. Although they are not real stem cells (they cannot self-renew), these cells divide asymmetrically to produce an anterior pIIb and a posterior pIIa cell that ultimately divide to generate the two outer (hair and socket) and the two inner (neuron and sheath) cells that constitute the sensory organ (Bardin, Le Borgne et al. 2004). The external sensory organs are not essential for fly viability, and mutations in cell fate genes generate visible morphological changes in these organs. For these reasons, SOP cells have been useful as a tool to analyze the mechanism of asymmetric cell division (Neumuller and Knoblich 2009). As described for neuroblast cells, also in SOP cells ACD is intrinsically regulated by the unequal segregation of cell fate determinants in only one of the two daughter cells. Numb asymmetric segregation, for example, was first discovered in SOP cells. This cell fate determinant is asymmetrically inherited only in the pIIb daughter cell, where it inhibits Notch signaling (See paragraph 3.1, Section 3, pagg. 27-30) (Rhyu, Jan et al. 1994) (Babaoglan, O'Connor-Giles et al. 2009) (Cotton, Benhra et al. 2013).

Similar to neuroblasts, the Par polarity complex has a conserved role in SOP cells. Here, Par3, Par6 and aPKC are asymmetrically localized at the posterior cortex and their localization follows the planar cell polarity (PCP) of the surrounding epithelium (Bellaiche, Radovic et al. 2001; Besson, Bernard et al. 2015). PCP represents the initial

symmetry-breaking signal that dictates the asymmetric localization of the Par complex. Moreover, in SOP cells, as well as in neuroblasts, aPKC phosphorylation of Numb on three serine residues (7, 276 and 295) seems to regulate Numb subcellular localization (Smith, Lau et al. 2007). Nevertheless, Insc is not expressed in SOP cells, suggesting a different mechanism for spindle alignment in this model (Neumuller and Knoblich 2009).

Recently, a novel population of stem cells has been described in the *D. melanogaster* adult midgut cells (Micchelli and Perrimon 2006) (Ohlstein and Spradling 2006). These cells are called adult **intestinal stem cells (ISCs)** and are located within the intestinal epithelial monolayer, in direct contact with the basement membrane (BM). Upon cell division, the ISCs produce a basal cell, which maintains the contact with the BM, and remains an ISC, and an apical, undifferentiated enteroblast (dos Santos, Rebbeck et al.), which directly differentiates into an enterocyte (EC) or a hormone-secreting entero-endocrine cell (dos Santos, Rebbeck et al.) (Micchelli and Perrimon 2006) (Ohlstein and Spradling 2006).

Recent studies from Goulas and colleagues showed that ISCs use a combination of intrinsic and extrinsic mechanisms to regulate self-renewal (Goulas, Conder et al. 2012). In particular, signals from the extracellular matrix, through integrins, are essential to define the apical localization of the Par polarity complex (Par3/Par6/aPKC) and the alignment of the mitotic spindle along the apico-basal polarity axis, so that the Par complex is inherited only by the apical daughter cell. It is the resulting difference in the amount of aPKC activity in the two daughter cells that seems to be responsible for cell fate specification. In fact, differently from what has been observed in neuroblasts, the overexpression of aPKC in ISCs and EBs inhibits self-renewal and promotes differentiation. These results imply that the cell that inherits the Par complex and aPKC is committed to differentiation (Goulas, Conder et al. 2012). In the same study, Goulas and colleagues demonstrated also that the apical asymmetric segregation of the Par complex is not accompanied by the basal

segregation of cell fate determinants into the opposite daughter cells. Even if the entire machinery for Numb asymmetric segregation is present (as assessed by the basal localization and asymmetric segregation of a Numb-GFP construct), endogenous Numb was not detected in ISCs and mutations in Numb did not cause lineage defects (Bardin, Perdigoto et al. 2010; Goulas, Conder et al. 2012). Hence, ISCs have adopted a mechanism to generate different cell lineages based on the segregation of the Par complex, rather than specific cell fate determinants, between the two daughter cells. The localization of the complex requires integrin-mediated adhesion (an extrinsic signal) in order to orient the mitotic spindle (Goulas, Conder et al. 2012).

The mechanisms that regulate ACD in *C.elegans* and *D.melanogaster* are quite similar, even though some of the players and determinants involved are different. In ***C. elegans***, the first cell division of the **zygote** is asymmetric and produces an anterior AB cell and a posterior P1 cell. In this model, asymmetry is achieved right after fertilization at the entry point of the sperm. The cue generated from the sperm centrosome-pronucleus complex induces the formation of a polarity axis, revealed by the formation of two cortical domains: an anterior domain, composed of PAR3, PAR6, and PKC-3 (the homologue of *D. melanogaster* aPKC) (Goldstein and Hird 1996) (Cuenca, Schetter et al. 2003) (Etemad-Moghadam, Guo et al. 1995) (Hung and Kemphues 1999) (Tabuse, Izumi et al. 1998) and a posterior domain defined by PAR1 and PAR2 (Boyd, Guo et al. 1996) (Cuenca, Schetter et al. 2003) (Guo and Kemphues 1995). These cortical domains are essential for both the orientation of the mitotic spindle and the segregation of specific cell fate determinants (such as MEX1, MEX5 and PIE-I) along the anterior-posterior axis (Knoblich 2010). Moreover, It has been proposed that, due to their cytoplasmic localization, the asymmetric localization of MEX5 and PIE-I in the *C. elegans* zygote is established through a reaction-

diffusion mechanism (Knoblich 2010) (Daniels, Perkins et al. 2009; Daniels, Dobrowsky et al. 2010).

1.2.3 Asymmetric cell division in mammalian model systems

Several examples of ACD have been described also in vertebrate systems, such as the developing mouse forebrain, the mouse epidermis and mouse muscle satellite cells. The mechanisms through which ACD is accomplished, however, are much less clear than in invertebrate systems. Surprisingly, most of the players involved in the regulation of polarity, spindle orientation and cell fate specification in invertebrates are conserved, at least in part, also in vertebrates and in mammals.

Most of what we know about mammalian ACD comes from studies of rapidly dividing **mouse neuroepithelial progenitor cells**. Within the developing mouse brain, cells are organized in a multi-layered structure in which proliferating stem cells are apically localized and face the lumen of the lateral ventricle. Differentiating neurons are instead located on the basal side of the epithelium. During early development, stem cells divide mainly symmetrically to increase the number of progenitors. From embryonic day 10 (E10) progenitor cells start expressing glial markers and become radial glia cells, a specialized type of neuroepithelial progenitors. Glial cells then switch their mode of division from symmetric to asymmetric: one daughter cell retains the progenitor fate and the other migrates towards the basal neuroepithelium and differentiates into a neuron (***Fig. 6***). Alternatively, the more "differentiated" daughter cell can behave as a so-called basal progenitor, which divides symmetrically to give rise to two differentiating neurons (Haubensak, Attardo et al. 2004) (Noctor, Martinez-Cerdeno et al. 2004).

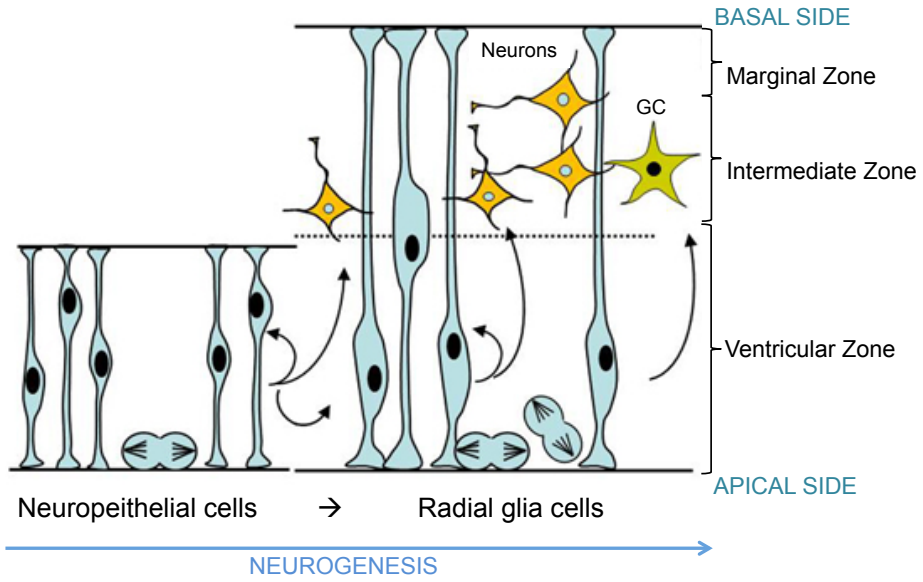

Figure 6. Schematic representation of mouse neurogenesis
Early neuroepithelial progenitors of the ventricular zone initially divide symmetrically to enrich the stem cell pool. At later stages of neurogenesis, neuroepithelial cells become radial glial cells and give rise to both neurons (yellow) and glial cells (green). Radial glia cells can divide either symmetrically, generating two progenitors, or asymmetrically, producing a neural progenitor and a neuron (adapted from (Leclerc, Neant et al. 2012).

Many of the players involved in ACD in invertebrate systems have a conserved role in the mammalian neuroepithelium. For example, spindle orientation in neuroepithelial progenitors requires Gαi, LGN (the mammalian homologue of Pins) and mInsc (the mouse homologue of Inscuteable) (Sanada and Tsai 2005) (Zigman, Cayouette et al. 2005) (Konno, Shioi et al. 2008). When one of these proteins is inhibited or silenced in neural progenitors, the number of vertical, symmetric cell division is increased, suggesting that spindle orientation is required for asymmetric but not symmetric cell division (Knoblich 2010).

As in *D. melanogaster*, Par3/Par6 and atypical PKCs (PKCζ and PKCλ/ι in vertebrates) are apically localized in mouse neuronal progenitors and concentrated at adherens junctions. Upon depletion of Par3 or Par6, progenitor cells are more prone to differentiate, while Par6 overexpression produces increased symmetric divisions (Costa, Wen et al. 2008).

Although many of the molecules involved in ACD are conserved from flies to mammals, the correlation between spindle orientation and cell fate determination in the mammalian neuroepithelium has not been clarified yet. An interesting hypothesis was proposed by Kosodo and colleagues in 2004. In their paper, they show that, at both early and advanced stages of mouse neurogenesis, the switch of neuropeithelial progenitors from proliferative to differentiating divisions is not associated with a rotation of the cleavage plane from vertical to horizontal but to a switch in the relative position of the apical membrane from symmetric to asymmetric in the two daughter cells (Kosodo, Roper et al. 2004). In particular, the apical surface of dividing neuroepithelial progenitors is very narrow, due to their elongated morphology, so that the apical domain can be inherited asymmetrically not only in horizontal but also in oblique divisions, in which the cleavage plane only slightly deviates from the vertical position (Knoblich 2010). This mechanism would explain why most of the dividing cells observed during neurogenesis display a quasi-vertical cleavage plane but give rise to asymmetric divisions. In the same paper, Kosodo and colleagues also show that the polarity protein Par3 is localized at the apical cortex of neuroepithelial progenitor cells, and that it is differentially inherited by the daughter cells arising from neurogenic divisions (Kosodo, Roper et al. 2004).

A more recent paper from Bultje and colleagues sustains this model, proposing that mammalian Par3 protein is asymmetrically inherited at mitosis of neural progenitors. Thus, the cell that inherits the greater amount of Par3 maintains the stem cell phenotype, while the other cell differentiates (Bultje, Castaneda-Castellanos et al. 2009). They also found that asymmetric inheritance of Par3 results in differential Notch signalling activation, which depends on the Numb protein. These findings suggest that asymmetric inheritance of Par3, which was shown to interact with Numb (Nishimura and Kaibuchi 2007), results in differential activation of Notch signalling in the two daughter cells of asymmetrically dividing neural progenitor cells (Bultje, Castaneda-Castellanos et al. 2009).

Although some of the cell fate determinants (e.g., Numb) described in *D. melanogaster* are expressed also in mammalian neuroepithelial progenitors, none of them has been found to behave as a segregating determinant in the mammalian brain. In particular, Numb was initially thought to localize apically in the developing neocortex and this has led to hypothesize that Numb could be asymmetrically inherited during horizontal divisions. Nevertheless, Numb ablation in this system did not affect asymmetric cell division or stem cell maintenance (Kuo, Mirzadeh et al. 2006). An interesting study from Rasin and colleagues in 2007 showed that the real function of Numb in the mammalian neuroepithelium appears to be the regulation of adherens junctions and E-cadherin trafficking (Rasin, Gazula et al. 2007). In neuroepithelial cells, Numb accumulates baso-laterally (and not apically, as previously observed) and regulates epithelial polarity by maintaining the integrity of adherens junctions (Rasin, Gazula et al. 2007).

The mechanism of ACD has also been extensively studied in mammalian adult stem cells. This is exemplified by ACD in the **mouse epidermal stem cells**. These cells are localized in the basal layer of the epidermis, in direct contact with the extracellular matrix (ECM), and divide periodically to sustain tissue homeostasis and repair. Epidermal stem cells use ACD to produce two different daughter cells: one cell that remains in contact with the ECM and maintains the stem cell identity, and another differentiating cell that detaches from the ECM and migrates to become a supra-basal cell. The supra-basal cell stops dividing and forms the external barrier layer of the skin. Similar mechanisms are used to produce skin stratification during embryonic development (***Fig. 7***) (Lechler and Fuchs 2005). Studies from Elaine Fuchs's laboratory provided evidences that asymmetrically dividing epidermal stem cells orient their spindle perpendicularly to the basement membrane, using integrins and cadherins, to attach to the ECM (***Fig. 7***) (Lecher and Fuchs 2005).

As in the case of the neuroepithelium, also in the mammalian skin most of the players involved in ACD are conserved from invertebrates to mammals. For example, the Par complex localizes at the apical cortex of basal epidermal stem cells, opposite to the basement membrane. Gαi, mInsc, LGN and NuMA (the mammalian homologue of Mud) are enriched at the apical cortex in asymmetrically dividing epidermal cells and are essential for perpendicular mitotic spindle alignment to the basement membrane (Lecher and Fuchs 2005). Moreover, Notch signalling has been shown to promote the basal to supra-basal switch, although the involvement of Numb in this process has not been clarified yet (Williams 2011).

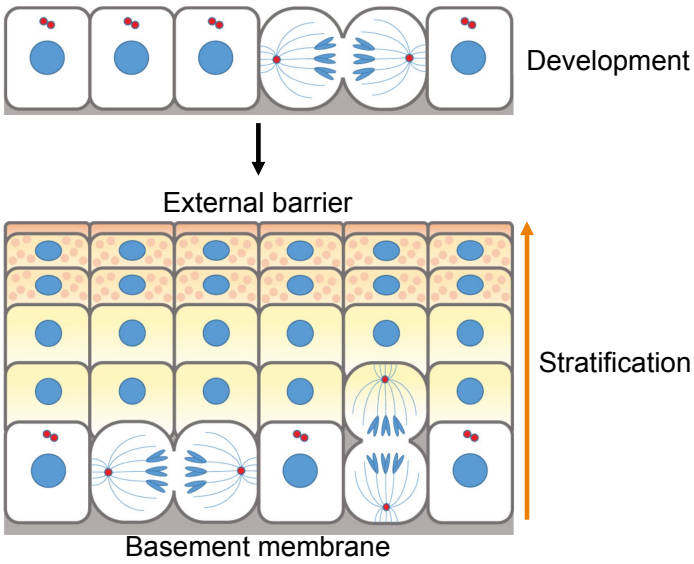

Figure 7. Skin stratification and asymmetric cell division
During early development of the skin, embryonic progenitor cells of the epidermis divide parallel to the basement membrane to enlarge the stem cell pool. As stratification and differentiation progress, epidermal progenitors switch to a perpendicularly oriented division to produce both a basal progenitor cell and a differentiating cell located in the suprabasal layer (adapted from (Kulukian and Fuchs 2013).

An additional example of ACD in adult mammalian stem cells is represented by **muscle satellite stem cells**. This population of cells is essential for the muscle tissue homeostasis and for regeneration upon injury (Cossu and Tajbakhsh 2007). Satellite cells have a precise location within the muscle tissue, which lies beneath the surrounding basal lamina and

outside the myofiber plasma membrane (PM) (Yin, Price et al. 2013). Satellite cells can undergo both symmetric and asymmetric cell divisions and their mode of division is influenced by their interaction with the stem cell niche. Due to their unique expression of Pax7, satellite cells can be easily visualized by immunofluorescence or isolated by FACS sorting, thereby making them a suitable model to study ACD (Knoblich 2010). Indeed, lineage-tracing studies have highlighted that satellite cells are a heterogeneous population of cells. In fact, only a small sub-population of these cells does not express the myogenic transcription factor Myf5 and is referred to as the "real" satellite stem cell population (Kuang, Kuroda et al. 2007). Myf5 expressing cells, which derive from $Myf5^-$ cells, are called satellite myogenic cells and differ from satellite stem cells in terms of regenerative potential. Following transplantation, satellite stem cells are able to reconstitute the stem cell niche and to repair muscle fibers, while satellite myogenic cell are more prone to differentiation (Kuang, Kuroda et al. 2007) (Yin, Price et al. 2013).

The mechanism of ACD in satellite cells is not completely understood. Upon muscle injury, these cells use the Par polarity complex (in particular PKCλ) to asymmetrically activate the p38/MAPK pathway, so that only one daughter cell, the one that inherits higher levels of this signalling pathway, continues to divide and reconstitutes the muscle, while the other cell retreats back to quiescence and repopulates the stem cells pool (Troy, Cadwallader et al. 2012).

Also the Notch signaling pathway plays an important role in satellite cells. When Notch is inhibited, satellite stem cells are not maintained and their differentiation is increased (Luo, Renault et al. 2005). Moreover, the cell fate determinant Numb, which is also a Notch inhibitor, is asymmetrically inherited at mitosis of satellite cells and its overexpression induces differentiation in these cells (Knoblich 2010). Thus, even if a direct demonstration is still missing, Numb could have a conserved role in the specification of cell fate also in the mouse muscle satellite stem cells compartment.

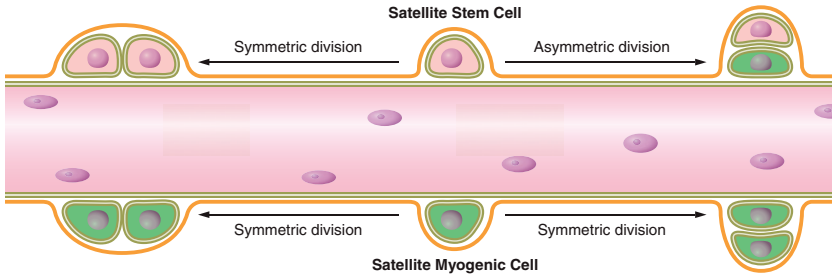

Figure 8. ACD in satellite stem cells
The satellite cell population is heterogeneous. Satellite cells that do not express the myogenic transcription factor Myf5 (satellite stem cells) are placed hierarchically above satellite cells that express Myf5 (satellite myogenic cells). These two populations of satellite cells have different regenerative potential. Upon transplantation, satellite stem cells can contribute to muscle regeneration and reconstitution of the stem cell reservoir, while satellite myogenic cells preferentially differentiate to muscle cells (adapted from Yin et al., 2013).

Asymmetric cell division has also been described in **stem cells of the mammary epithelium**. As previously described (see paragraph 1.2, Section 1, page 3), mouse and human mammary glands are hierarchically organised and are composed of multipotent stem cells, lineage restricted progenitors, and differentiated cells. A work from McCaffrey and Macara identified an essential role for the aPKC-Par3 interaction during end-bud remodelling and mammary gland morphogenesis (McCaffrey and Macara 2009). This study demonstrated that transplantation of Par3-depleted stem/progenitor cells into the mammary fat pad severely affects mammary outgrowth formation and results in hyperplasia and luminal filling. Furthermore, Par3-depleted glands show an expansion of K8+K14+ dual-positive progenitor cells, indicating a role for Par3 in the regulation of the number of mammary progenitors. This work also confirmed the role of aPKC in the MaSCs compartment, as aPKC inhibition also resulted in an expansion of K8+K14+ dual-positive progenitors (McCaffrey and Macara 2009).

On the other hand, a recent study suggests the involvement of Par3L - a protein closely related to Par3 but that cannot bind to Par6 and aPKC - in mammary stem cell maintenance

(Huo and Macara 2014). In this work, the authors demonstrate that Par3L-depletion from the mammary gland results in severe loss of stem cells. The mechanism they propose involves the binding of Par3L to the tumour suppressor protein Lkb1 and the inhibition of its kinase activity (Huo and Macara 2014) (Rejon, Al-Masri et al. 2016). It is, however, still unclear whether Par3L regulates ACD. An intriguing hypothesis would be that, like Par3, Par3L might bind to mINSC, thus controlling ACD through spindle orientation (Rejon, Al-Masri et al. 2016).

In addition, another polarity protein, called Scrib, was shown to have a role in mammary cell fate determination. Mislocalization or loss of Scrib promotes Notch activation and luminal commitment (Feigin, Akshinthala et al. 2014) (Godde, Sheridan et al. 2014). Despite all these studies, further studies are still needed to elucidate the role of cell polarity and polarity proteins in ACD of MaSCs.

In a recent study, Ballard and colleagues identified asymmetrically dividing basal and luminal cells in the mammary end bud of pubertal mammary glands (Ballard, Zhu et al. 2015). In this study, mInsc was reported to regulate the mode of mammary stem cell division. More in detail, the conserved extracellular molecule SLIT2, which interacts with the receptor ROBO1, regulates the expression levels and the localization of mInsc, which is known to play a role in spindle positioning. This regulation depends on the transcription factor SNAI1, whose transcriptional activity is increased by the SLIT2/ROBO1 interaction. Increased SNAI1 activity results in increased expression of mInsc, which in turn causes more basal cap cells within the end bud to divide symmetrically, leading to an expansion of the MaSCs pool and to larger epithelial outgrowths (Ballard, Zhu et al. 2015).

To conclude, our laboratory has recently demonstrated the involvement of the cell fate determinant Numb in the control of cell fate specification of MaSCs (Tosoni, Zecchini et

al. 2015). In these cells, Numb segregates asymmetrically into the cell that retains the stem cell identity, where it sustains high levels of the tumour suppressor p53 (see paragraph 3.4, Section 3, pagg.32-33). In addition, depletion of Numb in the mouse mammary gland leads to an expansion of the stem cell compartment, a phenotype that can be reversed by re-expression of Numb or restoration of p53 activity (Tosoni, Zecchini et al. 2015). Interestingly, aPKCs (ζ and λ/ι) have been shown to phosphorylate Numb *in vitro* and *in vivo* to control its localization in both *D. melanogaster* and mammalian systems (Smith, Lau et al. 2007). Nonetheless, no studies have investigated whether the activity of the Par polarity complex and aPKC has a crucial role in controlling the asymmetric segregation of Numb at mitosis of MaSCs.

Thus, aPKC and the Par polarity complex have been shown to control Numb localization and distribution in different cellular contexts (see Section 2). However, we do not have any knowledge about their possible implication in the process of MaSCs mitosis. These aspects will be investigated in this thesis work.

In the next Section, I will describe the multi-functional profile of Numb, from its discovery as a cell fate determinant to its recent involvement in breast cancer pathogenesis.

1.3 Numb: from cell fate specification to breast cancer

Numb is a 70 kDa protein and is expressed in almost all human tissues (data from the Human Protein Atlas). In cells, this protein is mainly localized at the PM and at vesicular structures of the endocytic pathway.

Structurally, Numb contains different protein-protein interaction domains: a phosphotyrosine-binding (PTB) domain, a proline-rich region (PRR) and Eps15 homology (EH) regions (DPF and NPF). Unlike the *D. melanogaster* Numb gene, the mammalian NUMB gene undergoes alternative splicing to produce four structurally and functionally different Numb isoforms, ranging from 65 to 72 KDa. Alternative splicing involves mainly the PTB and PRR domains. Numb1 (p72) and Numb3 (p71) isoforms (Numb-PRRL) differ from Numb2 (p66) and Numb4 (p65) (Numb-PRRS) by the presence of a large 48-amino acids insert in the PRR region. A smaller 11 amino acid insert in the PTB region, often referred to as "PTB-loop", is present in Numb1 and Numb2 but not in Numb3 and Numb4 (***Fig.9***). Based on their different structure, specific Numb isoforms might have specialized functions (Gulino, Di Marcotullio et al. 2010). Alternative splicing of Numb was recently shown to be developmentally regulated in differentiating P19 cells: Numb1 and Numb3 isoforms (which include the 48-aa fragment) are expressed in progenitors, while Numb2 and Numb4 isoforms are preferentially expressed in differentiated cells (Rajendran, Zhang et al. 2016).

The Numb protein has a multi-functional profile. Since its discovery in 1994 as a cell fate determinant in *D. melanogaster* SOP cells, Numb has been implicated in a number of biochemical functions including endocytosis, determination of cell polarity and ubiquitination (Pece, Confalonieri et al. 2011). These functions will be described in detail in the following paragraphs.

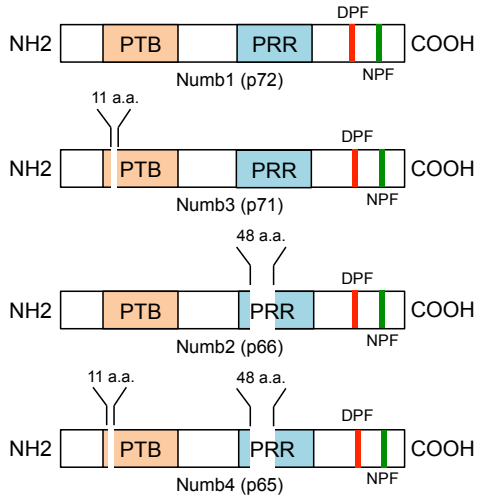

Figure 9. Schematic representation of Numb isoforms in mammals
In D. melanogaster, the NUMB gene encodes for a unique transcript (on the top). In mammalian cells (human, mouse, rat), instead, the Numb gene is alternatively spliced into four different isoforms that differ in the length of their PTB and PRR domain (See the main text for details) (adapted from Gulino, Di Marcotullio et al. 2009).

1.3.1 Numb as a cell fate determinant

The discovery of Numb goes back to 1994 when a pioneering work from the Jan group discovered that loss of Numb in *D. melanogaster* SOP cells results in the loss of external sensory organs and causes flies to become "numb". In this study, they determined that Numb is a membrane-associated protein that is asymmetrically localized in only one half of the dividing SOP cell. During cell division, Numb is thus inherited only by one of the two daughter cells - the pIIb cell - and determines the cell fate of the secondary precursors (Rhyu, Jan et al. 1994). In the same study, the authors demonstrated that Numb is asymmetrically inherited also at mitosis of neuroblast cells during the development of the *D. melanogaster* central nervous system, suggesting a broader role for Numb in asymmetric cell division (Rhyu, Jan et al. 1994). Successive studies confirmed the role of Numb in cell fate specification in additional model systems, such as in *D. melanogaster* muscle stem cells (Ruiz Gomez and Bate 1997), mouse satellite cells (George, Biressi et al. 2013) and mouse mammary stem cells (Tosoni, Zecchini et al. 2015). In all these systems, the asymmetric partitioning of Numb at mitosis is an intrinsic mechanism used to

determine a differential cell fate for the two daughter cells. However, the involvement of Numb in ACD does not appear to be a universal process. There are examples of asymmetrically dividing cells that do not rely on the differential inheritance of Numb (e.g., ISCs in Drosophila) or for which the role of Numb in ACD has not been clarified yet (mouse neural progenitors) (See also Section 2).

1.3.2 Numb and endocytosis

Endocytosis is an energy-consuming mechanism by which a cell can transport big molecules (such as proteins) into its cytoplasm. However, cells often use endocytosis as a tool to internalize portions of the PM and surface receptors in the context of specific signaling pathways. In particular, endocytosis is used for long-term attenuation of signaling cascades, when internalized receptors are destined to degradation into lysosomes through the intracellular endocytic compartments (early and late endosomes) (Pece, Confalonieri et al. 2011). Endocytosis is also relevant during cellular events that require polarization, such as directed cell migration. In these processes, endocytosis is used to selectively recycle specific molecules to restricted regions of the PM (Pece, Confalonieri et al. 2011) (Nishimura and Kaibuchi 2007).

As previously mentioned, the role of Numb in endocytosis is linked to the Notch signalling pathway (paragraph 2.2, Section 2, page 14). During ACD, Numb influences cell fate by antagonizing the Notch receptor. This counteracting influence was initially discovered in *D. melanogaster* SOP cells, and was then confirmed also in *D. melanogaster* neuroblasts and mammalian cells (Guo, Jan et al. 1996) (Spana and Doe 1996) (McGill and McGlade 2003).

The Notch signalling pathway is essential during the development of different organisms due to its roles in cellular differentiation, proliferation and apoptosis (Bray 2006). In the Notch system, signalling proceeds from a signal sending to a signal-receiving cell, which

expresses signal-sending molecules (Delta and Serrate/Jagged trans-membrane ligands) and signal-receiving molecules (the trans-membrane Notch receptors), respectively. When a ligand binds to the Notch receptor, the receptor undergoes a series of proteolytic cleavages that result in the release of a fragment of its C-terminal domain (NICD) into the cytoplasm of the signal-receiving cell. The NICD fragment then translocates to the nucleus, where it activates Notch-specific target genes, such as Hes1 and Hey1 (Pece, Confalonieri et al. 2011).

As mentioned above, the inhibitory role of Numb has been clearly elucidated in *D. melanogaster* SOP cells, where inhibition of Notch by Numb specifies the pIIb cell. In this system, Numb was initially described to interact with α-adaptin, a component of the AP-2 endocytic complex, to regulate Notch internalization (Reichardt and Knoblich 2013). Two recent studies demonstrated that Numb is actually involved in post-internalization and recycling events (Cotton, Benhra et al. 2013) (Couturier, Mazouni et al. 2013). In fact, in asymmetrically dividing SOP cells, Numb binds to the Notch receptor and to a four-pass trans-membrane protein called Sanpodo that is required for Notch signaling in the SOP lineage (O'Connor-Giles and Skeath 2003). Here, Numb acts during post-internalization events: it accumulates with Notch and Sanpodo at sub-apical sorting endosomes, where it inhibits the recycling of the Notch-Sanpodo complexes back to the PM (Cotton, Benhra et al. 2013; Reichardt and Knoblich 2013). Couturier and colleagues also demonstrated that Numb does not play any role in Notch and Sanpodo internalization, but that its role is restricted to post-internalization events (Couturier, Mazouni et al. 2013). The interaction of Numb with α-adaptin appears to be important for the recruitment of Numb and Notch to apical endosomes in dividing SOP cells rather than for Notch internalization (Couturier, Mazouni et al. 2013).

The mechanism of Notch inhibition mediated by Numb is less clear in mammalian cells, where Sanpodo is not conserved (Pece, Confalonieri et al. 2011). In mammalian cells,

Numb can bind the E3 ubiquitin-ligase Itch, which in turn can cause Notch1 ubiquitination and inactivation at the PM. Moreover, it was shown that the overexpression of Numb in this system promotes degradation of the NICD cytosolic fragment but not of the membrane-tethered Notch receptor (McGill and McGlade 2003). Although we are far from understanding the entire process in mammals, it appears that endocytosis and trafficking conserve their role from *D. melanogaster* SOP cells to mammals, even with different molecular players (e.g., absence of Sanpodo) (Pece, Confalonieri et al. 2011).

1.3.3 Numb, cell polarity and cell migration

In the context of a tissue, epithelial cells maintain their proper location and polarization by forming intercellular junctions, such as adherens junctions (AJ) and tight junctions (TJ). AJs are mainly composed of E-cadherin and α/β-catenins, and are connected to the actin cytoskeleton (Harris and Nelson 2010) (Hartsock and Nelson 2008) (Tanos and Rodriguez-Boulan 2008). On the other hand, TJs are maintained by transmembrane proteins (occludins and claudins) and junctional adhesion molecules, and are localized apically in polarized epithelial cells. Occludins and claudins associate with a cytoplasmic plaque that is mainly composed of proteins of the ZO family (Steed, Balda et al. 2010) (Hartsock and Nelson 2008).

TJ assembly is regulated by the Par polarity complex, which includes atypical protein kinase C (aPKC in Drosophila, PKCζ or λ/ι in mammals), Par3 and Par6. Par6 was shown to interact directly with the activated forms of Cdc42 and Rac GTPases, regulating the kinase activity of aPKC during TJ formation (Joberty, Petersen et al. 2000) (Yamanaka, Horikoshi et al. 2001) (Gopalakrishnan, Hallett et al. 2007).

In order to move and migrate, cells have to dissolve tight and adherens junctions, disrupt epithelial polarity, and undergo the so-called “epithelial-to-mesenchymal transition”, or EMT. This event is essential during development, as well as during physiological

processes, such as wound healing. EMT can be induced by different signals, such as the transforming growth factor-β1 receptor (TGF-β1R) or the hepatocyte growth factor receptor (HGF-R). In pathological conditions, such as cancer, cells can adopt this developmental process to acquire motility and form metastasis (Pece, Confalonieri et al. 2011).

The function of Numb in cell polarization and junction formation relies on its ability to interact with several factors implicated in these mechanisms. Numb was shown to directly bind to Par3 and aPKC during directional cell migration of mammalian cells (Nishimura and Kaibuchi 2007). The role of Numb in this process is related to the endocytosis of integrins from the rear to the front of migrating cells, which requires that, Numb interacts with β-integrins and AP-2 at clathrin coated vesicles and it is phosphorylated by aPKC/Par3 to allow integrin recycling at the leading edge of migrating cells (Nishimura and Kaibuchi 2007). Numb phosphorylation on specific serine residues (7, 276 and 295) impairs Numb binding to integrins and AP2 (Nishimura and Kaibuchi 2007).

An additional confirmation of the importance of Numb in epithelial polarity came from the observation that Numb interacts with E-cadherin for the maintenance of AJs in mouse neuronal progenitors (Rasin, Gazula et al. 2007). Moreover, during HGF-induced EMT in MDCK cells, Numb dissociates from E-cadherin and Par3 and associates with aPKC to sequester it from the cytosol (Wang, Sandiford et al. 2009). By using small hairpin RNA (sh-RNA)-mediated knockdown of Numb in MDCK cells, Wang and colleagues further demonstrated that the correct subcellular localization of E-cadherin, β-catenin and the Par3–Par6–aPKC polarity proteins requires the presence of Numb (Wang, Sandiford et al. 2009). In 2011, studies from Kaibuchi's laboratory demonstrated that Numb directly interacts with p120 catenin, which is one of the components of AJs. In this work, they proposed that aPKC phosphorylates Numb to maintain apico-basal polarity in MCF7 cells.

Numb phosphorylation, in fact, prevents its binding to p120 catenin and α-adaptin, and results in reduced E-cadherin endocytosis (Sato, Watanabe et al. 2011).

Finally, a very recent study in renal epithelial cells showed that Numb regulates EMT and E-cadherin adhesion dissolution during renal fibrosis (Ding, Ma et al. 2015). This study demonstrates that loss of Numb correlates with cell phenotypes that are associated with EMT, a highly important process during pathological conditions such as metastatic cancer.

1.3.4 Numb and ubiquitination: focus on the Numb-HDM2-p53 axis

Ubiquitin is a small protein of around 9 KDa, whose name is due to its ubiquitous expression in almost all tissues. The process that adds an ubiquitin molecule to a substrate protein is called ubiquitination (or ubiquitylation) and can affect target proteins in different ways: it can send proteins to the proteasome for degradation, alter their subcellular localization or interfere with their activity (Mukhopadhyay and Riezman 2007). Ubiquitination is a three-step process: activation, conjugation, and ligation, which are performed by ubiquitin-activating enzymes (E1s), ubiquitin-conjugating enzymes (E2s), and ubiquitin ligases (E3s), respectively.

As previously anticipated, Numb can interact with different E3-ubiquitin ligases. For example, Numb interacts with the E3-ubiquitin ligase Itch in mammalian cells to cause ubiquitination and degradation of Notch, thereby inhibiting the Notch signalling pathway. In the same system, overexpression of Numb promotes ubiquitination and proteasomal degradation of the NICD cytosolic fragment (McGill and McGlade 2003).

Interestingly, the same E3-ubiquitin ligase Itch is involved in the regulation of another developmental signalling route, the Hedgehog (Hh) signalling pathway. In this context, Numb was shown to target Itch to the Gli1 transcription factor for degradation, ultimately leading to the inhibition of the Hh signal (Di Marcotullio, Ferretti et al. 2007). Since both Notch and Hh have been implicated in normal developmental programs, as well as

tumourigenesis, it would be interesting to test whether Numb might act as a linker between these two essential morphogenetic pathways, to be validated as a target in pathological conditions.

Another important link between Numb and ubiquitination is represented by the Numb-HDM2-p53 axis. In our laboratory, Colaluca and colleagues demonstrated that Numb interacts with the E3-ubiquitin ligase HDM2, which is responsible for ubiquitylation and degradation of the tumour suppressor p53 (Colaluca, Tosoni et al. 2008). The interaction of Numb with HDM2, through the phosphotyrosine-binding domain (or PTB) of Numb, inhibits HDM2 activity, thereby leading to p53 protein stabilization (Colaluca, Tosoni et al. 2008). The mechanism by which Numb inhibits HDM2 activity is still undefined. Some hypothetical models are indicated in ***Figure 10***: Numb could prevent the interaction between HDM2 and p53 by intercalating between the two proteins; it could bind the p53-HDM2 complex, preventing the conformational changes that are necessary for catalysis; or, Numb could compete with p53 for HDM2 (***Fig. 10***). None of these models has been confirmed yet, although current studies in our laboratory are addressing this issue.

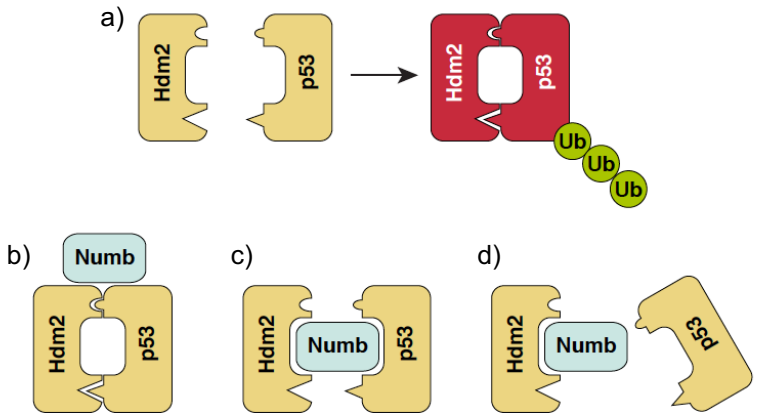

Figure 10. Numb regulation of p53 protein stability
a. *Schematic view of the process of p53 ubiquitination by Hdm2;* ***b-d.*** *Possible models of Numb inhibition of HDM2.* ***b,*** *Numb binds to the Hdm2/p53 complex, preventing the conformational changes required for catalysis.* ***c,*** *Numb localizes between p53 and HDM2, abolishing their binding.* ***d,*** *Numb competes with p53 for Hdm2. (taken from Colaluca et al. 2008).*

1.3.5 Numb and cancer

As anticipated in the previous paragraph (see paragraph 3.4, Section 3), Numb is considered a tumour suppressor. The first evidence for this function was described in *D. melanogaster*, in which Numb depletion from larval neuroblasts produces over-proliferation of self-renewing stem cells and tumour formation (Lee, Andersen et al. 2006) (Caussinus and Gonzalez 2005). Since then, Numb deficiency has been linked to a list of different human diseases, from neurodegenerative diseases to different types of human cancers (Pece, Serresi et al. 2004; Kyriazis, Wei et al. 2008) (Westhoff, Colaluca et al. 2009) (Ito, Kwon et al. 2010).

The link between Numb and tumour suppression can be easily explained by the multiple biological and biochemical functions exerted by Numb. In the absence of Numb, both Notch and Hh signaling pathways are boosted, while the TP53 signaling is attenuated, thus promoting cell proliferation and inhibiting apoptosis. Moreover, depletion of Numb could result in alterations of the endocytic machinery, which itself represents a tumour suppressor mechanism (Lanzetti and Di Fiore 2008) (Vaccari and Bilder 2009) (Polo, Pece

et al. 2004). In addition, the role of Numb in cell polarity and EMT has recently been demonstrated to contribute to cancer transformation events. More precisely, ablation of Numb has been associated with EMT, which is a strategy adopted by tumour cells to acquire motility, invasiveness and resistance to chemotherapy (see paragraph 1.3.3) (Singh 2010; Thiery 2009).

Finally, the involvement of Numb in cell fate specification raises the possibility that Numb could exert a tumour suppression function also by controlling stem cell homeostasis and preventing the emergence of CSCs. Contributions to this theory come from the finding that p53 (whose levels are surveyed by Numb) regulates the polarity of cell division in mammary SCs. Loss of p53 results in an increase of CSCs in breast cancer model systems due to augmented symmetric cell division (Cicalese, Bonizzi et al. 2009). Recent studies from our laboratory demonstrate that depletion of in Numb MaSCs associates with low p53 levels and results in the expansion of the stem cell compartment and in the emergence of CSCs (Tosoni, Zecchini et al. 2015). In detail, MaSCs were isolated as $PKH26^{pos}$ cells from mammospheres (see paragraph 1.3, Section 1, page 6) and this was used as an "ex-vivo" system in combination with transplantation assays to characterize the role of Numb in MaSCs homeostasis and polarized cell division. In asymmetrically dividing MaSCs, Numb is inherited only by the cell that retains the stem cell fate, which can be recognized as the cell that does not dilute the PKH26 dye and thus re-enters quiescence (Tosoni, Zecchini et al. 2015) (Cicalese, Bonizzi et al. 2009). Furthermore, in a mouse model of conditional Numb knockout (KO) in the mammary, Numb depletion resulted in hyperplasia and aberrant lineage specification, supporting the idea that loss of Numb is associated with aberrant mammary morphogenesis *in vivo*. This phenotype was associated with the expansion of the stem cell compartment in these glands and with the emergence of CSCs with unlimited proliferation and self-renewing potential. The mechanism proposed to explain these phenotypes involves the tumour suppressor p53, as low levels of Numb

were associated with low p53 levels and an increase in SCDs (***Fig.11***) (Cicalese, Bonizzi et al. 2009). Of note, Nutlin3, an inhibitor of p53 degradation, rescues the abnormal phenotype displayed by Numb-KO cells, confirming that Numb acts by regulating p53 activity in mammary cells (Tosoni, Zecchini et al. 2015) (Faraldo and Glukhova 2015). Remarkably, depletion of Numb was also accompanied by induction of EMT (up-regulation of Snail, Slug, and Sox9 transcription factors) and by reprogramming of progenitors and differentiated cells to a stem cell–like state (Guo et al., 2012). These data indicate that the role of Numb might not be restricted only to MaSCs but also to the progenitor compartment, where Numb appears to be re-expressed and to suppress EMT, ensuring the proper maturation of luminal cells (***Fig.11***) (Tosoni, Zecchini et al. 2015) (Faraldo and Glukhova 2015).

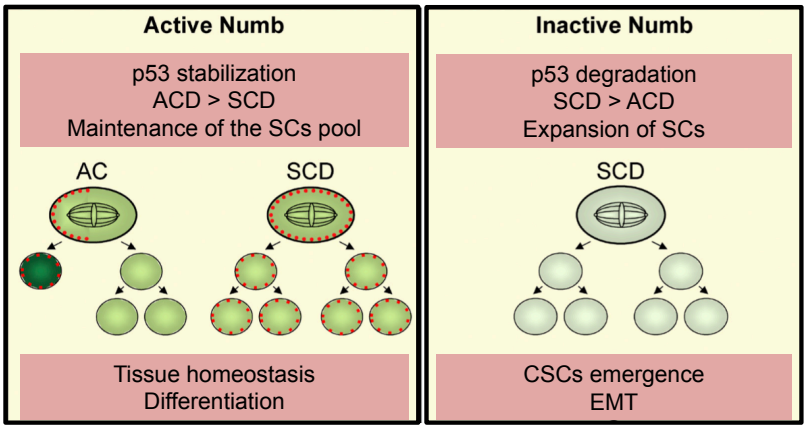

Figure 11. Role of Numb in the homeostasis of the mammary stem cell compartment
Left panel: In the bi-layered mammary epithelium, Numb (red dots) expression is found in all luminal (L) and rare basal (B) cells. Upon ACD, Numb segregates in the cell that retains stem cell fate, where it prevents p53 (dark green) degradation. In the normal mammary epithelium, ACDs prevail on SCDs, maintaining the stem cell pool and gland homeostasis. SCDs prevail in luminal progenitors where Numb suppresses EMT.
Right panel: In the absence of Numb, p53 is degraded and SCDs are increased. This increase results in the expansion of the stem- and progenitor pool, and the activation of the EMT program, leading to hyperplasia and tumourigenesis (taken from Faraldo and Glukhova, 2015).

Rationale of the project

The homeostasis of tissues and organs depends on the ability of adult stem cells to undergo asymmetric, self-renewing cell divisions (ACDs), in which one of the two daughter cells (DCs) retains the stem cell fate and withdraws into quiescence, while the other DC assumes a progenitor fate, characterized by mitotic expansion and subsequent terminal differentiation. Subversion of these mechanisms could result in the malignant transformation of a stem cell into a cancer stem cell.

One of the most relevant mechanisms aimed at controlling cell fate specification is the mechanism of unequal segregation of cell fate determinants, such as Numb, into the two DCs. In the *D. melanogaster* developing nervous system, Numb is asymmetrically inherited during ACD of both neuroblasts and sensory organ precursor cells (SOPs) (Jan and Jan 2001). More precisely, Numb is inherited by the differentiating daughter cell, in which it inhibits the Notch receptor signalling pathway and promotes differentiation. The molecular machinery that governs the asymmetric distribution of Numb in *D. melanogaster* neuroblasts has been characterized. The localization of Numb in *D. melanogaster* neuroblasts is regulated by the activity of the evolutionarily conserved Par Polarity complex (Par3/Par6/aPKC) together with the mitotic kinase Aurora A. The aPKC-mediated phosphorylation of Numb regulates its membrane localization, causing its exclusion from the apical cortex, where the Par complex is localized, and, instead, retaining it on the basal side of the membrane. Numb is, thus, inherited only by the basal DC (Wirzt-Peitz, Nishimura et al. 2008).

The role of Numb in ACD has also been described in mammalian systems, such as muscle satellite cells and mammary stem cells (Tosoni, Zecchini et al. 2015). Recent studies from our laboratory have pointed to a key role for Numb in maintaining the homeostasis of the mammary stem cell compartment. More precisely, in mammary adult stem cells, Numb segregates asymmetrically into the cell that retains the stem cell identity, where it sustains the activity of the tumour suppressor p53. In this context, Numb is able to bind to both p53 and the E3-ubiquitin ligase HDM2, resulting in the inhibition of p53 degradation (Colaluca, Tosoni et al. 2008). Loss of Numb in the mammary stem cell compartment causes decreasing levels of p53 and leads to the emergence of cancer stem cells (Tosoni, Zecchini et al. 2015). These finding are in line with previous observations that p53 regulates the homeostasis of the mammary stem cells by ensuring self-renewing divisions (Cicalese, Bonizzi et al., 2010).

There are evidences that the mechanisms underlying Numb asymmetric partitioning at mitosis are evolutionarily conserved from *D. melanogaster* to mammals. In mammalian cells, Numb is phosphorylated by several PKC enzymes (including PKCζ, the mammalian homologue of *D. melanogaster* aPKC) (Smith, Lau et al. 2007). Moreover, the interaction of mammalian Numb with Par3 and PKCζ is essential during mammary gland morphogenesis, as well as during integrin-mediated directed cell migration (Nishimura and Kaibuchi 2007) (McCaffrey and Macara 2009).

To our knowledge, no studies have identified the molecular machinery responsible for Numb asymmetric distribution at mitosis of mammalian cells.

Based on this knowledge, the main aim of this thesis work was to dissect the upstream events involved in controlling Numb asymmetry in the mammary stem cell compartment. In particular, we intended to address the role of the Par polarity complex and, specifically, of the PKCζ isoform in the regulation of Numb phosphorylation and their function in determining Numb subcellular localization and segregation. Moreover, we hypothesized that Numb phosphorylation by PKCζ could impact on the binding with p53, thus contributing to its role in the regulation of the polarity of mammary stem cell division.

Although not addressed here, it is important to note that both PKCζ and PKCι (another atypical PKC in mammals) are frequently amplified in breast cancer (CBioportal). This observation raises the possibility that dysfunction of the mechanisms that regulate Numb asymmetry could contribute to breast tumourigenesis and therefore represent a possible therapeutic target to fight the emergence of breast cancer stem cells.

Chapter 2

Materials and methods

2.1 Materials

2.1.1 Solutions

Phosphate-buffered saline (PBS)

NaCl	137mM
KCl	2.7mM
Na_2HPO_4	10mM
KH_2PO_4	2mM

8 g of NaCl, 0.2 g of KCl, 1.44 g of Na2HPO4, and 0.24 g of KH2PO4 were dissolved in 800 ml of distilled water. The pH was adjusted to 7.4 with HCl and the volume was brought to 1 litre with distilled water.

Tris-buffered saline (TBS)

NaCl	137mM
KCl	2.7mM
Tris HCl, pH7.4	25mM

8 g of NaCl, 0.2 g of KCl and 3 g of Tris base were dissolved in 800 ml of distilled water. The pH was adjusted to 7.4 with HCl and distilled water was added to bring the volume up to 1 litre.

10X SDS-PAGE running buffer

Glycine	192mM
Tris HCl, pH 8.3	250mM
SDS	1%

TAE (Tris-Acetate-EDTA) 50X

Glycine	192 mM
Tris HCl, pH 8.3	250 mM
Tris base	2M
Acetic acid	1M
EDTA, pH 8	10 mM

Distilled water was added to bring the volume up to 1 litre and the pH was adjusted to 8.5 with HCl.

2.1.2 Protein buffers

RIPA Buffer 1X

Tris HC, pH7.6	50mM
NaCl	150mM
NP-40	1%
SDS	0,1%
Sodium deoxycholate	0.5%
EDTA	1mM

JS Buffer 1X

HEPES, pH7.4	50mM
NaCl	150mM
Glycerol	10%
Triton X100	1%
$MgCl_2$	1.5mM
EGTA	5mM

500X Proteases inhibitor cocktail (Calbiochem) and 10X Phostop Phosphateses inhibitor (Roche), were added to the buffer just before use.

Ponceau

Ponceau	0.1% (w/v)
Acetic acid	5%

Laemmli buffer 1X

SDS	2%
Tris HCl, pH6.8	62.5mM
Bromophenol blue	0.1%
Beta-mercapto-ethanol	5% (v/v)
Glycerol	10%

SDS-PAGE sample buffer was prepared as 5X stock solution and stored at -20°C, protected from light.

2.1.3 Plasmids

The following constructs were used:

- pLKO.1-shCtrl, pLKO.1- shPar3 (Clone ID: TRCN0000094401) and pLKO.1-shPKCζ (Clone IDs: TRCN0000001220, TRCN0000010121 and TRCN0000010112) were purchased from Dharmacon;
- pLV-Venus and pLV-PKCζ-Venus lentiviral vectors were a kind gift from K.Kaibuchi;
- The pLVX.PURO-Numb-dsRed (FL) construct was previously produced in our lab (Tosoni, Zecchini et al., 2015);
- The pLL3.7-Numb FLAG (FL) construct was previously produced in our lab (Colaluca, Tosoni et al. 2008). It contains an shRNA sequence for endogenous Numb (5'-GGTTAAGTACCTTGGCCATGT-3') together with a sh-resistant sequence encoding for Numb-FLAG.
- The Numb-3A and -3D mutants were produced by PCR-based site directed mutagenesis of the pLVX.PURO-Numb-dsRed (FL) construct (see "Methods").
- The pLL3.7-Numb FLAG 3D mutant was produced by PCR-based site-directed mutagenesis on the pLL3.7-Numb FLAG (FL) construct (see "Methods").
- The pLVX.PURO-Numb ΔPTB and the pLL3.7-Numb FLAG ΔPTB plasmids were available in the lab (and were produced by PCR-mediated deletion with phosphorylated primers).

All constructs were sequence verified.

2.1.4 Chemicals

TPA (Phorbol 12-myristate 13-acetate) was purchased from Sigma-Aldrich and used at 1 μM. PKH26(red) and PKH488(green) were purchased from Sigma-Aldrich.

2.1.5 Antibodies

The following antibodies were used:

- *Immunoblot*: anti-Numb (AB21, homemade, 1:1000); anti-Numb phospho-Ser276 (Cell Signalling Technology, 1:1000); anti-Par3 (Millipore, 1:500); anti-PKCζ (C20, Santa Cruz Biotechnology, 1:500); anti-p53 (FL-393, Santa Cruz Biotechnology, 1:500); anti-α adaptin (AP2) (Santa Cruz Biotechnology, 1:1000); anti-Vinculin (Sigma Aldrich, 1:1000), anti-GRP94 (9G10, Santa Cruz Biotechnology, 1:1000), anti-Flag (Cell Signalling Technology, 1:1000); anti-mouse or anti-rabbit HRP-conjugated IgG (Cell Signalling Technology, 1:10000), anti-goat HRP-conjugated IgG (Santa Cruz Biotechnology, 1:10000).
- *Immunofluorescence*: anti-Numb (AB21, homemade, 1:1000), anti-mouse Alexa647-conjugated secondary antibody (1:400, Amersham).

2.2 Methods

2.2.1 Cloning techniques

PCR-based site-directed mutagenesis

Point mutations of Numb at Ser7, 276 and 295 were performed by PCR-based site-directed mutagenesis on the pLVX-PURO-Numb-dsRed / pLL3.7-Numb-FLAG wild-type constructs. Primers were designed on QuikChange Primer design Tool (Agilent Technologies, http://www.genomics.agilent.com/primerDesignProgram.jsp) by loading Numb-FL FASTA sequence (HGNC:HGNC:8060) and selecting the corresponding amino acid on the sequence. The PFU-Turbo enzyme (Agilent Technologies) was used, following manufacturer's instructions. For PCR amplification, the following protocol was used: 45'' 95°C, (1' 95°C, 1' 58°C, 13' 72°C) x 18 cycles, 5' 72°C. 5 µL of purified PCR product were used to transform 50 µL of TOP10 E.coli bacteria. Positive colonies were selected on LB-Agar with Ampicillin (50 µg/mL, Sigma-Aldrich). All fragments were confirmed by DNA sequencing.

Minipreps

Individual colonies were used to inoculate 3 ml LB (containing the appropriate antibiotic) and grown overnight at 37°C. Bacteria were transferred to Eppendorf tubes and centrifuged for 5 minutes at 16,000*xg* using a 5415 R centrifuge. Minipreps were performed with the Wizard Plus SV Minipreps Kit (Promega) following manufacturer's instructions. The plasmids were eluted in 30 µl nuclease free water.

Transformation of competent cells

An aliquot of competent cells TOP10 (Invitrogen) was thawed on ice for approximately 10 minutes prior to the addition of plasmid DNA. Cells were incubated with DNA on ice for 30 minutes and then subjected to a heat shock for 45 seconds at 42°C. Cells were returned to ice for an additional 5 minutes. Then, 900 µl of LB medium was added and the cells were left at 37°C for further 60 minutes before plating them onto agar plates with the appropriate antibiotic. Plates were incubated overnight at 37°C.

Large-scale plasmid preparation

Cells containing transfected DNA were expanded into 250-600 ml cultures overnight. Plasmid DNA was isolated from these cells using the Machery-Nagel Xtra Maxi-prep kit according to manufacturer's instructions.

Agarose gel electrophoresis

DNA samples were loaded on 1% agarose gels along with DNA markers (1 kb DNA Ladder, Promega). Gels were made in TAE buffer containing Gel Red (Biotium), according to manufacturer's instructions, and run at 100 V until desired separation was achieved. DNA bands were visualized under a UV lamp.

2.2.2 Cell culture

Cell culture media and cell lines.

We used the following mammary cell lines: MCF10A, Comma Dβ, ZR-75-1, ZR-75-30, AU565, HCC1569, MDA-MB 231, MDA-MB 453, SUM159, MDA-MB 175 VII, T47D, BT20.

MCF10A cells were cultured in DMEM:F12 medium (Invitrogen) 1:1, 5% Horse Serum (Invitrogen), Hydrocortisone (0.5 mg/mL, Sigma-Aldrich), Cholera toxin (100 ng/mL, Sigma-Aldrich), Insulin (10 µg/mL, Boehringer-Mannhaim), EGF (20 ng/mL, Vinci-Biochem).

Comma Dβ cells were cultured in RPMI1640 (Lonza), 5% Fetal Calf Serum (Bio-Whittacker), Insulin (5 µg/mL), HEPES (10 mM, Cell Biology Unit), EGF (20 ng/mL).

ZR-75-1, ZR-75-30, AU565 and HCC1569 cell lines were grown in RPMI 1640 (Lonza) supplemented with 10% NA Fetal Bovine Serum (FBS, Hyclone) and L-Glutamine (2 mM, Microtech). MDA-MB 231 cells were cultured in DMEM (Lonza) supplemented with 10% SA FBS (Biospa) and L-Glutamine (2mM). MDA-MB 453 were cultured in Leibovitz's L15 medium+Glutamax (Invitrogen) supplemented with 10% SA FBS. SUM159 cells were grown at 10% CO_2 in Hams' F12 95% (Life Technologies) supplemented with 5% NA FBS, L-Glutamine (2mM), Insulin (5 µg/mL), Hydrocortisone (1 µg/mL) and HEPES (10mM). MDAMB175 VII were cultured at 0% CO_2 in Leibovitz's L15 medium+Glutamax (90%, Invitrogen) supplemented with 10% NA FBS. T47D cells were grown in DMEM (90%, Lonza) supplemented with 10% NA FBS and L-Glutamine (2mM). BT-20 cells were cultured in MEM with Earl's Salts (90%, Life Technologies) supplemented with 10% NA FBS, L-Glutamine (2mM), Sodium Pyruvate (1mM), Non-essential amino acids (0.1mM).

HEK293T (Human Embryonic Kidney) cells were grown in DMEM 90%, supplemented with 10% SA FBS and L-Glutamine (2mM). These cells were used as packaging cells for lentivirus production.

2.2.3 Purification of primary cells:

Mammary epithelial cells (MECs) and Mammary stem cells (MaSCs)

FVB/Hsd mice

FVB/Hsd mice (Taketo, Schroeder et al. 1991)were used to isolate mammary epithelial and stem cells. This specific mouse strain was chosen due to its vigorous reproductive performance with large litters, that allows the explant of considerable amounts of breast tissue (Taketo et al, 1991).

Enzyme Digestion Mixture (EDM)

EDM was obtained from a solution of DMEM + Hams' F12 medium (1:1 ratio) supplemented with Insulin (1 µg/mL), Hydrocortisone (1 µg/mL) and L-Glutamine (2 mM). EDM was sterilized through a 0.2- µm vacuum filter unit and stored at 4°C until needed. Immediately before use, EGF (10 ng/mL), Collagenase type 1A (200 U/mL, Sigma) and Hyaluronidase (100 U/mL, Sigma) were added. EDM was pre-warmed at 37°C in a water bath before adding it to sample tissues.

Mammary Epithelial Stem Cell Medium (MESCM)

MEBM Basal Medium (Lonza) was supplemented with L –Glutamine (2 mM), Insulin (5 µg/mL), Hydrocortisone (0.5 µg/mL) and Heparin (1 U/mL, Wockhardt) (Dontu, Al-Hajj et al., 2003) (Tosoni, Di Fiore et al. 2012).

The complete MESCM medium was obtained by adding EGF (20 ng/mL), FGF (20 ng/mL, Peprotech), and B-27 Supplement (2%, Gibco) immediately before use.

B-27 is a serum-free supplement typically used in research for growth and long-term

viability of hippocampal neurons. The selection of its components makes B-27 successfully suitable for mammary epithelial and SCs research.

The complete medium was sterilized by filtering through a 0.2-µm filter before adding it on cells.

Sphere culture Supports

To obtain suitable supports for cell suspension culture, low adhesion plates were prepared using Non-Tissue culture treated flat bottomed plates (Falcon). These plates were doubly coated with an inert, chemically stable, non-toxic polymer named Poly-HEMA (2-hydroxyethylmethylmethacrylate) (Sigma).

A stock concentration (12%) Poly-HEMA solution was prepared by dissolving 25 g of Poly-HEMA crystal powder in 208 mL 95% ethanol overnight at 55°C under mechanical shaking. The stock solution was diluted 1:10 with 95% ethanol and sterilized through a 0.2-µm filter. The second bottom plate coating was applied only when the first volume of Poly-HEMA had completely dried (generally overnight).

Tissue collection, digestion and isolation of MECs

Five weeks-old female FVB/Hsd mice were used to collect both axillary and inguinal mammary glands. The explant was done under sterile hood and the fur was carefully disinfected before opening the carcass. Groups of 5 animals, for a total number of 20 mice per preparation, were used.

This particular age (5 weeks) was chosen since from 4 to 6 weeks of life, mice undergo puberty and their mammary tissue is enriched in SCs.

Collected mammary tissues (axillary and inguinal) were minced by sterile scissors into ~1−2 mm^3 pieces, immediately re-suspended in 10 mL pre-warmed EDM and incubated at 37°C in a 5% CO_2 humidified incubator for 4 hours. The tissue-EDM mixture was re-suspended up and down with a pipette (~5–7 times) every 20–30 minutes, to help tissue

dissociation or until all large fragments are digested.

The digested tissue suspension was then transferred in conical bottomed tubes and centrifuged at 80 x g for 5 minutes, at RT. This step of differential centrifugation allows the separation of stromal cells (mostly fibroblasts and endothelial cells) and fat tissue, which remain in the supernatant, from the epithelial fraction of the mammary tissue. The latter is composed of both single primary mammary epithelial cells (MECs) together with large clusters of partially digested epithelial tissue, we refer to as "organoids".

After that, the supernatant was carefully removed eliminating fat residues and stromal cells and the pellet was gently re-suspend in 10 mL DMEM supplemented with 2 mM L-Glutamine.

To yield a homogeneous single cell suspension, the material was then sequentially filtered, by using cell strainers (BD Falcon) of decreasing pore sizes. The first 100 µm cell-strainer retained gross digestion residues together with fur or possible muscle and skin fragments. The 100 µm-filtered suspension was sieved as first in 70 µm and than in 40 µm cell-strainer. Pure organoids were retained in the strainers during these steps, and were recovered in later phases. The last filtration with a 20 µm cell-strainer finally eliminates the digestion residues such as groups of aggregated cells. In this way, a single-cell suspension of MECs is obtained.

Blood cells are typically small sized and go through all the steps of filtration. To remove them, a hypotonic 0.2% NaCl solution was used for 45 seconds to induce a volume shock. To avoid any damage on the MECs population the physiological conditions were restored with the addition of a 1.6% NaCl solution.

After red blood cells lysis, MECs were thereby centrifuged at 1200 rpm for 5 minutes and then re-suspended in 10 mL complete MESCM. At this stage, the cell suspension typically contains ~2 x 10^6 cells/ ml (Cicalese, Bonizzi et al., 2009) (Pece, Tosoni et al., 2010).

MECs purification from organoids

In alternative to SCs purification, MECs for other purposes were obtained from the 70 and 40 μm organoids recovered during the filtration steps. These organoids were collected by washing the 70 and 40 μm strainers with complete MESCM medium, supplemented with 2% SA FBS (Biospa). The re-collected material was seeded on cell-culture treated plates, to let cells adhere to the bottom. After 48 hours, the organoids had spread onto the bottom of the plate and adhered MECs could be used for further analysis (lentiviral infection, WB, IF). We have to underline that MECs obtained with this procedure are, actually, differentiated cells, that represent a bulk population of mammary epithelial cells.

Mammosphere assay

Notwithstanding the accuracy of the purification procedure, a certain amount of contaminant cells (such as fibroblasts) remained in the MECs suspension. To remove this undesired fraction, we seeded MECs on Non-tissue culture treated supports to allow the adhesion of contaminants. One week of culture within these specific supports was sufficient to allow the isolation of pure MECs, which remained in suspension and we called the F0 generation of mammospheres (Cicalese, Bonizzi et al., 2009) (Pece, Tosoni et al., 2010).

After one week, F0 mammospheres were collected and enzymatically dissociated in pre-warmed 0.05% trypsin/0.5 mM EDTA for 10 minutes, plus filtering through a 40 μm cell strainer. Single cells were then counted and re-plated at 10^5 cells/mL in complete MESCM medium, on Poly-HEMA coated plates. Plates were incubated for 1 week at 37°C and 5% CO_2 to allow the formation of the first generation of mammospheres (F1). After 1 week the dissociation and replating procedure was repeated to produce the second generation of mammospheres (F2) (Cicalese, Bonizzi et al., 2009) (Pece, Tosoni et al., 2010).

In this study we didn't go beyond the F2 generation of mammospheres. In particular, we used F1 generation mammospheres for PKH labelling and lentiviral infections. F2 generation mammospheres formation was visualized instead in most of our Time Lapse video-microscopy experiments.

PKH-labelling

In this study we used two different PKH labelling dyes, PKH26 (red epifluorescence) or PKH2-GL (PKH488, green epifluorescence), both purchased from Sigma-Aldrich.

For PKH staining, F1 generation mammospheres were harvested, enzymatically dissociated and counted with a Burker chamber. Up to 10^7 cells were re-suspended in sterile PBS 1X (Lonza) and mixed with an equivalent amount of a 1:5000 dilution of PKH in PBS 1X (PKH final dilution 1:10000, that corresponds to 10^{-7} M). The mix was incubated for 5 minutes at RT in dark. After that, cells were pelleted at 1200rpm for 5 minutes and re-suspended in complete MESCM. Re-suspended cells were seeded at 5.000 cells/mL on Poly-HEMA coated 6-well-plates, to form the F2 generation of mammospheres. After 7 days, the dissociation procedure was repeated on F2 spheres and PKH positive cells were isolated by FACS (Fluorescence-activated cell sorting) assay (Cicalese, Bonizzi et al., 2009) (Pece, Tosoni et al., 2010).

FACS analysis for the isolation of PKH^{high} MaSCs

For FACS analysis we used the Vantage SE flow cytometer (Becton&Dickinson) equipped with an argon ion laser tuned to 488 nm (Enterprise Coherent) and a band-pass 575/26 nm optical filter (FL2 channel).

Single-cell suspensions from disaggregated PKH-labelled mammospheres were re-suspended in L-15 medium with 0.1% EDTA at a concentration of around 3 x 10^6 cells /

ml and subjected to FACS sorting. An average sorting rate of 800-1000 events per second at a sorting pressure of 20 PSI was maintained.

Mammary stem cells were purified as the top bright epifluorescent cells (PKH^{high}), which represent around 0,2-0,4% of the entire population sorted. The cut-off value considered to identify the PKH^{high} region in FACS output data was defined, for each experiment, according to the calculated percentage of SCs in the mammospheres (Cicalese, Bonizzi et al. 2009) (***Fig. 12***). This value depends on sphere dimensions and the expected sphere forming efficiency (SFE) of each experiment (see Tosoni, Di Fiore et al. 2012 for further details).

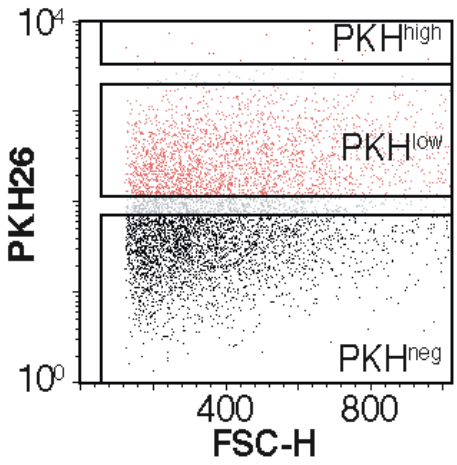

Figure 12. Representative FACS-distribution of PKH cell subsets from mammospheres
Dissociation of PKH stained mammospheres leads to a heterogeneous distribution of stained cells. PKH^{high}, PKH^{low} and PKH^{neg} cells can be separated. Only PKH^{high} cells represent true MaSCs.

2.2.4 Lentiviral infection

Transfection of HEK293T packaging cells

On day one, HEK293T packaging cells were plated in 10 cm plates at $5x10^6$ cells/plate. In the evening, the medium was replaced by 9 ml of complete medium and 1 ml of transfection mix.

Transfection mix was prepared as follows:

- mix 1: 500 µl of HBSS 2X;
- mix 2: 10 µg Lentiviral DNA construct (pLVX, pLV-Venus, pLL3.7 or pLKO.1 constructs), 2.8 µg ENV, 5 µg pMDL, 2.5 µg REV, 62.4 µl $CaCl_2$ 2M, sterile TE 0.1X up to 500 µl.
- Transfection mix: mix2 was added to bubbling mix1 and incubated 5 minutes at room temperature before use.

On day 2, the cell supernatant was replaced with 5ml of fresh HEK293T cell medium, to achieve a higher virus concentration.

For the infection of primary cells, the cell supernatant was replaced with 5ml of either fresh MESCM with 2% B27 and 2% NA FBS (for the infection of MECs in adhesion) or fresh MESCM with 2% B27 alone (for mammosphere cells infection). In both cases FGF and EGF were not included in the medium and were added only at the moment of the infection.

Lentiviral infection of MCF10A and MDA MB 231 cells

MCF10A were transduced with pLV-Venus, pLV-PKCζVenus, pLL3.7-Numb FLAG (FL), pLL3.7-Numb3D FLAG and pLL3.7-NumbΔPTB FLAG. MDA MB 231 cells were

transduced with pLKO.1 shCtrl, pLKO.1-shPKCζ #1, pLKO.1-shPKCζ #2 and pLKO.1-shPKCζ #3.

48 hours after transfection of packaging cells, supernatant was collected and passed through a 0.45 μm filter. After the addition of 8 μg/ml polybrene (Hexadimethrine bromide, Sigma), the supernatant was added to target cells plated on 10 cm cell culture dishes at 50% confluency. Two cycles of infection (of 16 hours each) were repeated, after which the medium was replaced with standard medium according to the cell line (see above "Cell culture media and cell lines"). 48 hours post-transduction, infected cells were used for further assays.

Lentiviral infection of primary cells

Primary cells (MECs) were transduced with pLKO.1-shCtrl and pLKO.1-shPar3 vectors. Single-cell suspensions from F1 mammospheres (MaSCs and progenitors) were transduced with pLKO.1-shCtrl, pLKO.1-shPar3 or pLVX-PURO-Numb dsRed constructs (FL, 3A, 3D and ΔPTB). Viruses were produced in MESCM to avoid the differentiation of MaSCs and progenitors (N.B. HEK293T cells medium contains serum, that stimulates differentiation). As described for cell lines, 48 hours after transfection of packaging cells, supernatant was collected and passed through a 0.45 μm filter. After the addition of polybrene, EGF (20 ng/mL) and FGF (20 ng/mL), the collected virus was either directly added to adherent MECs, or used to re-suspend dissociated cells from first generation mammospheres.

For all primary cells, two overnight cycles of infection were performed. 48 hours post-transduction, infected cells were used for further studies. Cells infected with pLVX.PURO or pLKO.1 constructs were selected for 1 week in puromycin (1 μg/ml in complete MESCM).

For double transduction experiments (shPar3 in MaSCs), we first transduced single-cell suspensions from first generation mammospheres with the pLKO.1 constructs (pLKO.1-shCtrl or pLKO.1-shPar3). Cells were selected for 48hours in puromycin and then transduced with the second construct (pLVX-PURO-Numb dsRed). Co-transduced cells were then re-selected in puromycin for 48hours and finally used for videomicroscopy (see paragraph 2.2.5, "Methods").

Lentiviral infection of KO1 (Numb-KO) tumour cell line

The KO1 (Numb-KO) cell line was previously established and characterized in our laboratory (Tosoni, Zecchini et al. 2015). These cells derive by tumours formed by the orthotopic transplantation of Numb-KO MECs from K5-Cre/Numb-flox/flox mice (Tosoni, Zecchini et al. 2015). KO1 cells were grown in suspension, as mammospheres (see "Mammosphere assay"), and display an immortal behaviour. These cells were grown in complete MESCM medium in poli-HEMA coated plates.

For this reason, for the infection of KO1 cells with pLVX-PURO-Numb dsRed constructs (FL, 3A, 3D and ΔPTB) we used the same procedures used for primary cells (see previous paragraph "Lentiviral infection of primary cells").

Gene knock-down: shRNA interference

To knock-down selected genes (PKCζ and Par3) we used pLKO.1 lentiviral vectors carrying specific shRNA sequences (See Plasmids paragraph). To infect both cell lines and primary cells we used the general procedures described above for lentiviral vectors.

2.2.5 Time Lapse (TL) live imaging analysis

We exploited TL analysis to visualize the first mitotic division of MaSCs. We used the Microscope Cage Incubator (Okolab), which encloses the IX81-ZDC bright field/fluorescent microscope station (Olympus). This system has a laser-based Z-drift compensator and works as a dynamic scanner. The associated software builds a virtual grid above the sample and it can capture images of the same field at different time points, by keeping more fields on focus. Cell viability during the entire record period was guaranteed by the Cage Incubator, which maintained a microenvironment as close as possible to the culture incubator (37°C 5% CO_2).

To visualize Numb distribution at mitosis, cells from F1 generation mammospheres were infected with the pLVX.PURO-Numb dsRed construct (or one of its mutants; see paragraphs 2.1.3 and 2.2.4).

After selection in puromycin, cells were collected and prepared for video-microscopy. For this purpose, cells were harvested, enzymatically dissociated (as previously described) and re-suspended in complete MESCM medium at a concentration of 5,000 cells/30 µl. To maintain cells static during the recording period, the single cell suspension was embedded in Methylcellulose-based medium. This particular medium was prepared by adding 10X MESCM (containing 10-fold concentrated supplements) to pre-casted methylcellulose (MethoCult™ Stemcell Technologies), so that the final concentration of supplements is 1X in 1.8% methylcellulose. 370 µl of Methylcellulose-based medium were added to 30 µl of re-suspended cells (5000 cells) and gently mixed. The so obtained 400 µl of re-suspension were then plated on glass bottom wells (MatTek Corporation™) and loaded into the Microscope Cage Incubator for video-microscopy. Video recording lasted for 7 days (168 hours), and images were captured every 30 minutes for each defined field with a 10X 0.4 NA objective.

TL analysis and interpretation

The statistical analysis on TL videos was performed only on single living cells without considering the small groups or cells aggregates. Only cells that gave rise to fully formed (70 μm diameter) mammospheres at the end of the recording time were considered as MaSCs and thus considered in the analysis. Numb segregation was assessed during the first mitotic division of MaSCs. An average of 30 MaSCs were analysed in each experimental setting.

Numb distribution was scored as “Symmetric” or “Asymmetric” at each mitotic division analysed. All events were double-checked by two independent operators. Intermediate phenotypes were excluded from the quantification.

To score the ratio between asymmetric versus symmetric cell divisions in KO1 cells, the first, second and third mitotic divisions were analysed. In particular, a 1-2-3-5 pattern of cell number progression was considered as the result of an initial asymmetric division, followed by symmetric divisions of the progenitors. Conversely, a 1-2-4-8 progression pattern was the result of an initial symmetric division.

2.2.6 Immunofluorescence (IF)

IF on cell lines and adherent primary MECs

Cells were plated on glass coverslips pre-incubated with 0.1% gelatine in PBS at 37°C for 30 minutes. Cells were fixed in 4% paraformaldehyde (in 1X PBS) for 10 minutes, washed with PBS and permeabilized in 0.1% Triton X-100 in 1X PBS for 4 minutes at room temperature. To prevent non-specific binding of the antibodies, cells were then incubated with 1X PBS in presence of 3% BSA and 10% Normal Donkey Serum (blocking solution) for 1 hour at room temperature. Next, cells were incubated for 1 hour with primary antibody in blocking solution, washed 3 times with 1X PBS and incubated for 45 minutes with fluorescently labelled secondary antibodies (Amersham). After 3 washes with PBS, nuclei were DAPI-stained for 5 minutes and washed again 3 times with 1X PBS. Coverslips were immediately mounted with glycerol and examined under a Leica TCS SP2 AOBS confocal microscope equipped with 405, 488, 543, and 633 nm laser lines. For the quantitative analysis of IF experiments, the ImageJ image analysis software (W. Rasband, National Institutes of Health) was used.

IF on PKH^{high} MaSCs

For IF on MaSCs, PKH^{high} cells were isolated from F2 generation mammosphere by FACS sorting. Single-cell suspensions were plated on poly-lysine coated coverslips and cells were then fixed with 4% formaldehyde (10 minutes at RT). We then used the same IF procedure described for cell lines and MECs.

Quantification of Numb localization by IF

Numb subcellular localization was scored as “Plasma membrane” or “Cytoplasm”, at a single-cell level. Intermediate phenotypes were excluded from the quantification. All images were double-checked by two independent individuals.

2.2.7 Protein procedures

Cell lysis

Cells were washed with PBS 1X and then lysed in 1X JS or RIPA buffer, directly in the cell culture plates and with the help of a cell-scraper. Lysates were then clarified by centrifugation at 13000 rpm for 20 minutes at 4°C, using a 5415 R centrifuge. Protein concentration was measured by the Bradford assay (Biorad) following manufacturer’s instructions.

Western Blot (WB)

Desired amounts of proteins were loaded onto 10% SDS-PAGE gels for electrophoresis (Criterion™ TGX Stain-Free™ Precast Gels, Biorad). Running was performed in Running buffer 1X at 200V for 45 minutes. Proteins were transferred to nitrocellulose in WB transfer systems (Trans-Blot® Turbo™ Transfer System, Biorad), at 25 V for 15 minutes. Ponceau staining was used to determine the efficiency of protein transfer onto the filters. Filters were then blocked for 1 hour (or overnight) in 5% milk or BSA in TBS supplemented with 0.1% Tween (TBS-T). After blocking, filters were incubated with the primary antibody, diluted in TBS-T 5% milk or BSA, for 1 hour at room temperature, followed by three washes of ten minutes each in TBS-T. Filters were then incubated with the appropriate horseradish peroxidase-conjugated secondary antibody diluted in TBS-T for 30 minutes. After the incubation with the secondary antibody, the filter was washed 3

times in TBS-T (10 minutes each) and the bound secondary antibody was revealed using the ECL method (Amersham).

Co-immunoprecipitation assay

For co-IP experiments, MCF10A were transduced with pLL3.7-Numb FLAG, pLL3.7-Numb 3D FLAG and pLL3.7-NumbΔPTB FLAG. 48 hours post-transduction, lysates were prepared in JS buffer and quantified by Bradford assay. 3 mg/lysate was incubated in the presence of anti-FLAG antibody-conjugated beads (30 μL/sample) (Sigma) for 2 hours at 4°C, with rocking. The supernatant (Input) was then removed and beads were washed 4 times with JS buffer. Immunoprecipitated proteins were eluted in Laemli buffer 2x and analysed by WB.

2.2.8 RNA procedures

RNA extraction

Total RNA was extracted from cells by using the RNeasy® Mini Kit (Qiagen), following manufacturer's instructions.

cDNA synthesis

1μg of purified total RNA was used for first strand cDNA syntesis by using Superscript VILO cDNA Synthesis Kit (Invitrogen), following manufacturer's instructions.

Real-Time Quantitative PCR (rt-qPCR)

The relative quantity of mRNA transcripts for PRKCZ (human and mouse), CDKN1A (p21) and MDM2 was determined by rt-qPCR, using specific TaqMan® Gene Expression

Assays (Thermo Scientific). The selected assays are indicated in ***Table 1***. The data were normalized by using GAPDH and GUSB as housekeeping genes. To perform rtqPCR, we used the Roche LightCycler® 480 Real-Time PCR System and each PCR reaction was performed as technical triplicate, according to the following thermal cycling conditions: polymerase activation 95°C 10 min, 40 cycles: 95°C 15'', 55°C 1 min. The output data were analysed for gene expression according to the ΔΔCt method.

Gene	Assay
Human PRKCZ	Hs00177051_m1
Mouse PRKCZ	Mm00776345_g1
Mouse CDKN1a	Mm00432448_m1
Mouse MDM2	Mm00487656_m1

Table 1. TaqMan™ Gene Expression Assays used in this work

Chapter 3

Results

3.1 Treatment with TPA induces Numb phosphorylation and re-localization to the cytosol in mammary cells

In order to study the role of Numb phosphorylation in mammary epithelial cells, we employed TPA (12-O tetradecanoylphorbol-13-acetate), a potent activator of different classes of PKC enzymes. TPA has been shown to cause phosphorylation and rapid release of Numb from the PM in mammalian cells (Dho, Trejo et al. 2006) (Nishimura and Kaibuchi 2007) (Smith, Lau et al. 2007).

To test the efficacy of TPA on Numb phosphorylation in mammary cells, we used three different mammary epithelial cell lines:

- the non-tumourigenic human mammary MCF10A cell line;
- the quasi-normal mouse mammary epithelial Comma-Dβ cell line;
- mouse primary mammary epithelial cells (MECs), isolated from FVB/Hsd mice (5 weeks old, axillary and inguinal glands; see "Materials and Methods").

We found that Numb phosphorylation levels on Ser276 (pSer-276), a well-established PKC phosphorylation site in Numb (Smith, Lau et al., 2007), were augmented upon treatment with 1μM TPA for 10 minutes, in all cell lines (***Fig. 13***).

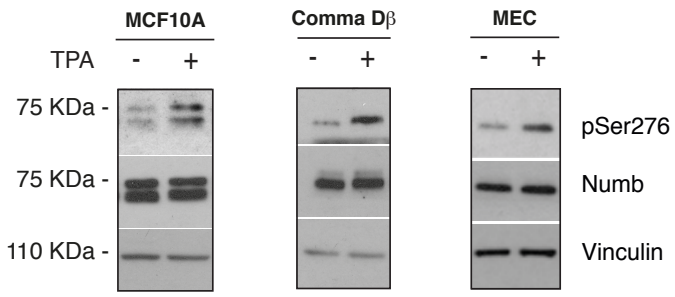

Figure 13 – TPA treatment increases Ser276 phosphorylation levels in mammary cells
The indicated cell lines (MCF10A, Comma-Dβ, mouse MECs) were treated with TPA (+; 1 μM for 10 minutes) or vehicle alone (DMSO, -). Cells were then lysed in RIPA buffer and total cell lysates were subjected to SDS-PAGE and immunoblotted with the indicated antibodies (see "Materials and Methods"). Vinculin was used as loading control.

We next analyzed the effects of TPA treatment on Numb subcellular localization in mammary epithelial cells. In the cell lines that we tested, Numb was mainly associated with the PM and with endosomes (***Fig. 14a-c, left panels***). The degree of partitioning between these two compartments varied among the cell lines: Numb was predominantly associated with the PM in human MCF10A cells, while it was distributed between PM and endocytic vesicles in mouse cells. (***Fig.14a-c, left panels***). Treatment with TPA led to a significant re-distribution of Numb from the biomembranes (PM + endosomes) to the cytosol, in all cell lines (***Fig. 14a-c, right panels***).

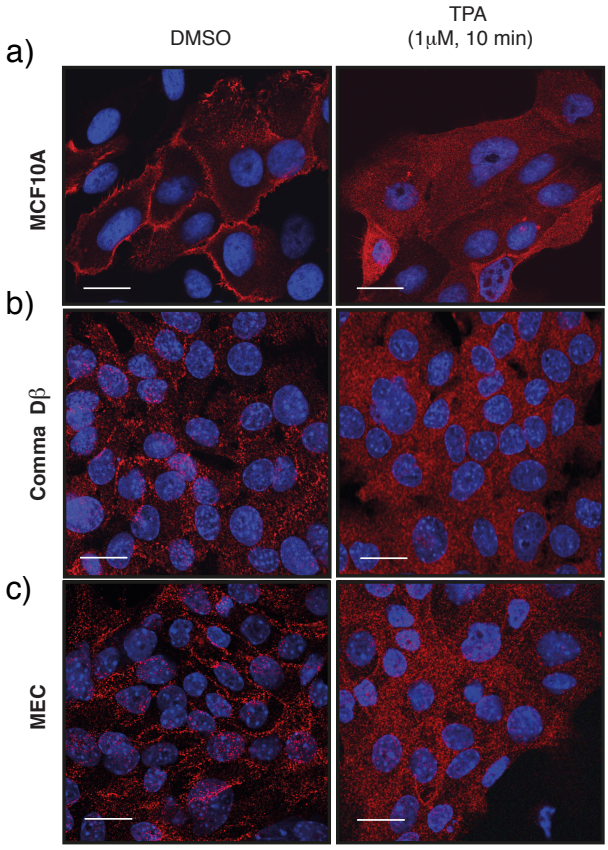

Figure 14 - TPA treatment of mammary epithelial cells re-localizes Numb to the cytosol
The indicated cell lines (MCF10A; Comma-Dβ; mouse MECs) were treated with TPA (+, 1 μM for 10 minutes) or vehicle alone (DMSO). Cells were then fixed in 4% paraformaldehyde and Numb localization was analyzed by immunofluorescence (IF) and confocal microscopy (see "Materials and Methods"). Numb, red; DAPI, blue. Bar, 10 μm. Merged channels are shown.

Based on these results, we then tested the effect of TPA on Numb localization in mouse mammary stem cells (MaSCs). We isolated MaSCs, using the PKH26-labelling technique coupled with mammosphere (MS) culture assays (Cicalese, Bonizzi et al., 2009, Pece, Tosoni et al., 2010). PKH26^{high} cells were isolated from second-generation MSs and treated with 1μM TPA (or DMSO as vehicle) for 10 minutes. Numb localization was then analyzed by IF (see "Methods"). In interphasic PKH26^{high} cells, Numb was predominantly associated with the PM and vesicles (***Fig.15, left panel***). Upon TPA treatment, Numb staining became dispersed in the cytosol (***Fig. 15, left panel***). The effect of TPA was quantified by calculating the percentage of cells with either PM or cytosolic (not-PM) staining of Numb. The quantification was performed on three different technical replicas (sample size: 100 cells) and is reported in **Fig. 15** (***Fig. 15, right panel***).

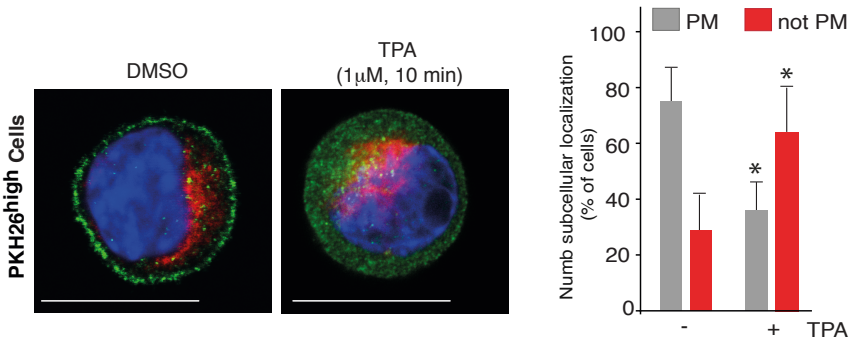

Figure 15 - TPA treatment of PKH26^{high} MaSCs re-localizes Numb to the cytosol
Left: *PKH26^{high} cells were purified from second-generation mammospheres, cultured in suspension and treated with TPA (1 μM for 10 minutes) or vehicle only (DMSO). Cells were fixed on coverslips and subsequently analyzed by IF and confocal microscopy (see "Materials and Methods"). Numb, green; PKH26, red; DAPI, blue. Bar, 10 μm. Merged channels are shown. Sample size: 100 cells/treatment.*
Right*: Quantitation of the IF experiment. Cells were scored as PM or not-PM (in this latter case, Numb localised in endosome-like structures) based on their prevalent pattern of Numb staining at the individual cell level. The percentage of cells showing the two staining patterns is reported for each experimental condition. *, p value < 0.05.*

3.2 Numb phosphorylation is functional to its partitioning in mammary stem cells.

We next decided to evaluate the effect of Numb phosphorylation on its distribution at mitosis of MaSCs. For this purpose, we exploited TPA as a tool to induce Numb phosphorylation in order to study the downstream effects of this modification on Numb distribution. Since MaSC-based experiments would require exposure to TPA for long periods (at least for 36 hours, which comprises the first mitotic division of a MaSC), we first assessed whether the effects of TPA on Numb localization and Ser-276 phosphorylation were long-lasting. For this purpose, we incubated mouse primary MECs with TPA for 10 minutes, 24 hours and 48 hours, and analyzed Numb localization by IF. As shown in ***Fig.16***, we established that TPA treatment was efficient in re-localizing Numb to the cytosol for treatments up to 48 hours.

We also verified by Western blot (WB) analysis that TPA treatment was able to increase Ser276 phosphorylation levels for treatments up to 48 hours (***Fig. 17)***.

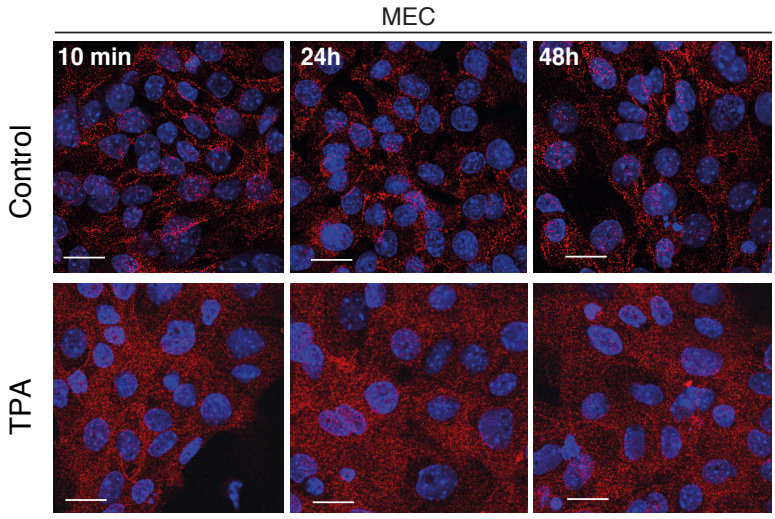

Figure 16 - TPA efficiency on Numb re-localization lasts at least 48 hours
Mouse MECs were treated with TPA (1 μM) for the indicated time points (10 minutes, 24 hours, 48 hours) and then analyzed for Numb localization by IF. Numb, red; DAPI, blue. Bar, 10 μm. Merged channels are shown. Note that the images corresponding to the time point "+ TPA 10 minutes" is the same as the one shown in Fig. 14 (panel c).

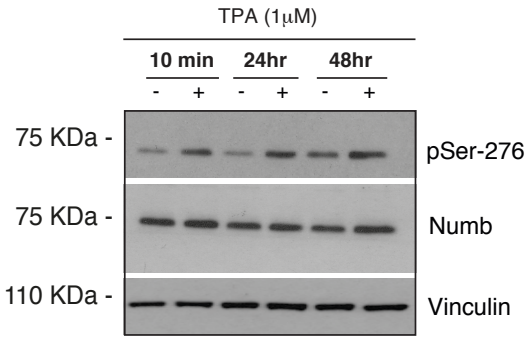

Figure 17. TPA efficiency on Ser276 phosphorylation levels lasts 48 hours
Mouse MECs were treated with TPA (1 μM) for the indicated time points (10 minutes, 24 hours, 48 hours) and then lysed in RIPA buffer. Total cell lysates were subjected to SDS-PAGE and immunoblotted with the indicated antibodies (see "Materials and Methods" section). Vinculin was used as loading control.

We then analyzed Numb distribution at MaSCs mitosis in the presence of TPA. To visualize Numb distribution, we infected primary mammary cells, isolated from first-generation MSs, with a lentiviral construct encoding for Numb fused to the dsRed protein (Numb-dsRed). Transduced cells were then selected with puromycin and re-suspended in Methylcellulose-based medium in the presence of either TPA or vehicle (DMSO). In these conditions, the formation of the second generation of MSs was recorded by video microscopy (see paragraphs 2.2.4 and 2.2.5, "Methods"). Only cells that gave rise to fully formed MSs at the end of the experiment were considered as MaSCs and, hence, included in further analysis.

We analyzed Numb-dsRed distribution at the first mitotic event of MaSCs. In the presence of TPA, we observed a significant alteration in the pattern of Numb distribution between the two daughter cells. In detail, we scored 32% Numb asymmetric partitioning and 68% Numb symmetric partitioning in TPA treated cells ***(Fig. 18***). These values contrasted with those detected in control cells, where we scored 75% Numb asymmetric partitioning and 25% Numb symmetric partitioning (***Fig. 18***).

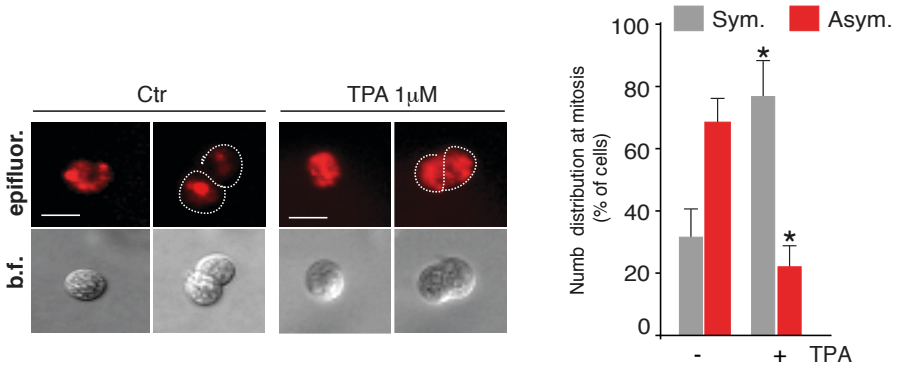

Figure 18 - TPA induces symmetric partitioning of Numb at mitosis of MaSCs
Left: *Mammary cells were dissociated from first-generation mammospheres, lentivirally transduced with Numb-DsRed, and monitored by time-lapse video-microscopy throughout the formation of the next generation of mammospheres. In this type of analysis, MaSCs are retrospectively identified based on their ability to generate fully formed (> 70 μm) mammospheres at the end of the recording time (~ 7 days). Only cells that formed fully formed mammospheres were considered for the analysis. Epifluorescent Numb (red); b.f., bright field. Bar, 10μm.*
Right: *Quantitation of the experiment. *, p value < 0.05. Sample size: 30 cells/treatment.*

3.3 Mammalian Par3 is essential for Numb phosphorylation during mitosis of mammary stem cells

In the light of a possible link between Numb phosphorylation and its distribution at mitosis of MaSC, we became interested in defining the mechanism underlying this modification. Previous studies on *D. melanogaster* neuroblasts demonstrated that the evolutionary conserved Par polarity complex (Par3, Par6, aPKC) directs the polarised distribution and the asymmetric segregation of Numb by controlling its phosphorylation status. In particular, Par3 is required for Numb recruitment at the apical membrane of the dividing neuroblast, where Numb is phosphorylated by aPKC (Wirzt-Peitz et al., 2008). This event is crucial for Numb asymmetric confinement in the basal sibling cell.

In mammalian cells, Par3 was also shown to interact with Numb and to control atypical PKC-mediated phosphorylation of Numb (Nishimura and Kaibuchi, 2007). Moreover, the interaction between Par3 and PKCζ has been found to be important for end-bud

remodelling and progenitor differentiation during mammary gland morphogenesis; this was, however, not directly linked to the control of asymmetric cell division (McCaffrey and Macara, 2009).

Based on this knowledge, we hypothesized that these roles of the Par complex could be conserved in vertebrate epithelia and in the mammary epithelium. To test this hypothesis, we analyzed the role of Par3 in our model system. We knocked-down Par3 in mouse primary MECs by using a lentiviral construct encoding for a specific shRNA, targeted to the murine PAR3 sequence (pLKO.1-shPar3). As control, we used an unrelated, scrambled shRNA, and we first looked at Numb phosphorylation levels by WB analysis. In Par3-KD cells, we observed a reduction of Numb phosphorylation on Ser276 (***Fig.19***).

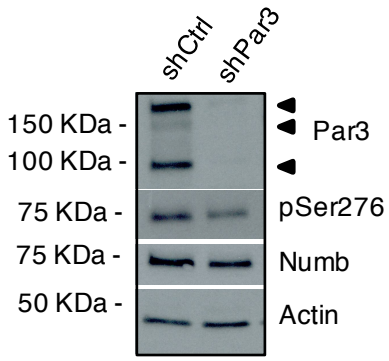

Figure 19 - Par3-KD decreases Ser276 phosphorylation in mouse MECs
Mouse MECs were subjected to KD of Par3 by pLKO.1-shRNA lentiviral transduction. Cells were then lysed in RIPA buffer and analyzed by SDS-PAGE and immunoblotting with the indicated antibodies. Black arrows indicate the three Par3 isoforms found in mammalian cells (100, 150,180 KDa).

We then analyzed Numb subcellular localization by IF. In control cells, Numb localized both at the PM and in the cytoplasm, mainly at the level of endosomes. The ablation of Par3 resulted in a significant accumulation of Numb at the PM (***Fig.20***).

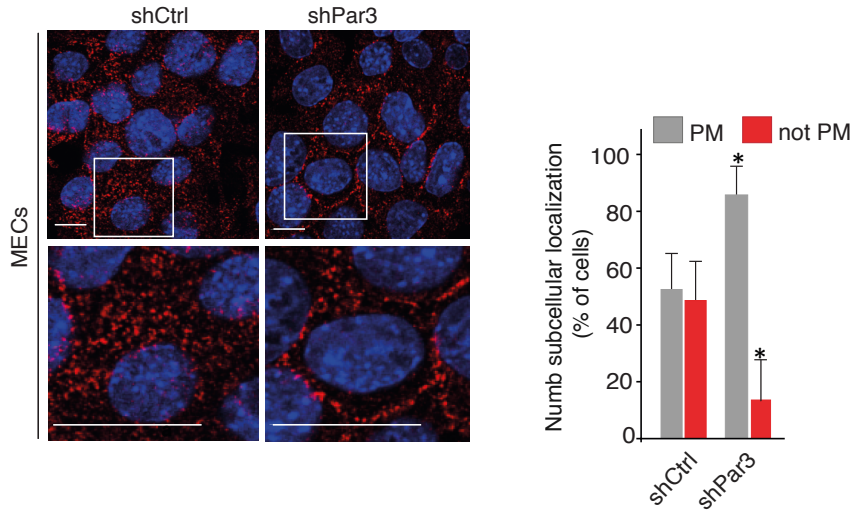

Figure 20- Par3-KD reinforces Numb staining at the PM
Left: *Mouse MECs were subjected to KD of Par3 by pLKO.1-shRNA lentiviral infection, and then analyzed by IF for Numb localization. Numb, red; DAPI, blue. Bar, 10μm.*
Right: *Quantitation of the IF experiment. Cells were scored as PM or not PM (in this latter case, Numb localised in endosome-like structures), based on their prevalent pattern of Numb staining at the individual cell level. The percentage of cells showing the two staining patterns is reported. *, p value < 0.05.*

Since we found that the distribution of Numb at mitosis is influenced by Numb phosphorylation status, we next investigated the role of Par3 in the control of Numb partitioning. For this purpose, we performed Par3 knockdown in MaSCs, using the same shRNA construct described for MECs. We co-transduced MaSCs from second-generation mammospheres with the shPar3 (or shCtrl) lentiviral construct and the Numb-dsRed lentiviral vector (see paragraph 2.2.4, "Methods"). As previously described, we analyzed Numb-dsRed distribution at the first mitotic division of MaSCs. Upon Par3-KD, we scored a 30% increase in symmetric distribution of Numb (69% symmetric partitioning and 31% asymmetric partitioning; ***Fig. 21***) compared to control cells (30% symmetric partitioning and 70% asymmetric partitioning; ***Fig. 21***).

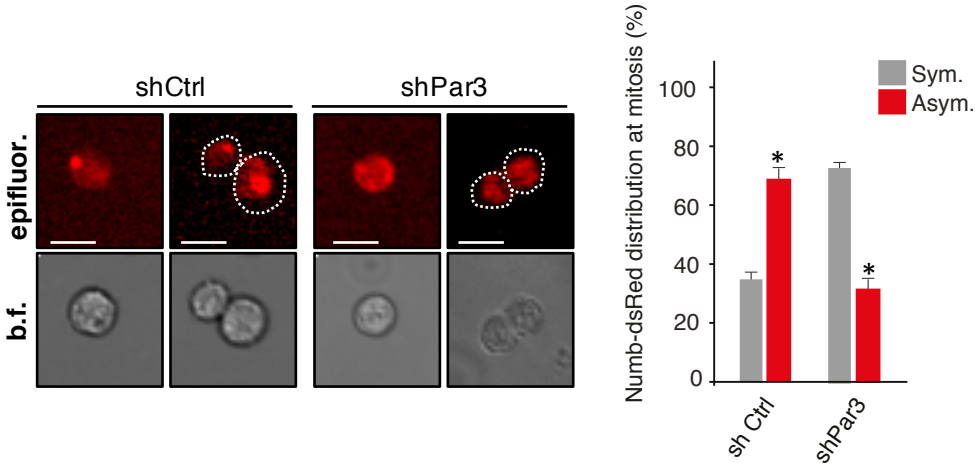

Figure 21 - Par3-KD increases symmetric distribution of Numb at mitosis of MaSCs
Left: *Mammary cells were dissociated from first-generation mammospheres, lentivirally transduced with Numb-DsRed and shPar3 (or shCtrl) and selected in puromycin for 1 week. Mammospheres formation was monitored by time-lapse video-microscop. MaSCs were retrospectively identified as in the experiment shown in Fig. 18. Epifluorescent Numb (red); b.f., bright field. Bar, 10μ m.*
Right: *Quantitation of the experiment. *, p value < 0.05. Sample size: 30 cells/treatment*

3.4 PKCζ promotes Numb phosphorylation in mammary epithelial cells

To better characterize the involvement of the Par polarity complex in the regulation of Numb distribution in MaSCs, we focused our attention on PKCζ, one of the two mammalian homologues of *D. melanogaster* aPKC. This enzyme has been shown to interact with Par3 (Nishimura and Kahibuchi, 2007) and to phosphorylate Numb in human cells (Smith, Lau et al., 2007).

3.4.1 PKCζ overexpression in mammary cells

To start, we tested the effects of PKCζ overexpression on Numb phosphorylation on Ser276 in mammary epithelial cells. To this aim, we transduced MCF10A cells with a lentiviral vector encoding for PKCζ fused to the Venus fluorescent protein (PKCζ- Venus). We used empty vector (EV-Venus)-transduced cells, expressing only the Venus protein, as

control. By WB analysis, we observed increased levels of pSer276 in PKCζ overexpressing cells, compared to control cells (***Fig. 22***).

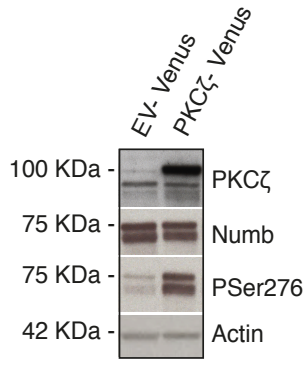

Figure 22 - PKCζ overexpression increases Ser276 phosphorylation in MCF10A cells *MCF10A cells were transduced with PKCζ-Venus or EV-Venus lentiviral constructs. Cells were then lysed in RIPA buffer and analyzed by SDS-PAGE and immunoblotting with the indicated antibodies. Actin was used as loading control.*

We then analyzed Numb localization by IF upon PKCζ overexpression (***Fig. 23***). While Numb was predominantly localized at the PM in EV-Venus transduced cells, in PKCζ overexpressing cells, instead, Numb was re-distributed from the PM to the cytosol (***Fig.23***). To quantify this observation, we analyzed Numb staining at the single cell level and quantified the number of cells that displayed Numb staining at the PM, in both EV-Venus (75,1%±2,4*; sample size: 1180 cells) and PKCζ-Venus (23,1%±2,6*, sample size: 950 cells) transduced cells (*=confidence interval of the proportion at 95%) (***Fig. 23***).

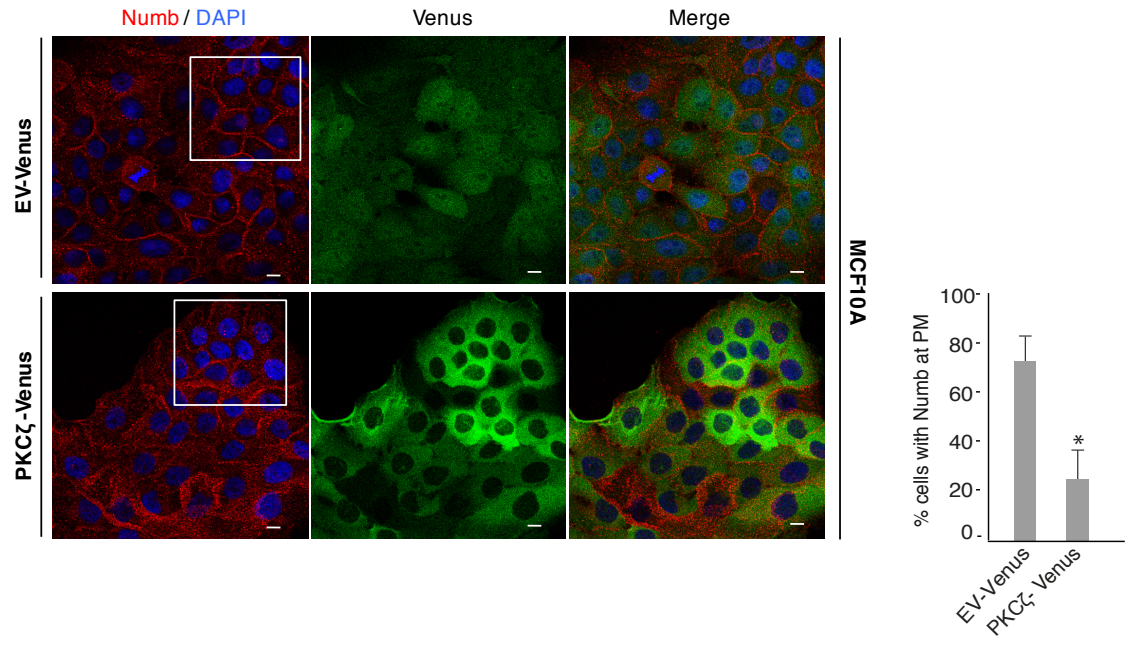

Figure 23 - PKCζ overexpression re-localizes Numb to the cytosol in MCF10A cells
Left*: MCF10A cells were transduced with PKCζ-Venus or EV-Venus lentiviral constructs, grown on glass coverslips and fixed with 4% paraformaldehyde. Numb localization was then analyzed by IF. Numb, red; DAPI, blue; Venus, green. Bar, 10μm.*
Right: *Quantitation of the IF experiment. Cells were analyzed on the basis of their prevalent pattern of Numb staining at the individual cell level. Only cells with Numb at the PM were counted and reported as a percentage over the total number of analyzed cells for both experimental conditions. *, p value < 0.05. Sample size: 1180 cells (EV); 950 cells (PKC* ζ-Venus).

3.4.2 PKCζ knockdown in mammary cells

To further corroborate the involvement of PKCζ in the control of Numb phosphorylation in the mammary epithelium, PKCζ was knocked down in mammary epithelial cells. In order to find a suitable model system that would allow an appreciable effect on Numb phosphorylation, we decided to screen different human mammary breast cancer cell lines for their levels of pSer276 (***Fig. 24)***. Among the analyzed cell lines, we chose MDAMB231 cells due to their high levels of Numb phosphorylation at Ser276. We also detected high levels of pSer276 in T47D, BT20 and AU565 cells, but this was correlated with high Numb endogenous levels in these cell lines (***Fig. 24***).

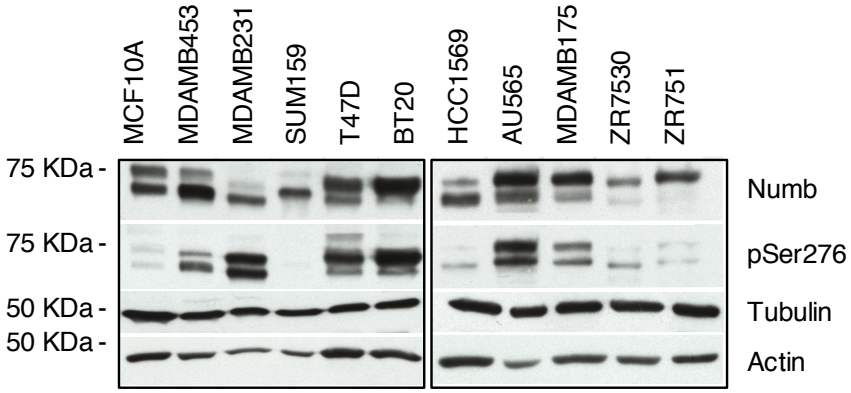

Figure 24 - MDAMB231 cells display high levels of pSer276
The indicated cells were lysed in RIPA buffer and analyzed by SDS-PAGE and immunoblotting, with the indicated antibodies. Actin and tubulin were used as loading control.

We then performed PKCζ-KD in MDAMB231 cells by using three different lentiviral shRNA-constructs (sh1, 2 and 3). As control, we used an unrelated, scrambled shRNA-construct (shCtrl). PKCζ gene expression was quantified by real-time, quantitative PCR, and calibrated on the shCtrl sample (***Fig. 25***). PKCζ-KD was achieved with all three shRNA constructs and highest efficiency was obtained with the sh1 construct (percentage of KD: sh#1, 81.1%; sh#2, 66.3%; sh#3, 51.2%; ***Fig. 25***).

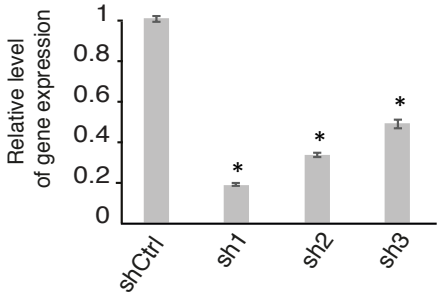

Figure 25 –Efficiency of PKCζ-KD in MDAMB231 cells
*MDAMB231 cells were subjected to KD of PKCζ with three different pLKO.1-shRNA constructs and PKCζ mRNA levels were analyzed by rt-qPCR (see "Methods"). The levels of PKCζ gene expression for each sample, calibrated on the shCtrl sample, are shown. GUSB and GAPDH mRNA levels were used as normalizers. *, p value < 0,01.*

We then assessed Numb phosphorylation levels by WB analysis and scored a reduction in pSer276 levels in all three KD samples, with higher efficiency in sh1 infected cells (***Fig.26***).

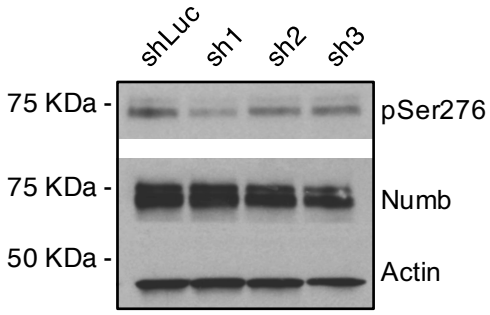

Figure 26. PKCζ-KD impairs Numb phosphorylation at Ser276 in MDAMB231 cells
MDAMB231 cells were subjected to KD of PKCζ with three different pLKO.1-shRNA lentiviral constructs. The cells were then lysed in RIPA buffer and analyzed by SDS-PAGE and immunoblotting with the indicated antibodies. Actin was used as loading control.

We also analyzed the effects of PKCζ-KD on Numb localization by IF. In control MDAMB231 cells, unlike what we observed in other breast cell lines, Numb immunostaining was mainly diffused into the cytosol. Upon PKCζ-KD, we scored a significant redistribution of Numb from the cytosol to the PM in all three PKCζ-KD cell lines (***Fig.27***). We also quantified this phenotype by analysing Numb staining at the single cell level and by calculating the percentage of cells that displayed Numb localization at the PM, in each sample (shCtrl: 10,4%±2,4*, sample size: 644; sh1: 77,4%±2,3*, sample size: 606; sh2: 72,1%±3,1*, sample size: 811; sh3: 58±4,2*, sample size: 514) (***Fig. 27***).

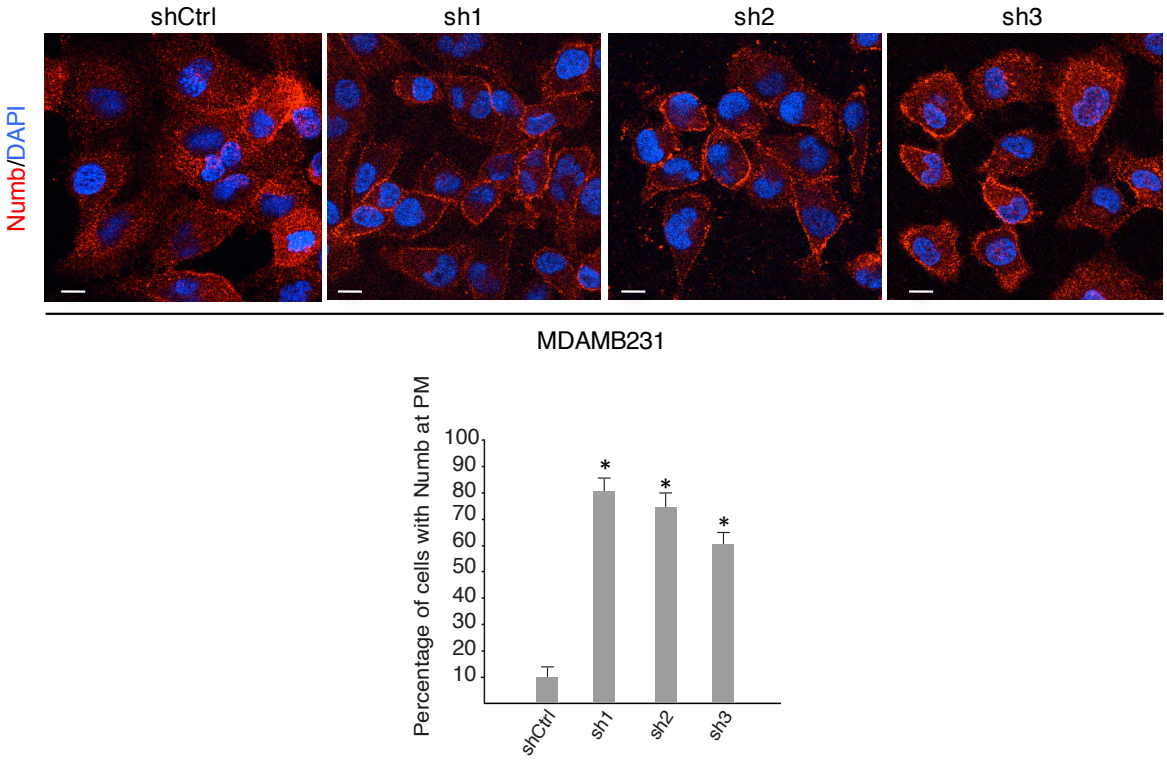

Figure 27 - Numb re-localizes to the PM upon PKCζ-KD in MDA MB231 cells
Up*: MDAMB231 cells were subjected to KD of PKCζ with three different shRNA lentiviral constructs. The cells were then fixed with 4% paraformaldehyde and Numb localization was analyzed by IF. Numb, red; DAPI, blue. Bar 10μm. Merged channels are shown.*
Bottom*: Quantitation of the IF experiment. The cells were analyzed based on their prevalent pattern of Numb staining at the individual cell level. Only cells with Numb at the PM were counted and reported as a percentage over the total number of analyzed cells for all the experimental conditions. *, p value < 0,01. Sample size: 644 cells (shCtrl); 606 cells (sh1); 811 cells (sh2); 514 cells (sh3).*

3.5 Mutations of PKC phosphorylation sites on Numb impair its distribution at mitosis of MaSCs.

To obtain further evidences that Numb phosphorylation is involved in the asymmetric partitioning of Numb at mitosis in MaSCs, we decided to use a molecular genetics approach. As stated in the Introduction, mammalian Numb is phosphorylated by PKC isoenzymes on multiple sites, including Ser7, Ser276 and Ser295, which are evolutionarily conserved throughout evolution (Dho, Trejo et al. 2006) (Nishimura and Kaibuchi, 2007) (Smith, Lau et al., 2007).

Previous studies have exploited the use of phospho-mimetic (Ser to Asp) or phospho-deficient (Ser to Ala) mutants of Numb to unravel the contribution of PKC-mediated phosphorylation of Numb during ACD (Dho, Trejo et al. 2006) (Nishimura and Kaibuchi, 2007) (Smith, Lau et al., 2007) (Sato, Watanabe et al., 2011). Thus, we also engineered, on the lentiviral Numb-dsRed backbone (full-length, FL), mutants in which all the three serine residues were mutated to aspartic acid (phospho-mimetic mutant, Numb-3D, ***Fig. 28***) or to alanine (phospho-deficient mutant, Numb-3A, ***Fig. 28***), as previously described (Nishimura and Kaibuchi, 2007). A Numb mutant deprived of the phosphotyrosine-binding domain (ΔPTB), which lacks the region of binding to p53 and to the PM, was used as a putative lack-of-function control mutant (***Fig.28***).

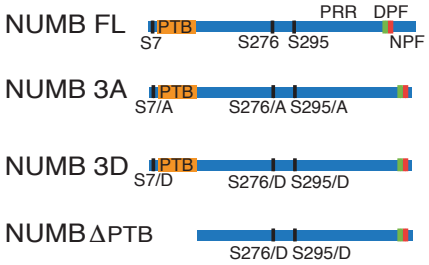

Figure 28 - Schematic representation of Numb phosphomutants. *The four engineered pLVX-PURO – Numb dsRed constructs are shown (FL, 3A, 3D and ΔPTB). The position of the Numb phospho-tyrosine binding (PTB) domain, proline-rich region (PRR), endocytic motifs (NPF, DPF), and of the relevant serine residues (S7, S276, S295) are indicated. The dsRed tag protein (N-terminal) is not depicted in this scheme.*

Upon transduction in MaSCs, these phosphomutants showed outstanding differences in their subcellular localization (***Fig. 29***). In particular, the Numb-3A mutant was predominantly localized at the PM, as well as the FL Numb-dsRed. Conversely, the Numb-3D and the ΔPTB mutants localized mainly to the cytosol (***Fig. 29***)

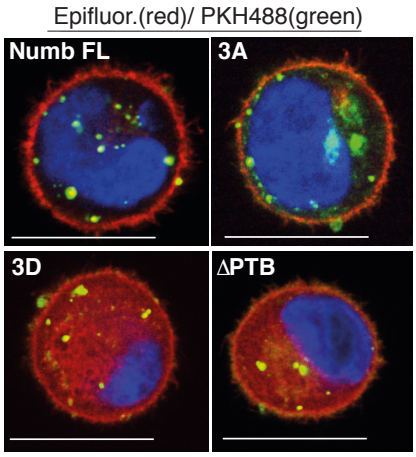

Figure 29 - Localization of Numb phosphomutants in MaSCs
PKH488+ cells were purified from mammospheres that stably expressed Numb-DsRed (Numb FL) or its mutants (3A, 3D, or ΔPTB) and analyzed by IF and confocal microscopy for Numb-dsRed constructs localization. Numb (and Numb mutants), red; PKH, green; DAPI, blue. Bar, 10μm.

Next, we analyzed the distribution of the Numb phosphomutants at the first mitotic event of MaSCs by TL video-microscopy. As shown in ***Fig. 30***, while the FL Numb-dsRed

protein is asymmetrically partitioned in the majority of the divisions observed (*Numb-FL:* 70% Numb asymmetric partitioning, 30% Numb symmetric partitioning), both the Numb-3A and Numb-3D mutants (and the Numb-ΔPTB) were symmetrically distributed between the two daughter cells (*Numb 3A*: 10% asymmetric partitioning, 90% symmetric partitioning; *Numb-3D*: 8% asymmetric partitioning, 92% symmetric partitioning; *Numb ΔPTB*: 6% asymmetric partitioning, 94% symmetric partitioning) (***Fig. 30***).

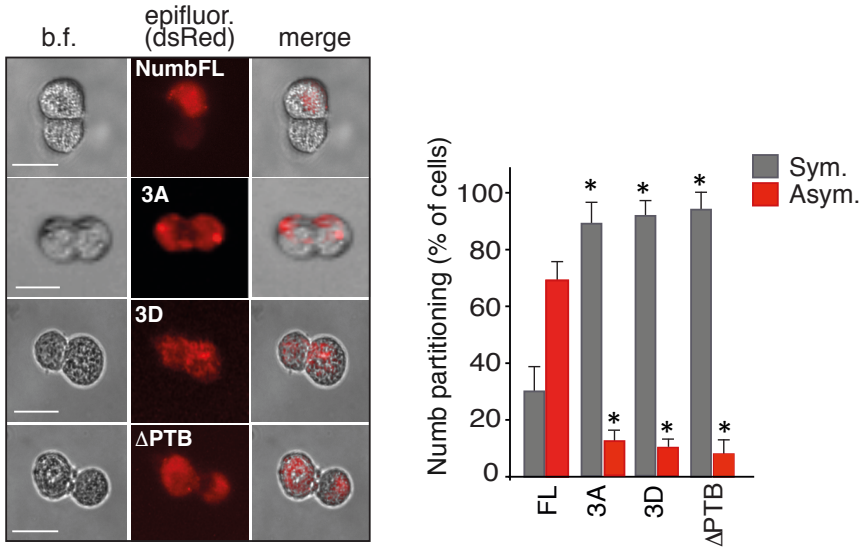

Figure 30 – Numb phosphomutants partition symmetrically in MaSCs
Left*: Single cell suspensions from first-generation mammospheres were lentivirally transduced with Numb-DsRed (or its mutants), and then monitored by time-lapse video-microscopy throughout the formation of the next generation of mammospheres. MaSCs were retrospectively identified as in the experiment shown in Fig. 6. Epifluorescent Numb (red); b.f., bright field. Bar, 10μm.*
Right: *Quantitation of the video-microscopy experiment. *, p value < 0.05 vs. comparable condition in FL. Sample size: 30 cells/treatment.*

We also produced single point-mutants in Ser7, Ser276 or Ser295 residues, either to alanine or to aspartic acid, as previously described by Nishimura and Kaibuchi (Nishimura and Kaibuchi, 2007). However, once transduced in MaSCs, none of these mutants displayed any of the phenotypes showed by the triple-mutant constructs (data not shown).

3.6 Numb phosphomutants cannot rescue the biochemical and biological phenotypes of Numb-KO cells

To investigate the effects of the mutagenesis of PKC-phosphorylation sites on Numb biological and biochemical activity, we expressed the Numb phosphomutants in a Numb-KO context. To this aim, we used the KO1 cell line (previously described in our laboratory), which derives from a tumour obtained by orthotopic transplantation of Numb-KO primary MECs (Tosoni, Zecchini et al., 2015). KO1 cells, due to the lack of Numb expression, display low levels of the tumour suppressor p53 (***Fig.31, "Ctr" lane***) and of p53-dependent transcripts (p21, Mdm2) (***Fig.32, "Ctr"***), and show a symmetric pattern of division at mitosis (***Fig. 33, "Ctr"***). The re-expression of FL Numb-dsRed in KO1 cells rescued all these phenotypes to the WT level (***Fig.31, 32, 33***). When the Numb-3A and Numb-3D mutants (and the Numb-ΔPTB as a lack-of-function mutant) were expressed in the same cell line (KO1), they failed to rescue any of the phenotypes induced by loss of Numb expression (***Fig. 31, 32, 33***).

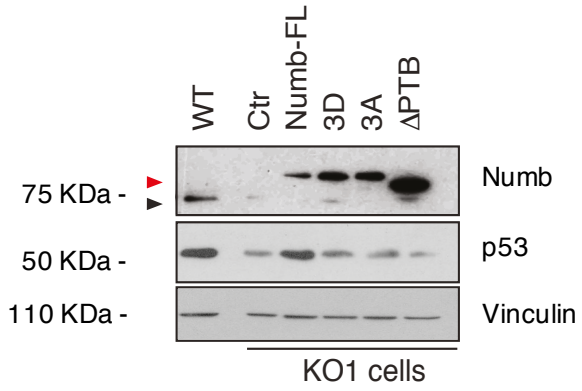

Figure 31 - Effects of Numb phosphomutants on p53 protein levels in Numb-KO cells
KO1 cells were transduced with the indicated constructs (WT indicates wild-type MECs form FVB/Hsd mice; Ctr indicates not infected KO1 cells) and analyzed by SDS-PAGE and immunoblot, with the indicated antibodies. Arrows indicate the position of endogenous Numb (in WT MECs, black) or of transduced Numb proteins (red).

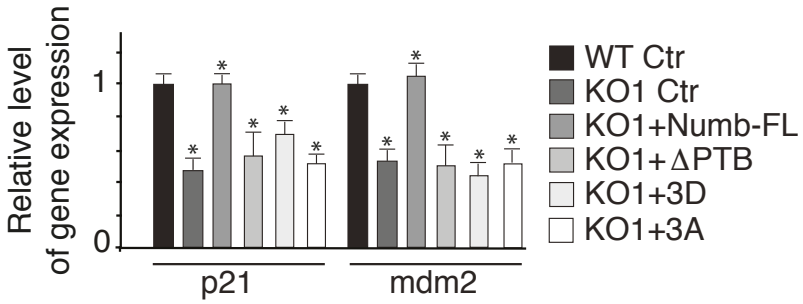

Figure 32 - Effects of Numb phosphomutants on p21 and mdm2 mRNA levels in Numb-KO cells

*KO1 cells were transduced with the indicated constructs and analyzed by rt-qPCR for the expression of p21 and mdm2. *, p value < 0.05.*

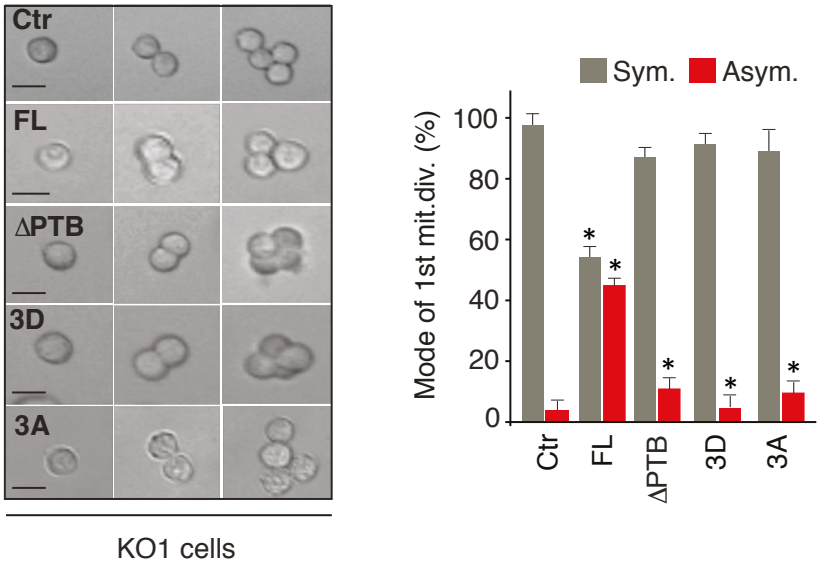

Figure 33 – Numb phosphomutants cannot rescue the symmetric mode of division of Numb-KO cells

Left: *Single cell suspensions from KO1 mammospheres were lentivirally transduced with Numb-DsRed (or its mutants), and then monitored by time-lapse video-microscopy throughout the formation of the next generation of mammospheres. In this type of analysis, a 1-2-4 pattern of cell divisions was scored as symmetric cell division, while a 1-2-3-5 pattern was scored as asymmetric cell division. Scale bar, 10 μm.*

Right*: Quantitation of the video-microscopy experiment. *, p value < 0.05. Sample size: 30 cells/treatment.*

3.7 Numb phosphorylation impairs the binding of Numb to p53

We showed that none of the Numb phosphomutants are able to rescue p53 levels of Numb-KO cells. To explain these results, we first hypothesized that Numb phosphorylation could impact on the binding of Numb to p53 (Colaluca, Tosoni et al., 2008). Thus, we generated, on a lentiviral Numb-FLAG FL backbone, a mutant in which all three serine residues phosphorylated by PKC were mutated to three aspartic acids (Numb-FLAG 3D). To produce this mutant, we used the pLL3.7 lentiviral backbone, which contains an shRNA sequence targeted to the endogenous Numb sequence, together with an sh-resistant sequence encoding for Numb-FLAG (C-ter). As in the case of the Numb-dsRed phosphomutants described above (see paragraph 3.5), we used a Numb-FLAG ΔPTB construct as negative control, since the PTB region is responsible for the binding to p53.

Indeed, we found that the Numb-FLAG 3D mutant co-immunoprecipitate with p53, but in lower amount compared to the Numb-FL protein (***Fig. 35***). We also analyzed the effects of Numb phosphorylation on the interaction with alpha-adaptin (AP2), a well-known binding partner of Numb (Dho, Trejo et al. 2006). Like p53, also AP2 showed a decreased interaction with Numb-FLAG 3D compared to Numb-FLAG FL (***Fig. 34***).

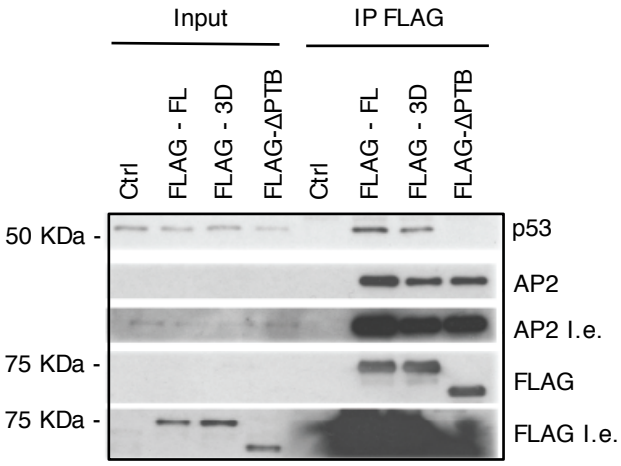

Figure 34 – Numb phospho-mimetic mutant displays reduced interaction with p53. *MCF10A cells were lentivirally transduced with either Numb-FLAG FL, Numb-FLAG 3D or Numb-FLAG ΔPTB constructs. The cells were then lysed in JS buffer and subjected to co-immunoprecipitation assay with an anti-FLAG antibody. Co-immunoprecipitated proteins were analyzed by SDS-PAGE and immunoblotting with the indicated antibodies. Not infected cells were used as control (Ctrl). Increased exposures ((I.e) are reported to shown the Input.*

Chapter 4

Discussion

A “stem cell” is a cell with the ability to self-renew and to produce differentiating daughter cells. One of the mechanisms that stem cells use to fulfill these properties is asymmetric cell division (ACD). Although the existence of ACD has been proved in several mammalian systems (skin, gut, muscle, mammary gland), the mechanisms that govern these events are still poorly understood. In a review of ACD, A. Knoblich stated that “transferring our detailed understanding of the process from *D. melanogaster* and *C. elegans* to vertebrates has been much more challenging than expected” (Knoblich 2010). In fact, although almost all players involved in the regulation of ACD are conserved in vertebrates, the function of these proteins has not been clearly elucidated. We know, for example, that Par proteins and aPKC are apically localized and asymmetrically inherited during mitosis of mouse neural progenitor cells (Kosodo, Roper et al. 2004). However, only few of these divisions are aligned along the axis determined by the Par complex, suggesting that the polarity of cell division is not coupled to spindle orientation in this system (Kosodo, Roper et al. 2004). Also the basolateral localization of Numb is conserved in mouse neural progenitors, but this was shown to be connected to the regulation of E-cadherin trafficking, rather than to cell fate specification (Rasin, Gazula et al. 2007). Intriguingly, in 2009, Bultje and colleagues showed that mammalian Par3 is asymmetrically inherited during mitosis of mouse neural progenitor cells and that it regulates cell fate specification by controlling Notch signalling (Bultje, Castaneda-Castellanos et al. 2009).

While the discussion on ACD in mammalian neural progenitors is still open, in the mammary gland epithelium, adult mammary stem cells (MaSCs) have been clearly shown to undergo ACD to produce either luminal or myoepithelial progenitor cells (Stingl, Eirew et al., 2006) (Ballard, Zhu et al. 2015). Concerning polarity proteins, both Par3 and aPKC have been shown to regulate the asymmetric division of MaSCs during mammary gland

morphogenesis. In fact, both Par3-KD and aPKC inhibition result in the expansion of K8/K14 dual positive progenitors (McCaffrey and Macara 2009).

Recent studies from our laboratory provided evidences for asymmetric segregation of Numb in MaSCs (Tosoni, Zecchini et al. 2015) and for the involvement of the Numb-p53 axis in cell fate determination. To our knowledge, the molecular mechanisms that specify Numb asymmetric partitioning in MaSCs have not yet been characterized.

With the present study, we argue that the molecular machinery responsible for Numb asymmetric segregation at mitosis is conserved, at least in part, from *D. melanogaster* neuroblasts to MaSCs. In particular, we demonstrate that Numb asymmetric distribution at mitosis of MaSCs depends on its phosphorylation status, as well as on the presence of Par3, which is necessary to guarantee the asymmetric distribution of Numb at mitosis of MaSCs. Our data also suggest that Numb phosphorylation, mediated by PKCζ, determines Numb subcellular localization and impairs the binding of Numb to p53, thus linking the regulation of ACD to cell fate specification and tumourigenesis.

4.1 Numb phosphorylation at PKCζ target sites is relevant for its localization in mammary cells

As previously mentioned, the role of Numb as a cell fate determinant at mitosis has been originally clarified in the neural system of *D. melanogaster* (Caussinus and Gonzales 2005) (Knoblich 2010). In this model, the phosphorylation status of Numb determines its asymmetric inheritance in only one of the two daughter cells, by controlling its subcellular localization. For these reasons, we started our investigations by evaluating the relevance of Numb phosphorylation on its localization in mammary epithelial and stem cells.

In our experiments, we used TPA (12-*O*-TetradecanoylPhorbol-13-Acetate) as a tool to induce Numb phosphorylation (as previously described by Dho, Trejo et al. 2006 and

Smith, Lau et al., 2006). TPA is a potent activator of classical and novel PKC isoenzymes and it was shown to induce Numb phosphorylation at conserved serine residues (Smith, Lau et al., 2006). One of these residues - Ser276, which we used as readout in our experiments - was also predicted to be phosphorylated by atypical PKCζ (Nishimura and Kaibuchi, 2007). We found that, in mammary epithelial cells, treatment with TPA increases Numb phosphorylation levels on Ser276 and induces a re-localization of the protein from cellular biomembranes to the cytosol. In accordance with these results, we observed the same re-localization of Numb in PKH26^{high} mouse MaSCs upon treatment with TPA (see paragraph 3.1, "Results"). These results suggest that the phosphorylation of Numb, on conserved serine residues, can influence its subcellular localization in mammary cells.

To directly address the impact of Numb phosphorylation on its partitioning at mitosis of MaSCs, we analyzed Numb distribution in the presence of TPA. We found that TPA treatment imparted a shift from asymmetric to symmetric distribution of Numb at mitosis of MaSCs, indicating that Numb distribution may depend on its phosphorylation status (see paragraph, 3.2"Results"). In other words, our findings suggest that variations in the phosphorylation status of Numb may influence the asymmetric *vs.* symmetric outcome of Numb distribution into daughter cells.

4.2 The Par complex regulates Numb phosphorylation in the mammary stem cell compartment

Since our data may suggest a role for Numb phosphorylation on its distribution at mitosis, we then concentrated our efforts on identifying the players that specifically cause this modification in mammary cells. We showed that both Par3-KD (see paragraph 3.3, "Results") and PKCζ-KD (see paragraph 3.4.2, "Results") in mammary epithelial cells

impaired Numb phosphorylation on Ser276 and caused the accumulation of Numb at biomembranes, allowing us to conclude that Par3 and atypical PKCζ might control Numb phosphorylation and localization in mammary cells. These data are supported by previous findings, showing that Par3, PKCζ and Numb actually interact in mammalian cells, and that Par3 is functional to the PKCζ-mediated phosphorylation of Numb (Nishimura and Kaibuchi, 2007). In this paper, the authors show that Numb is phosphorylated by PKCζ in vitro on three conserved serine residues (Ser7, 276 and 295). Moreover, the McGlades laboratory showed in 2006 that overexpression of a constitutively active form of PKCζ in HeLa cells results in the redistribution of endogenous Numb from the cortical membrane to the cytoplasm (Smith, Lau et al., 2006). We therefore overexpressed PKCζ (PKCζ-Venus) in mammary epithelial cells and found that, as in the case of TPA treatment, it increased pSer276 levels and promoted the release of Numb from the PM to the cytosol (see paragraph 3.4.1, "Results"). All together, these data support the involvement of the atypical PKCζ isoform in the processes of Numb phosphorylation and localization in mammary cells.

We also found that the ablation of Par3 in MaSCs causes a switch from asymmetric to symmetric segregation of Numb at mitosis (see paragraph 3.3, "Results"). This observation demonstrates that, also in the mammary epithelium, Par3 is necessary for the asymmetric partitioning of Numb during mitosis of stem cells. Of note, Lee and colleagues observed a similar phenotype of increased symmetric cell division in *D. melanogaster* neuroblasts upon overexpression of aPKC. This increase was associated with ectopic neuroblast self-renewal and tumour formation (Lee, Andersen et al., 2006). For this reason, to further corroborate the involvement of atypical PKCζ in the control of asymmetric distribution of Numb at MaSCs mitosis, we plan to study the effect of PKCζ depletion directly in MaSCs.

4.3 Studies on phospho-mimetic and phospho-deficient Numb mutants confirmed the involvement of PKCζ in the phosphorylation of Numb at mitosis of MaSC

As discussed above, mammalian Numb is phosphorylated by PKCζ on three specific residues - Ser7, Ser276 and Ser295 (Smith, Lau et al., 2006; Nishimura and Kaibuchi, 2007). To gain more insight into the role of these phosphorylation sites in MaSCs, we generated two different Numb phosphomutants, in which we mutated all three serine residues to either alanine (phospho-deficient mutant, Numb-3A) or aspartic acid (phospho-mimetic mutant, Numb-3D). In PKH26^{high} isolated MaSCs, the Numb-3D mutant localized mainly in the cytoplasm, while the Numb-3A mutant was predominantly associated with the PM (see paragraph 3.5, "Results"). These observations further validate our previous finding that the phosphorylation of Numb by PKCζ directs its subcellular localization in mammary cells (see paragraph 3.4, "Results").

We also showed that both the Numb-3D and the Numb-3A mutants are symmetrically distributed at mitosis of MaSCs. These results are consistent with a difference in subcellular localisation observed between mutants, and suggest a dynamic mechanism underlying the distribution of Numb during mitosis. In fact, the Numb-3A mutant is associated with the PM, like the WT protein, but cannot be phosphorylated by PKCζ. Hence, it cannot be released from the PM in a spatially restricted fashion. Thereby, this mutant remains associated with the entire PM throughout the mitotic division and segregates equally in the two daughter cells. Conversely, the Numb-3D mutant mimics the phosphorylation status that follows PKCζ phosphorylation and the resulting release of Numb from the PM. This mutant is totally localized in the cytoplasm of the dividing MaSC, without any spatial restriction, and therefore it is equally partitioned in the two daughter cells.

Our observation that both phosphomutants were segregated symmetrically during mitosis of MaSCs suggests that a proper cycle of Numb phosphorylation and de-phosphorylation is likely necessary to allow its asymmetric partitioning. However, it is possible that additional serine residues (or a different set of them) are involved in coupling Numb phosphorylation and asymmetric segregation in mammary stem cells. Further investigations are required to better characterize the entire mechanism that leads to Numb asymmetric segregation in the mammary stem cell compartment.

It did not escape our attention that other PKC isoforms have been shown to phosphorylate Numb (Smith, Lau et al., 2006) (Martin-Blanco, Checquolo et al. 2014) (Mah, Soloff et al. 2015). For example, Smith and colleagues showed that Numb is phosphorylated *in vitro* by PKCα, β1, β2 and ε (Smith, Lau et al. 2007). In addition, Martin-Blanco et al. showed that Numb is phosphorylated by the novel PKCθ isoform in early thymocyte precursors, which leads to its exclusion from the nucleus and the promotion of p53 degradation (Martin-Blanco, Checquolo et al. 2014). We also took into consideration that individual PKC isozymes exhibit different tissue distribution, subcellular localization, and biochemical properties, which indicate that each member of the family plays specialized roles in different tissues. The breast tissue expresses almost all isoforms but shows higher expression of PKCα, PKCδ and PKCι (ProteinDB, www.proteomicsdb.org).

The PKCι isoenzyme, together with PKCζ, is an atypical PKC isoform. In 2015, Mah and colleagues showed that PKCι depletion from mouse embryonic cells results in a marked increase in the number of various stem/progenitor cells. Furthermore, PKCι depletion lead to a marked decrease in pSer276 levels. The authors suggest that the mechanism underlying these phenotypes involves phosphorylation, inactivation and symmetric localization of Numb, leading to the activation of Notch1 and its effectors (Mah, Soloff et al. 2015).

In the present thesis work, we did not investigate the involvement of other PKC isoforms than PKCζ during MaSC division. As previously mentioned, we chose to evaluate PKCζ for several reasons: i) PKCζ interacts with Numb and Par3 in mammalian cells (Nishimura and Kaibuchi, 2007); ii) PKCζ is essential for end-bud formation and progenitor differentiation during mammary gland morphogenesis (McCaffrey and Macara, 2009); and iii) PKCζ phosphorylates Numb on conserved residues between *D. melanogaster* and mammals (Smith, Lau et al., 2006). Nevertheless, PKCζ and PKCι share 73% homology in their amino acid sequences (ProteinBLAST, http://blast.ncbi.nlm.nih.gov/Blast.cgi). Moreover, it was recently shown that PKCι interacts with Par3 (Guyer and Macara, 2015) and that its expression correlates with breast cancer progression and the clinical-pathological state (Kojima, Akimoto et al. 2008). In light of all these observations, our future plans include the study of a possible role for both atypical PKCs (ζ and ι) in ACD of MaSCs.

4.4 Numb phosphorylation impacts on the Numb-p53 interaction: consequences on cell fate determination and cancer

During asymmetric cell division of MaSCs, Numb is inherited by the daughter cell that retains the stem cell fate, where it ensures the stability of the tumour suppressor p53 (Tosoni, Zecchini et al., 2015). p53, in turn, is essential for the maintenance of the stem cell phenotype, and its loss favours symmetric cell divisions and the expansion of cancer stem cells (Cicalese, Bonizzi et al., 2009). Since the phosphorylation of Numb determines its asymmetric partitioning at mitosis, assessment of the consequences of this modification on the interaction between Numb and p53, and thus on the control of cell fate specification, gains importance.

Recently, Siddique and colleagues demonstrated that, in liver cancer stem cells (CSCs), the phosphorylation of Numb by PKCζ disrupts its binding to p53, ultimately leading to p53 degradation and the expansion of CSCs (Siddique, Feldman et al. 2015). In this paper, the authors show that activation of PKCζ is mediated by the mitotic kinase Aurora A, and this event causes Numb phosphorylation and p53 destabilization (Siddique, Feldman et al. 2015). Of note, the authors also show that the Numb-3D phospho-mimetic mutant does not interact with p53 and that its ectopic expression decreases the levels of p53 in liver CSCs (Siddique, Feldman et al. 2015). These data are in line with our findings in the mammary epithelium, in which we found that neither the Numb-3A nor the Numb-3D mutants are able to rescue the low p53 levels displayed by Numb-KO cells (see "Results", paragraph 7). These results are also confirmed by our observation that both mutants do not rescue the mRNA levels of well-established p53 target genes, such as MDM2 and TP21, in Numb-KO cells (see "Results", paragraph 7). Of note, the same mutants are not able to revert the symmetric mode of division of Numb-KO cells, which allows us to conclude that Numb phosphorylation impairs the interaction between Numb and p53. To strengthen these results, we tested the direct effect of Numb phosphorylation on its binding to p53. In co-immunoprecipitation assays, the Numb-3D mutant (Numb-FLAG 3D) exhibited lower affinity for p53 compared to full length Numb (FL Numb-dsRed; see "Results", paragraph 8), suggesting that Numb phosphorylation on PKCζ sites directly destabilizes the binding of Numb to p53.

At the moment, we do not have clear data on the binding of the Numb-3A mutant to p53. However, the fact that this mutant could not rescue the p53-related phenotypes of Numb-KO cells suggests that a correct cycle of phosphorylation and de-phosphorylation might be important for the regulation of the Numb-p53 binding. To complete our characterization,

we are currently testing the possible involvement of Aurora A in the activation of PKCζ in MaSCs.

As previously highlighted, a correct balance between symmetric and asymmetric cell division is critical during development and in adult tissue homeostasis. When this fine-tuned balance is disrupted, normal tissue morphogenesis goes awry. Alteration of this process is also relevant to cancer, as strongly supported by recent evidence that dysfunctions of the Numb/p53 circuitry in MaSCs lead to the emergence of cancer stem cells with unlimited self-renewal potential (Tosoni, Zecchini et al., 2015). This finding is in line with previous observations that p53 controls the mode of MaSCs division and its loss is correlated with tumourigenesis (Cicalese, Bonizzi et al., 2009). Therefore, we can speculate that the dysfunction of the molecular circuitries that control the distribution of Numb might result in the subversion of the homeostasis of the MaSC compartment, and could represent a source of malignant transformation. In support of this idea, both PKCζ and PKCι are amplified or mutated in 2 and 5% of breast cancer patients, respectively, as reported in multiple databases (www.cbioportal.org). It has also been demonstrated that aberrantly expressed PKCζ in mammary cells induces phenotypic alterations associated with malignant transformation and tumour progression (Urtreger, Kazanietz et al. 2012).
To our knowledge, no studies have directly addressed the possible contribution of Numb phosphorylation to breast cancer tumourigenesis. To assess whether a correlation exists between an aberrant regulation of Numb phosphorylation and clinical-pathological parameters in breast cancer, we plan to assess PKCζ/ι and Numb phosphorylation levels (pSer276) in a cohort of breast cancer patients from the IEO hospital in Milan, Italy. This analysis will allow us to demonstrate that the presence of Numb and its correct partitioning at mitosis is essential to safeguard the homeostasis of MaSCs, and that the molecular

mechanisms that govern Numb asymmetric distribution act as an additional tumour suppressor barrier in the physiology of the mammary epithelium.

To summarize, in this thesis work we propose that a proper cycle of Numb phosphorylation and de-phosphorylation is essential to allow Numb asymmetric partitioning at mitosis of MaSCs. In particular, we show that Numb phosphorylation at three specific serine residues (Ser7, 276 and 295) is responsible for its subcellular localization in MaSCs. Our data also support the involvement of the Par polarity complex - and in particular of Par3 and aPKCζ - in the process of Numb phosphorylation.

Finally, we propose that Numb phosphorylation can affect its binding to the tumour suppressor p53, with critical implications on MaSCs homeostasis.

Acknowledgments

I thank my supervisor Pier Paolo Di Fiore for the opportunity to contribute to this project.

I also thank my co-supervisors, Daniela Tosoni and Salvatore Pece, for helpful discussions.

I thank my internal supervisor, Giorgio Scita, and my external supervisor, Marcos Gonzales-Gaitan, for their useful suggestions.

I thank Wessen Maruwge and Maria Grazia Malabarba for their critical revision of this thesis.

I especially thank everyone who helped me during these four years at the IEO Hospital and at the IFOM-IEO Campus, including all Facilities and the SEMM Office.

Bibliography

Al-Hajj, M., M. S. Wicha, et al. (2003). "Prospective identification of tumorigenic breast cancer cells." Proceedings of the National Academy of Sciences of the United States of America **100**(7): 3983-3988.

Babaoglan, A. B., K. M. O'Connor-Giles, et al. (2009). "Sanpodo: a context-dependent activator and inhibitor of Notch signaling during asymmetric divisions." Development **136**(24): 4089-4098.

Badders, N. M., S. Goel, et al. (2009). "The Wnt receptor, Lrp5, is expressed by mouse mammary stem cells and is required to maintain the basal lineage." PloS one **4**(8): e6594.

Ballard, M. S., A. Zhu, et al. (2015). "Mammary Stem Cell Self-Renewal Is Regulated by Slit2/Robo1 Signaling through SNAI1 and mINSC." Cell reports **13**(2): 290-301.

Bardin, A. J., R. Le Borgne, et al. (2004). "Asymmetric localization and function of cell-fate determinants: a fly's view." Current opinion in neurobiology **14**(1): 6-14.

Bardin, A. J., C. N. Perdigoto, et al. (2010). "Transcriptional control of stem cell maintenance in the Drosophila intestine." Development **137**(5): 705-714.

Becker, A. J., C. E. Mc, et al. (1963). "Cytological demonstration of the clonal nature of spleen colonies derived from transplanted mouse marrow cells." Nature **197**: 452-454.

Bellaiche, Y., A. Radovic, et al. (2001). "The Partner of Inscuteable/Discs-large complex is required to establish planar polarity during asymmetric cell division in Drosophila." Cell **106**(3): 355-366.

Bello, B. C., N. Izergina, et al. (2008). "Amplification of neural stem cell proliferation by intermediate progenitor cells in Drosophila brain development." Neural development **3**: 5.

Berika, M., M. E. Elgayyar, et al. (2014). "Asymmetric cell division of stem cells in the lung and other systems." Frontiers in cell and developmental biology **2**: 33.

Besson, C., F. Bernard, et al. (2015). "Planar Cell Polarity Breaks the Symmetry of PAR Protein Distribution prior to Mitosis in Drosophila Sensory Organ Precursor Cells." Current biology : CB **25**(8): 1104-1110.

Betschinger, J. and J. A. Knoblich (2004). "Dare to be different: asymmetric cell division in Drosophila, C. elegans and vertebrates." Current biology : CB **14**(16): R674-685.

Bonnet, D. and J. E. Dick (1997). "Human acute myeloid leukemia is organized as a hierarchy that originates from a primitive hematopoietic cell." Nature medicine **3**(7): 730-737.

Boone, J. Q. and C. Q. Doe (2008). "Identification of Drosophila type II neuroblast lineages containing transit amplifying ganglion mother cells." Developmental neurobiology **68**(9): 1185-1195.

Bowman, S. K., R. A. Neumuller, et al. (2006). "The Drosophila NuMA Homolog Mud regulates spindle orientation in asymmetric cell division." Developmental cell **10**(6): 731-742.

Bowman, S. K., V. Rolland, et al. (2008). "The tumor suppressors Brat and Numb regulate transit-amplifying neuroblast lineages in Drosophila." Developmental cell **14**(4): 535-546.

Boyd, L., S. Guo, et al. (1996). "PAR-2 is asymmetrically distributed and promotes association of P granules and PAR-1 with the cortex in C. elegans embryos." Development **122**(10): 3075-3084.

Bray, S. J. (2006). "Notch signalling: a simple pathway becomes complex." Nature reviews. Molecular cell biology **7**(9): 678-689.

Brooks, M. D., M. L. Burness, et al. (2015). "Therapeutic Implications of Cellular Heterogeneity and Plasticity in Breast Cancer." Cell stem cell **17**(3): 260-271.

Buchman, J. J. and L. H. Tsai (2007). "Spindle regulation in neural precursors of flies and mammals." Nature reviews. Neuroscience **8**(2): 89-100.

Bultje, R. S., D. R. Castaneda-Castellanos, et al. (2009). "Mammalian Par3 regulates progenitor cell asymmetric division via notch signaling in the developing neocortex." Neuron **63**(2): 189-202.

Caussinus, E. and C. Gonzalez (2005). "Induction of tumor growth by altered stem-cell asymmetric division in Drosophila melanogaster." Nature genetics **37**(10): 1125-1129.

Chamberlain, G., J. Fox, et al. (2007). "Concise review: mesenchymal stem cells: their phenotype, differentiation capacity, immunological features, and potential for homing." Stem cells **25**(11): 2739-2749.

Choksi, S. P., T. D. Southall, et al. (2006). "Prospero acts as a binary switch between self-renewal and differentiation in Drosophila neural stem cells." Developmental cell **11**(6): 775-789.

Cicalese, A., G. Bonizzi, et al. (2009). "The tumor suppressor p53 regulates polarity of self-renewing divisions in mammary stem cells." Cell **138**(6): 1083-1095.

Colaluca, I. N., D. Tosoni, et al. (2008). "NUMB controls p53 tumour suppressor activity." Nature **451**(7174): 76-80.

Cossu, G. and S. Tajbakhsh (2007). "Oriented cell divisions and muscle satellite cell heterogeneity." Cell **129**(5): 859-861.

Costa, M. R., G. Wen, et al. (2008). "Par-complex proteins promote proliferative progenitor divisions in the developing mouse cerebral cortex." Development **135**(1): 11-22.
Cotton, M., N. Benhra, et al. (2013). "Numb inhibits the recycling of Sanpodo in Drosophila sensory organ precursor." Current biology : CB **23**(7): 581-587.
Couturier, L., K. Mazouni, et al. (2013). "Numb localizes at endosomes and controls the endosomal sorting of notch after asymmetric division in Drosophila." Current biology : CB **23**(7): 588-593.
Cuenca, A. A., A. Schetter, et al. (2003). "Polarization of the C. elegans zygote proceeds via distinct establishment and maintenance phases." Development **130**(7): 1255-1265.
Daniel, C. W., K. B. De Ome, et al. (1968). "The in vivo life span of normal and preneoplastic mouse mammary glands: a serial transplantation study." Proceedings of the National Academy of Sciences of the United States of America **61**(1): 53-60.
Daniels, B. R., T. M. Dobrowsky, et al. (2010). "MEX-5 enrichment in the C. elegans early embryo mediated by differential diffusion." Development **137**(15): 2579-2585.
Daniels, B. R., E. M. Perkins, et al. (2009). "Asymmetric enrichment of PIE-1 in the Caenorhabditis elegans zygote mediated by binary counterdiffusion." The Journal of cell biology **184**(4): 473-479.
Deome, K. B., L. J. Faulkin, Jr., et al. (1959). "Development of mammary tumors from hyperplastic alveolar nodules transplanted into gland-free mammary fat pads of female C3H mice." Cancer research **19**(5): 515-520.
Dho, S. E., J. Trejo, et al. (2006). "Dynamic regulation of mammalian numb by G protein-coupled receptors and protein kinase C activation: Structural determinants of numb association with the cortical membrane." Mol Biol Cell **17**(9): 4142-4155.
Di Marcotullio, L., E. Ferretti, et al. (2007). "Multiple ubiquitin-dependent processing pathways regulate hedgehog/gli signaling: implications for cell development and tumorigenesis." Cell cycle **6**(4): 390-393.
Ding, X., M. Ma, et al. (2015). "Numb induces e-cadherin adhesion dissolution, cytoskeleton reorganization, and migration in tubular epithelial cells contributing to renal fibrosis." Current molecular medicine **15**(4): 368-379.
Doe, C. Q., Q. Chu-LaGraff, et al. (1991). "The prospero gene specifies cell fates in the Drosophila central nervous system." Cell **65**(3): 451-464.
Dontu, G., M. Al-Hajj, et al. (2003). "Stem cells in normal breast development and breast cancer." Cell proliferation **36 Suppl 1**: 59-72.
dos Santos, C. O., C. Rebbeck, et al. (2013). "Molecular hierarchy of mammary differentiation yields refined markers of mammary stem cells." Proceedings of the National Academy of Sciences of the United States of America **110**(18): 7123-7130.
Etemad-Moghadam, B., S. Guo, et al. (1995). "Asymmetrically distributed PAR-3 protein contributes to cell polarity and spindle alignment in early C. elegans embryos." Cell **83**(5): 743-752.
Faraldo, M. M. and M. A. Glukhova (2015). "Regulating the regulator: Numb acts upstream of p53 to control mammary stem and progenitor cell." The Journal of cell biology **211**(4): 737-739.
Feigin, M. E., S. D. Akshinthala, et al. (2014). "Mislocalization of the cell polarity protein scribble promotes mammary tumorigenesis and is associated with basal breast cancer." Cancer research **74**(11): 3180-3194.
Fishell, G. and A. R. Kriegstein (2003). "Neurons from radial glia: the consequences of asymmetric inheritance." Current opinion in neurobiology **13**(1): 34-41.
Fuchs, E. (2008). "Skin stem cells: rising to the surface." The Journal of cell biology **180**(2): 273-284.
Fuchs, E. and J. A. Nowak (2008). "Building epithelial tissues from skin stem cells." Cold Spring Harbor symposia on quantitative biology **73**: 333-350.
Fuerstenberg, S., J. Broadus, et al. (1998). "Asymmetry and cell fate in the Drosophila embryonic CNS." The International journal of developmental biology **42**(3): 379-383.
George, R. M., S. Biressi, et al. (2013). "Numb-deficient satellite cells have regeneration and proliferation defects." Proceedings of the National Academy of Sciences of the United States of America **110**(46): 18549-18554.
Godde, N. J., J. M. Sheridan, et al. (2014). "Scribble modulates the MAPK/Fra1 pathway to disrupt luminal and ductal integrity and suppress tumour formation in the mammary gland." PLoS genetics **10**(5): e1004323.
Goldstein, B. and S. N. Hird (1996). "Specification of the anteroposterior axis in Caenorhabditis elegans." Development **122**(5): 1467-1474.
Gopalakrishnan, S., M. A. Hallett, et al. (2007). "aPKC-PAR complex dysfunction and tight junction disassembly in renal epithelial cells during ATP depletion." American journal of physiology. Cell physiology **292**(3): C1094-1102.

Goulas, S., R. Conder, et al. (2012). "The Par complex and integrins direct asymmetric cell division in adult intestinal stem cells." Cell stem cell **11**(4): 529-540.
Gulino, A., L. Di Marcotullio, et al. (2010). "The multiple functions of Numb." Experimental cell research **316**(6): 900-906.
Guo, M., L. Y. Jan, et al. (1996). "Control of daughter cell fates during asymmetric division: interaction of Numb and Notch." Neuron **17**(1): 27-41.
Guo, S. and K. J. Kemphues (1995). "par-1, a gene required for establishing polarity in C. elegans embryos, encodes a putative Ser/Thr kinase that is asymmetrically distributed." Cell **81**(4): 611-620.
Harris, E. S. and W. J. Nelson (2010). "VE-cadherin: at the front, center, and sides of endothelial cell organization and function." Current opinion in cell biology **22**(5): 651-658.
Hartsock, A. and W. J. Nelson (2008). "Adherens and tight junctions: structure, function and connections to the actin cytoskeleton." Biochimica et biophysica acta **1778**(3): 660-669.
Haubensak, W., A. Attardo, et al. (2004). "Neurons arise in the basal neuroepithelium of the early mammalian telencephalon: a major site of neurogenesis." Proceedings of the National Academy of Sciences of the United States of America **101**(9): 3196-3201.
Hennighausen, L. and G. W. Robinson (2005). "Information networks in the mammary gland." Nature reviews. Molecular cell biology **6**(9): 715-725.
Hoshino, K. (1962). "Morphogenesis and growth potentiality of mammary glands in mice. I. Transplantability and growth potentiality of mammary tissue of virgin mice." Journal of the National Cancer Institute **29**: 835-851.
Hoshino, K. and W. U. Gardner (1967). "Transplantability and life span of mammary gland during serial transplantation in mice." Nature **213**(5072): 193-194.
Hsu, Y. C. and E. Fuchs (2012). "A family business: stem cell progeny join the niche to regulate homeostasis." Nature reviews. Molecular cell biology **13**(2): 103-114.
Hung, T. J. and K. J. Kemphues (1999). "PAR-6 is a conserved PDZ domain-containing protein that colocalizes with PAR-3 in Caenorhabditis elegans embryos." Development **126**(1): 127-135.
Huo, Y. and I. G. Macara (2014). "The Par3-like polarity protein Par3L is essential for mammary stem cell maintenance." Nature cell biology **16**(6): 529-537.
Inaba, M. and Y. M. Yamashita (2012). "Asymmetric stem cell division: precision for robustness." Cell stem cell **11**(4): 461-469.
Inman, J. L., C. Robertson, et al. (2015). "Mammary gland development: cell fate specification, stem cells and the microenvironment." Development **142**(6): 1028-1042.
Ito, K. and Y. Hotta (1992). "Proliferation pattern of postembryonic neuroblasts in the brain of Drosophila melanogaster." Developmental biology **149**(1): 134-148.
Ito, T., H. Y. Kwon, et al. (2010). "Regulation of myeloid leukaemia by the cell-fate determinant Musashi." Nature **466**(7307): 765-768.
Izumi, Y., N. Ohta, et al. (2006). "Drosophila Pins-binding protein Mud regulates spindle-polarity coupling and centrosome organization." Nature cell biology **8**(6): 586-593.
Joberty, G., C. Petersen, et al. (2000). "The cell-polarity protein Par6 links Par3 and atypical protein kinase C to Cdc42." Nature cell biology **2**(8): 531-539.
Joshi, P. A., H. W. Jackson, et al. (2010). "Progesterone induces adult mammary stem cell expansion." Nature **465**(7299): 803-807.
Knoblich, J. A. (2008). "Mechanisms of asymmetric stem cell division." Cell **132**(4): 583-597.
Knoblich, J. A. (2010). "Asymmetric cell division: recent developments and their implications for tumour biology." Nature reviews. Molecular cell biology **11**(12): 849-860.
Kojima, Y., K. Akimoto, et al. (2008). "The overexpression and altered localization of the atypical protein kinase C lambda/iota in breast cancer correlates with the pathologic type of these tumors." Human pathology **39**(6): 824-831.
Konno, D., G. Shioi, et al. (2008). "Neuroepithelial progenitors undergo LGN-dependent planar divisions to maintain self-renewability during mammalian neurogenesis." Nature cell biology **10**(1): 93-101.
Kosodo, Y., K. Roper, et al. (2004). "Asymmetric distribution of the apical plasma membrane during neurogenic divisions of mammalian neuroepithelial cells." The EMBO journal **23**(11): 2314-2324.
Kraut, R. and J. A. Campos-Ortega (1996). "inscuteable, a neural precursor gene of Drosophila, encodes a candidate for a cytoskeleton adaptor protein." Developmental biology **174**(1): 65-81.
Kuang, S., K. Kuroda, et al. (2007). "Asymmetric self-renewal and commitment of satellite stem cells in muscle." Cell **129**(5): 999-1010.
Kulukian, A. and E. Fuchs (2013). "Spindle orientation and epidermal morphogenesis." Philosophical transactions of the Royal Society of London. Series B, Biological sciences **368**(1629): 20130016.
Kuo, C. T., Z. Mirzadeh, et al. (2006). "Postnatal deletion of Numb/Numblike reveals repair and remodeling capacity in the subventricular neurogenic niche." Cell **127**(6): 1253-1264.

Kyriazis, G. A., Z. Wei, et al. (2008). "Numb endocytic adapter proteins regulate the transport and processing of the amyloid precursor protein in an isoform-dependent manner: implications for Alzheimer disease pathogenesis." The Journal of biological chemistry **283**(37): 25492-25502.

Lanzetti, L. and P. P. Di Fiore (2008). "Endocytosis and cancer: an 'insider' network with dangerous liaisons." Traffic **9**(12): 2011-2021.

Lechler, T. and E. Fuchs (2005). "Asymmetric cell divisions promote stratification and differentiation of mammalian skin." Nature **437**(7056): 275-280.

Leclerc, C., I. Neant, et al. (2012). "The calcium: an early signal that initiates the formation of the nervous system during embryogenesis." Frontiers in molecular neuroscience **5**: 3.

Lee, C. Y., R. O. Andersen, et al. (2006). "Drosophila Aurora-A kinase inhibits neuroblast self-renewal by regulating aPKC/Numb cortical polarity and spindle orientation." Genes & development **20**(24): 3464-3474.

Li, L. and T. Xie (2005). "Stem cell niche: structure and function." Annual review of cell and developmental biology **21**: 605-631.

Luo, D., V. M. Renault, et al. (2005). "The regulation of Notch signaling in muscle stem cell activation and postnatal myogenesis." Seminars in cell & developmental biology **16**(4-5): 612-622.

Mah, I. K., R. Soloff, et al. (2015). "Atypical PKC-iota Controls Stem Cell Expansion via Regulation of the Notch Pathway." Stem cell reports **5**(5): 866-880.

Martin-Blanco, N. M., S. Checquolo, et al. (2014). "Numb-dependent integration of pre-TCR and p53 function in T-cell precursor development." Cell death & disease **5**: e1472.

McCaffrey, L. M. and I. G. Macara (2009). "The Par3/aPKC interaction is essential for end bud remodeling and progenitor differentiation during mammary gland morphogenesis." Genes & development **23**(12): 1450-1460.

McGill, M. A. and C. J. McGlade (2003). "Mammalian numb proteins promote Notch1 receptor ubiquitination and degradation of the Notch1 intracellular domain." The Journal of biological chemistry **278**(25): 23196-23203.

Micchelli, C. A. and N. Perrimon (2006). "Evidence that stem cells reside in the adult Drosophila midgut epithelium." Nature **439**(7075): 475-479.

Mukhopadhyay, D. and H. Riezman (2007). "Proteasome-independent functions of ubiquitin in endocytosis and signaling." Science **315**(5809): 201-205.

Neumuller, R. A. and J. A. Knoblich (2009). "Dividing cellular asymmetry: asymmetric cell division and its implications for stem cells and cancer." Genes & development **23**(23): 2675-2699.

Nishimura, T. and K. Kaibuchi (2007). "Numb controls integrin endocytosis for directional cell migration with aPKC and PAR-3." Developmental cell **13**(1): 15-28.

Nishimura, T. and K. Kaibuchi (2007). "Numb controls integrin endocytosis for directional cell migration with aPKC and PAR-3." Dev Cell **13**(1): 15-28.

Noctor, S. C., V. Martinez-Cerdeno, et al. (2004). "Cortical neurons arise in symmetric and asymmetric division zones and migrate through specific phases." Nature neuroscience **7**(2): 136-144.

O'Connor-Giles, K. M. and J. B. Skeath (2003). "Numb inhibits membrane localization of Sanpodo, a four-pass transmembrane protein, to promote asymmetric divisions in Drosophila." Developmental cell **5**(2): 231-243.

Ohlstein, B. and A. Spradling (2006). "The adult Drosophila posterior midgut is maintained by pluripotent stem cells." Nature **439**(7075): 470-474.

Pece, S., S. Confalonieri, et al. (2011). "NUMB-ing down cancer by more than just a NOTCH." Biochimica et biophysica acta **1815**(1): 26-43.

Pece, S., M. Serresi, et al. (2004). "Loss of negative regulation by Numb over Notch is relevant to human breast carcinogenesis." The Journal of cell biology **167**(2): 215-221.

Pece, S., D. Tosoni, et al. (2010). "Biological and molecular heterogeneity of breast cancers correlates with their cancer stem cell content." Cell **140**(1): 62-73.

Plaks, V., A. Brenot, et al. (2013). "Lgr5-expressing cells are sufficient and necessary for postnatal mammary gland organogenesis." Cell reports **3**(1): 70-78.

Polo, S., S. Pece, et al. (2004). "Endocytosis and cancer." Current opinion in cell biology **16**(2): 156-161.

Rajendran, D., Y. Zhang, et al. (2016). "Regulation of Numb isoform expression by activated ERK signaling." Oncogene.

Rasin, M. R., V. R. Gazula, et al. (2007). "Numb and Numbl are required for maintenance of cadherin-based adhesion and polarity of neural progenitors." Nature neuroscience **10**(7): 819-827.

Reichardt, I. and J. A. Knoblich (2013). "Cell biology: Notch recycling is numbed." Current biology : CB **23**(7): R270-272.

Rejon, C., M. Al-Masri, et al. (2016). "Cell Polarity Proteins in Breast Cancer Progression." Journal of cellular biochemistry **117**(10): 2215-2223.

Reya, T., S. J. Morrison, et al. (2001). "Stem cells, cancer, and cancer stem cells." Nature **414**(6859): 105-111.
Rhyu, M. S., L. Y. Jan, et al. (1994). "Asymmetric distribution of numb protein during division of the sensory organ precursor cell confers distinct fates to daughter cells." Cell **76**(3): 477-491.
Rios, A. C., N. Y. Fu, et al. (2014). "In situ identification of bipotent stem cells in the mammary gland." Nature **506**(7488): 322-327.
Ruiz Gomez, M. and M. Bate (1997). "Segregation of myogenic lineages in Drosophila requires numb." Development **124**(23): 4857-4866.
Sanada, K. and L. H. Tsai (2005). "G protein betagamma subunits and AGS3 control spindle orientation and asymmetric cell fate of cerebral cortical progenitors." Cell **122**(1): 119-131.
Sato, K., T. Watanabe, et al. (2011). "Numb controls E-cadherin endocytosis through p120 catenin with aPKC." Molecular biology of the cell **22**(17): 3103-3119.
Shackleton, M., F. Vaillant, et al. (2006). "Generation of a functional mammary gland from a single stem cell." Nature **439**(7072): 84-88.
Siddique, H. R., D. E. Feldman, et al. (2015). "NUMB phosphorylation destabilizes p53 and promotes self-renewal of tumor-initiating cells by a NANOG-dependent mechanism in liver cancer." Hepatology **62**(5): 1466-1479.
Siller, K. H., C. Cabernard, et al. (2006). "The NuMA-related Mud protein binds Pins and regulates spindle orientation in Drosophila neuroblasts." Nature cell biology **8**(6): 594-600.
Smith, C. A., K. M. Lau, et al. (2007). "aPKC-mediated phosphorylation regulates asymmetric membrane localization of the cell fate determinant Numb." The EMBO journal **26**(2): 468-480.
Smith, C. A., K. M. Lau, et al. (2007). "aPKC-mediated phosphorylation regulates asymmetric membrane localization of the cell fate determinant Numb." EMBO J **26**(2): 468-480.
Smith, G. H. (1996). "Experimental mammary epithelial morphogenesis in an in vivo model: evidence for distinct cellular progenitors of the ductal and lobular phenotype." Breast cancer research and treatment **39**(1): 21-31.
Smith, G. H. and D. Medina (1988). "A morphologically distinct candidate for an epithelial stem cell in mouse mammary gland." Journal of cell science **90 (Pt 1)**: 173-183.
Spana, E. P. and C. Q. Doe (1996). "Numb antagonizes Notch signaling to specify sibling neuron cell fates." Neuron **17**(1): 21-26.
Steed, E., M. S. Balda, et al. (2010). "Dynamics and functions of tight junctions." Trends in cell biology **20**(3): 142-149.
Stingl, J., P. Eirew, et al. (2006). "Purification and unique properties of mammary epithelial stem cells." Nature **439**(7079): 993-997.
Tabuse, Y., Y. Izumi, et al. (1998). "Atypical protein kinase C cooperates with PAR-3 to establish embryonic polarity in Caenorhabditis elegans." Development **125**(18): 3607-3614.
Taketo, M., A. C. Schroeder, et al. (1991). "FVB/N: an inbred mouse strain preferable for transgenic analyses." Proceedings of the National Academy of Sciences of the United States of America **88**(6): 2065-2069.
Tanos, B. and E. Rodriguez-Boulan (2008). "The epithelial polarity program: machineries involved and their hijacking by cancer." Oncogene **27**(55): 6939-6957.
Tosoni, D., P. P. Di Fiore, et al. (2012). "Functional purification of human and mouse mammary stem cells." Methods in molecular biology **916**: 59-79.
Tosoni, D., S. Zecchini, et al. (2015). "The Numb/p53 circuitry couples replicative self-renewal and tumor suppression in mammary epithelial cells." The Journal of cell biology **211**(4): 845-862.
Troy, A., A. B. Cadwallader, et al. (2012). "Coordination of satellite cell activation and self-renewal by Par-complex-dependent asymmetric activation of p38alpha/beta MAPK." Cell stem cell **11**(4): 541-553.
Urtreger, A. J., M. G. Kazanietz, et al. (2012). "Contribution of individual PKC isoforms to breast cancer progression." IUBMB life **64**(1): 18-26.
Vaccari, T. and D. Bilder (2009). "At the crossroads of polarity, proliferation and apoptosis: the use of Drosophila to unravel the multifaceted role of endocytosis in tumor suppression." Molecular oncology **3**(4): 354-365.
Van Keymeulen, A., A. S. Rocha, et al. (2011). "Distinct stem cells contribute to mammary gland development and maintenance." Nature **479**(7372): 189-193.
Visvader, J. E. (2009). "Keeping abreast of the mammary epithelial hierarchy and breast tumorigenesis." Genes & development **23**(22): 2563-2577.
Visvader, J. E. and H. Clevers (2016). "Tissue-specific designs of stem cell hierarchies." Nature cell biology **18**(4): 349-355.
Wang, D., C. Cai, et al. (2015). "Identification of multipotent mammary stem cells by protein C receptor expression." Nature **517**(7532): 81-84.

Wang, Z., S. Sandiford, et al. (2009). "Numb regulates cell-cell adhesion and polarity in response to tyrosine kinase signalling." The EMBO journal **28**(16): 2360-2373.

Westhoff, B., I. N. Colaluca, et al. (2009). "Alterations of the Notch pathway in lung cancer." Proceedings of the National Academy of Sciences of the United States of America **106**(52): 22293-22298.

Wirtz-Peitz, F., T. Nishimura, et al. (2008). "Linking cell cycle to asymmetric division: Aurora-A phosphorylates the Par complex to regulate Numb localization." Cell **135**(1): 161-173.

Wodarz, A. and W. B. Huttner (2003). "Asymmetric cell division during neurogenesis in Drosophila and vertebrates." Mechanisms of development **120**(11): 1297-1309.

Woodward, W. A., M. S. Chen, et al. (2005). "On mammary stem cells." Journal of cell science **118**(Pt 16): 3585-3594.

Yamanaka, T., Y. Horikoshi, et al. (2001). "PAR-6 regulates aPKC activity in a novel way and mediates cell-cell contact-induced formation of the epithelial junctional complex." Genes to cells : devoted to molecular & cellular mechanisms **6**(8): 721-731.

Yin, H., F. Price, et al. (2013). "Satellite cells and the muscle stem cell niche." Physiological reviews **93**(1): 23-67.

Yu, F., C. T. Kuo, et al. (2006). "Drosophila neuroblast asymmetric cell division: recent advances and implications for stem cell biology." Neuron **51**(1): 13-20.

Zeng, Y. A. and R. Nusse (2010). "Wnt proteins are self-renewal factors for mammary stem cells and promote their long-term expansion in culture." Cell stem cell **6**(6): 568-577.

Zigman, M., M. Cayouette, et al. (2005). "Mammalian inscuteable regulates spindle orientation and cell fate in the developing retina." Neuron **48**(4): 539-545.